Faculty of Engineering and Science

Performance of Variable Helix and Pitch Cutting Tools on Chatter Vibration in End Milling of Inconel 718

Hoe Chen Hou

This thesis is presented for the Degree of
Master of Philosophy (Mechanical Engineering)
of
Curtin University

September 2018

DECLARATION

To the best of my knowledge and belief this thesis contains no material previously published by any other person except where due acknowledgment has been made.

This thesis contains no material which has been accepted for the award of any other degree or diploma in any university.

Signature : Hoe Chen Hou

Date : 27/09/2018

ABSTRACT

Machining processes constitute a major part of manufacturing activity that stimulate the growth of the global economy. Most of the research and development focus on improving the machining performance through advanced tools and materials especially in machining difficult to cut materials such as Nickel based superalloys. Inconel 718 is one of the Nickel based superalloys which are widely manufactured for high temperature applications such as gas turbine blade, aerospace components and nuclear reactor. It is frequently used in the high performance applications due to its unique characteristics. Inconel 718 has the ability of maintaining high mechanical strength at elevated temperature and also high corrosion and chemical wear resistance. However, Inconel 718 is extremely difficult to machine due to rapid work hardening, low thermal conductivity, and high chemical reactivity which often causes high cutting temperature, short tool life and chatter vibrations. In order to ensure good machinability, chatter vibration aspect of the machining process has to be addressed. Chatter vibrations is a detrimental phenomenon that will lead to poor surface quality, premature tool wear, excessive cutting force and noise, and reduction in metal removal rate. One of the recent developed cutting tools known as variable helix and pitch cutting tool shows promising in mitigating the chatter vibration in the milling process. These geometrical variations of tool are expected to induce irregular interval between the cutting edges, thereby chatter vibration can be disrupted. However, there has not been much experimental research conducted with these tools in the milling process of Inconel 718. In this study, the performance of variable helix and pitch cutting tools are experimentally investigated. The influences of tool corner geometry, cutting speed, feed rate, and depth of cut on the vibration responses, surface roughness and tool wear progression were studied. The results show that variable helix and pitch cutting tool are able to enhance the stability in the milling process of Inconel 718 at low cutting speed. Furthermore, the results also revealed that tool corner geometry plays a significant role in reducing chatter vibration at least by 15%, improving surface roughness and conserving longer tool life at high cutting speed. This research work also proposed the best combination cutting parameters based on the experimental results to achieve high stability, thereby good machinability in machining of Inconel 718.

ACKNOWLEDGEMENT

First of foremost, I would like to express my sincere appreciation to the main supervisors – Associate Professor Dr.Sujan Debnath for his valuable and constructive feedback during the course of my MPhil study. I would also like to express my deep gratitude to the co-supervisor, –Associate Professor Dr. Mohan Reddy Moola and Associate Professor Dr. Vincent Lee for their patient guidance, enthusiastic encouragement and support at all time. I am really grateful to all of them for giving me the opportunity to pursuit my MPhill Degree. Throughout the MPhil journey, there has been up and down, the constant motivation from the thesis committee is one of the strength that keep me going. The completion of the project will not be possible without the support from the thesis committee.

This research project was fully funded by the (FRGS) Fundamental Research Grant Scheme from the Minister of Higher Education which I am truly appreciate for awarding such opportunity to me.

I would like to express my gratitude to every Curtin University Staff who assisted me throughout my MPhil candidatures, especially the mechanical lab technician – Mr Micheal Ding and Mr Aspindy for their assistance during my study. In addition, I will like to thanks the staff from graduate school who help me in many ways to ensure that I am able to keep up in my progress during my study.

Next, I would like to thank all my HDR friends for their moral supports and the encouragement throughout my MPhil journey. This journey will not be such delightful without them.

Most importantly, I would like to express my deepest appreciation to my dad, Hoe Chai Lee, and my mom, Marry Chong Sin Lan who support me wholeheartedly throughout my MPhil journey. I will not forget the sacrifices they made for me to ensure the completion of the study. Thank you with love!

My sincere gratitude to everyone!

Hoe Chen Hou

TABLE OF CONTENTS

LIST OF FIGURES

LIST OF TABLES

NOMENCLATURE

Nomenclatures	Description	Units
V	Cutting speed	m/min
f	Feed rate	mm/z
DoC_a	Axial depth of cut	mm
DoC_R	Radial depth of cut	mm
g	Gravitational acceleration	m/s^2
N	Spindle speed	RPM
Z	Number of flute	-
F	Force	N
m	Mass	kg
$\ddot{x}$	Acceleration	m/s^2
c	Damping coefficient	Ns/m
$\dot{x}$	Velocity	m/s
k	Stiffness	N/m
x	Displacement	m
R_a	Surface roughness	µm
R	Corner radius	mm
β_1 , β_2	Helix angle	°
$\varphi_1, \varphi_2, \varphi_3, \varphi_4$	Pitch angle	°

ABBREVIATION

ANOVA	-	Analysis of Variance
Al_2O_3	-	Aluminum Oxide
CBN	-	Cubic Boron Nitride
CNC	-	Computer Numerical Control
CrN	-	Chromium Nitride
CVD	-	Chemical Vapor Deposition
FRF	-	Frequency Responses Function
HSS	-	High Speed Steel
LQL	-	Low Quantity Lubrication
MQCL	-	Minimum Quantity Cooling Lubrication
MQL	-	Minimum Quantity Lubrication
PCD	-	Polycrystalline Diamond
PCBN	-	Polycrystalline Cubic Boron Nitride
PVD	-	Physical Vapor Deposition
RMS	-	Root Mean Square
TiN	-	Titanium Nitride
TiCN	-	Titanium Carbonitride
TiAlN	-	Titanium Aluminum Nitride
TiAlCrN	-	Titanium Aluminum Chromium Nitride

Chapter 1: Introduction

Manufacturing is an essential activities in the industries. Manufacturing processes primarily consist of processing operation and assembly operation. Processing operation focus on transforming the raw material to final product through changing of shape, properties, appearance, and etc. Meanwhile, assembly operation aims to combine multiple components into final product by using welding, brazing, soldering, and etc. Ideally, the final product should be manufactured with high quantity and quality in a short period of time.

Machining process is one of the manufacturing process, it is used to remove material from raw material into desired shape and dimension. There are various types of conventional machining process, namely, turning, milling, and drilling process. Milling process is regarded as one of the universal operation process for the ability to machine flat, curved and all kind of contour surface at high-quality finish. Milling process is one of the favourite process in the industry due to its versatility. Therefore, machining process in term of milling is one of the key improvement area in order to increase profit in the manufacturing industries.

The performance of the machining process often relates to the term machinability, it defines as how ease of a material (often a metal) can be machined using appropriate tooling and cutting conditions. Good machinability indicates longer tool life, low cutting force and power, good surface finish (low surface roughness value), and ease of chip disposal (Pervaiz et al. 2014). In order to achieve good machinability, machining operation, choice of tool and cutting parameters play a significant role. The quality and quantity of a final product from machining process is directly affected by the machinability. Therefore, understanding metal cutting fundamentals is one of the key factors in order to improve machinability.

However, the performance of machining process is often hindered by the mechanical phenomena known as vibration especially milling process. Unlike turning process, milling process is an intermittent cutting process that involves instantaneous force. The cutting force during the milling process varies periodically as a function of

time-varying immersion. Therefore, analysing the vibration aspect of milling process is more difficult compared to turning process.

In general, mechanical vibrations can occur due to lack of dynamic stiffness on the system which are referring to the machine structure, machine-tool, the tool holder, the cutting tool, workpiece material, or combination of elements. There are three types of vibration, namely, free vibration, force vibration and self-excited vibration. Free vibration occurs when the mechanical system is shifted from its equilibrium and it is allowed to vibrate freely. Forced vibration develops due to external excitations by the rotation of spindle head. Free and forced vibrations can be reduced or avoided when the source of the vibrations is identified. However, the self-excited vibrations also known as the chatter vibrations, which occur due to the interaction between the cutting tool and workpiece, are difficult to analyse.

Based on the theory, self-excited vibrations are categorised into primary chatter and secondary chatter vibrations. Primary chatter vibrations usually occur due to the frictional force between cutting tool and workpiece, the thermo-mechanical effects in the machining process and the superposition of cutting force and thrust force (Wiercigroch and Budak 2001; Wiercigroch and Krivtsov 2001). However, the term "chatter", is usually focused on the secondary chatter vibrations. It is the most common form of self-excited vibrations. The source of vibration energy is extracted from the cutting process itself, the entry and exit of every cutting edge generates a small amount of vibration and eventually the vibration energy accumulates to a certain point and become unstable (chatter vibrations occurs), which is known as the regenerative effect (Altintas 2012).

Chatter vibrations is a detrimental phenomenon that will lead to poor surface quality, premature tool wear, damaged machine, excessive noise, reduction in metal removal rate, waste of material, increase of the spindle bearing, etc. Therefore, there is a need to suppress or reduce the chatter vibrations in the machining process in order to obtain good machinability. Nowadays, the advancement of technology and sensors has made monitoring and measurement of chatter vibrations possible. Therefore, there has been considerable amount of research carried out to avoid, mitigate or control chatter vibration.

Chatter vibrations are even more severe when machine a difficult-to-cut material, for example, the superalloys (nickel based superalloy, titanium superalloy, Haynes superalloy). Inconel 718 is one of the nickel based superalloys that have high strength at elevated temperature, good resistance to chemical wear and corrosion, and high strength to weight ratio. Inconel 718 is one of the favourite materials in the high temperature application industries such as aerospace, marine equipment, gas turbine, nuclear reactor, petrochemical plants, and engine components. It is frequently used in the high performance applications due to its unique characteristics as mentioned above. However, Inconel 718 is extremely hard to machine due to its metallurgical stability at high temperature, it has high tendency to work hardening and generates high cutting temperature during the machining process. Thus, Inconel 718 are rated as one of the lowest machinability rating as shown in ***Fig. 1.1***.

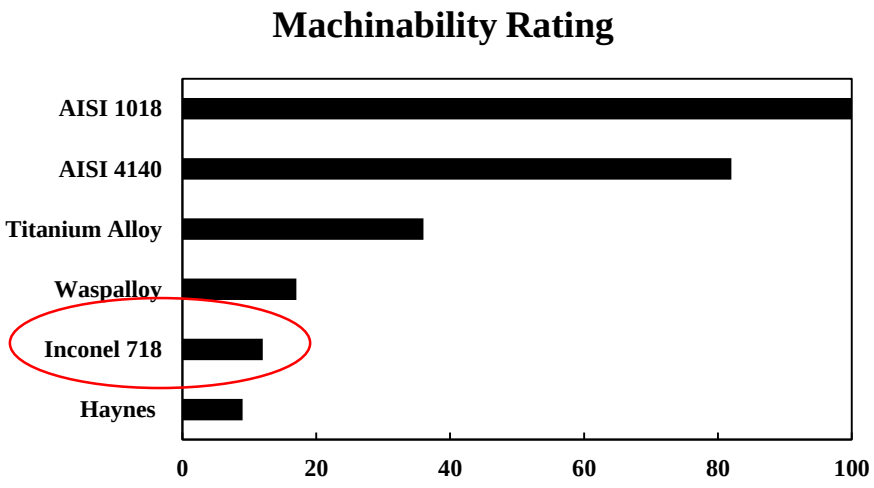

Fig. 1.1: Metal machinability rating (Pervaiz et al. 2014)

As mentioned previously, the selection of appropriate tooling is one of the factors that affect machinability. The recently developed tools, with geometric features such as variable helix and pitch angle, are able to disrupt the regenerative effect in the milling process. These geometrical variations of tool are expected to induce irregular interval between the cutting edges, thereby chatter vibration can be disrupted. Hence, it has the potential to mitigate the chatter vibrations in the milling process. However, according to the literature, variable helix and pitch cutting tool has yet to receive enough attention in the milling process of Inconel 718. As such, there is a need to

investigate the effect of variable helix and pitch end mill with the recently developed tool edge geometries in the machining process of Inconel 718.

In this study, variable helix and pitch cutting tool is utilized to perform experimental investigation in order to evaluate the performance of the milling process on Inconel 718. The surface roughness and vibration responses of the process are monitored in the experimentation. The experimental data are recorded, analysed and discussed to evaluate performance of the variable helix and pitch cutting tool. The best combination of cutting parameters are recommended to improve the machinability of Inconel 718. In this experimentation, dry cutting condition is incorporated in order to eliminate health and environmental problems which is associated with the cutting fluids. Therefore, this study also encourage machining process to work towards green manufacturing.

1.1 Problem Statement and Research Gap

Difficult to machine materials such as Inconel 718 pose many challenges towards achieving good machinability. Based on literatures, various research work have been conducted on addressing the machinability of Inconel 718. Most of the research work focused on the conventional cutting tool with regular geometry, coated tool materials, and under different cutting conditions. However, one of the main factors identified is chatter vibration which influences the machinability of Inconel 718 are rarely discussed in the literatures. In milling process, the cutting tool geometry is generally complex, especially for the helical end mill. Helical end mill consists of multiple flute and helical geometry that develops dynamic chip load and it is susceptible to chatter vibration. The recently developed cutting tools with advanced features (ie. Variable helix and pitch cutting tool), offer the ability to increase the stability limit by disrupting the regenerative effect. In addition, the variable helix and pitch cutting tool that equipped with corner radius which design to spread the overall thermal load across a larger surface area are able to reduce cutting temperature and increase tool life. However, there has not been much experimental research conducted with the recently developed cutting tool (variable helix and pitch tool) especially machining Inconel 718. Therefore, the investigation of the variable helix and pitch cutting tool is expected to stabilize the vibration (regenerative vibration), thereby improve the machinability of Inconel 718. The research work are expected to provide

the manufacturer with essential understanding in the performance of variable helix and pitch cutting tool while milling Inconel 718.

1.2 Research Question

This research is aimed to improve the machinability of difficult-to-cut materials (Inconel 718) by evaluating the vibration responses incorporated with variable helix and pitch cutting tools.

The specific research questions are as follows:

1. How is the performance of the variable helix and pitch cutting tool in the end milling process of Inconel 718 in term of chatter vibrations and its machinability?
2. What is the best combination of cutting parameters and cutting tool geometrical effects in the machining process of Inconel 718 under a specific test data?

1.3 Scope of the Study and Objective

This research mainly focus on determining the vibration responses and surface roughness of the Inconel 718 in end milling process with variable helix and pitch cutting tool.

The main objective of the research are derived as follows:

Objective 1.	To experimentally study the vibration responses and surface quality by utilising variable helix and pitch cutting tool with/without corner radius.
Objective 2.	To identify the best cutting parameters under a specific test range in order to achieve low vibration response and low surface roughness.
Objective 3.	To evaluate the progression of tool wear with the best combination of cutting parameters.

1.4 Thesis Outline

This thesis consists of five chapters. The first chapter introduced the research topic and also includes the problem statements, research gap, research questions, and the scope and objective.

Chapter two presented a literature review on the machinability of Inconel 718 and the mitigation of chatter vibration strategies. It covered an introduction to the terms machinability and chatter vibration. It also discussed the influencing factors and the assessment of good machinability while machining Inconel 718.

Chapter three provided a detail description of the experimental including workpiece and cutting tool used in this experimental study. Subsequently, it discussed the methodology of measurement on vibration response and surface roughness. Particularly, the chapter explained the Phase I and Phase II of the experiments which had been carried out in this study.

Chapter four presented the experimental results on the end milling process of Inconel 718. This chapter discussed and analysed the vibration responses and surface roughness produced by the variable helix and pitch cutting tool. It also discussed the progression of tool wear and its vibration responses on the consecutive cutting process.

Chapter five concluded the key findings on the performance of the end milling process of Inconel 718 by using variable helix end mill. It also provided the recommendations for future research in this area.

Chapter 2: Literature Review

2.1 Introduction

This chapter presents a literature review on the machinability of Inconel 718, it discusses the influence of cutting parameters, cutting conditions, cutting tool geometry, tool material and coating, and milling mode on the machinability of Inconel 718. In addition, the term chatter vibration are introduce and provided with further insight on the phenomena that could aid in the significance of the research. The chapter also highlights the strategies used in the literature to avoid and reduce chatter vibration. In the end of the chapter, a summary is presented.

2.2 Machinability of Inconel 718

Machinability is defined as the relative ease of a material that can be machined under a given cutting parameters (Groover 2007). Machinability term is also used as an assessment to the machining performance. The key factors that affect machinability are: cutting parameters (cutting speed, feed rate, and depth of cut), cutting conditions (with or without lubrications), cutting temperature, cutting tool material, and geometry. A good machinability indicates high quality of surface finish, low cutting forces, long tool life and less power consumption (Ezugwu et al. 2003).

Inconel 718 is one of the nickel based superalloys which is able to sustain high strength at elevated temperatures, superior resistance to chemical degradation and strong wear resistance under severe temperature and harsh environment (Kuo et al. 2010). It is widely used in gas turbine, aerospace, chemical plants, and other high temperature application industries (Le Coz and Dudzinski 2014). However, it is difficult to be machined (low machinability) due to its superior properties, such as high chemical reactivity (chemical affinity between nickel-based alloys and tool material), low thermal conductivity (poor heat dissipation during machining process), and rapid work hardening (toughness of the material increase at high cutting temperature). As Inconel 718 are widely manufactured for high temperature applications, it is important to ensure good machinability to reduce cost and increase productivity to meet the demand of the industries.

2.2.1 The Influences of Cutting Parameters and Cutting Conditions on the Cutting Force and Surface Integrity

In milling process, the cutting parameters are referring to the cutting speed (m/min), axial depth of cut (mm), radial depth of cut (mm), and feed per tooth (mm/z). On the other hand, the cutting conditions are referring to the usage of lubrication/coolant or under dry condition during the machining process. The selection of cutting parameters and cutting conditions are crucial because they directly influence the cutting force, surface intergrity and tool wear. When machining Inconel 718, the cutting speed region (from low speed, transition speed and high speed) are generally lower as compared to other metals as shown in ***Fig. 2.1*** which is due to the low machinability rating of nickel based superalloys.

Fig. 2.1: Publication has been removed due to copyright restrictions

Many research work has been conducted on the behavior of cutting force in machining of Inconel 718 (Alauddin et al. 1998; Nalbant et al. 2007; Liao et al. 2008; Junxue et al. 2014). According to Alauddin et al. (1996) and Alauddin et al. (1998), the cutting forces decreases with the increase of cutting speed, and the cutting forces increases with the increase of feed rate and depth of cut when machining Inconel 718. Liao et al. (2008) covered a wide range of cutting speed between 22.6m/min to 169.7m/min to observe the variation of cutting force in milling process (end milling and slot milling) of Inconel 718. They stated that the cutting speed ranging from 55 to 135m/min are suitable for end milling process, while 90 to 110m/min are suitable for slot milling process based on the variation of cutting forces. In addition, the authors also highlighted that chip disposal in slot milling are difficult due to the increase of cutting temperatures which causes the chip to weld on the workpiece.

Cai et al. (2014) investigated the effect of cutting parameters on the cutting force and surface integrity in the end milling process of Inconel 718. They discovered that surface topography and roughness are significantly affected by the cutting speed and feed rates, the surface roughness varied from 0.5 to 2.3 µm. The authors also observed that cutting forces increase with the increase of cutting speeds. They concluded that cutting speed of 110m/min and feed rate of 0.1mm/z are optimum

parameters to achieve better surface roughness and topography. Anhai et al. (2011) investigated on the surface roughness and chip morphology in milling process of Inconel 718. The study concluded that surface roughness decreases with the increase of cutting speed from 40 to 100m/min. The study also indicated that feed rate and depth of cut have insignificant influence on surface roughness. The surface roughness obtained was within 0.15 to 0.25µm. In term of chip morphology, the degree of chip serration increased with cutting speed.

Li et al. (2014) studied the effect of tool wear on the surface integrity and its impact to the fatigue life of Inconel 718 in the end milling of Inconel 718 under low cutting speed from 40 to 60m/min. They found that the surface roughness obtained are ranging from 0.25µm to 0.4µm. The authors concluded that the fatigue life of the Inconel 718 was not affected by the flank wear when it is less than 0.2µm. Tian et al. (2013) analysed the cutting force, tool wear progression and tool failure mechanism in high speed milling of Inconel 718 in the range of 600 to 3000m/min. The results showed that cutting forces tend to decrease first and increase with the increase of cutting speeds, the surface roughness obtained varies from 0.4 to 1.8µm. In addition, the authors concluded that notch wear is the dominant wear mechanism in low cutting speed (600 to 1400m/min) while flank wear is the dominant at high cutting speed (1800 to 3000m/min).

Thakur et al. (2009) optimised the cutting speeds and feed rate in order to achieve better surface finish and longer tool life in machining of Inconel 718. In the research work, an extensive analysis of machining characteristic was carried out which involved: (1) measurement of cutting force, cutting temperatures, surface roughness and tool life (2) prediction of specific cutting pressure (3) analysis of chip morphology, acoustic emission and tool wear mechanism. Later, Thakur et al. (2010) utilized coolant/lubrication to enhance the performance of machining process. They optimised the quantity of lubrications and pressure of nozzle to reduce cutting forces, cutting temperatures and longer tool life.

Inconel 718 has low thermal conductivity and therefore, the temperature of the cutting edge is usually very high due to poor heat dissipation during the machining process (Yan et al. 2014). The cutting temperatures during machining process of Inconel 718 under dry cutting condition was investigated by Le Coz and Dudzinski (2014). They found that maximum surface temperature at 0.5mm thickness of the workpiece was 600°C when it is machined under cutting speed of 320m/min. They suggested that 60m/min is the optimum cutting speed to achieve minimum cutting temperature and to prolonged tool life.

Cutting temperature is affected when machining processes are carried out under wet conditions. Devillez et al. (2011) compared the surface integrity and cutting forces when machine Inconel 718 under dry and wet conditions. The results suggested that under wet condition, the optimum cutting speed is 60m/min to achieve good surface integrity

Coolant and lubrication are used to reduce the cutting temperature during machining process. However, the usage of coolant and lubrication causes environmental and health problem (Shashidhara and Jayaram 2010). Therefore, in order to reduce the usage of coolant and lubrication under conventional method, minimum quantity lubrication (MQL) and low quantity lubrication (LQL) were adopted (Zhong et al. 2010). On the other hand, coolant and lubrication can be replaced with bio-based cutting fluids to avoid environmental and health problem (Debnath et al. 2014). Besides that, another environmental friendly method are the application of cryogenic cooling system which uses liquid nitrogen as cooling medium to reduce cutting temperature during machining process (Aramcharoen and Chuan

2014). Most of the methods stated above have been investigated to improve the machinability of Inconel 718.

Zhang et al. (2012) compared dry cutting and minimum quantity cooling lubrications (MQCL) in the milling process of Inconel 718. The results showed that wear mechanism under both cutting conditions are similar, significant flank wear and severe chipping of the cutting edge was observed. However, the tool life obtained under MQCL conditions is 1.57 times higher as compared to dry cutting conditions. In addition, they also observed lower cutting forces produced when machine under MQCL conditions. Aramcharoen and Chuan (2014) investigated the influences of cryogenic cooling, dry, and conventional oil-based coolant on machinability of Inconel 718. The results showed that cryogenic cooling perform better than dry conditions and conventional oil-based coolant which shows a significant reduction in cutting temperatures. The authors also stated that accessibility of cryogenic cooling between tool-chip interfaces provide better cooling effects which improves the tool life and surface finish. On the other hand, Patil et al. (2014) employed compressed cold carbon dioxide as the cooling medium in machining of Inconel 718, they found that compressed cold carbon dioxide caused cold work hardening to the workpiece which increases the cutting forces as compared to dry cutting conditions. Nevertheless, the surface roughness improved when machine under compressed cold carbon dioxide and also shows higher microhardness at surface of the workpiece.

Kumar et al. (2017) optimised the cutting conditions, cutting tool geometry and cutting parameters to achieve good surface roughness. The study reported that there is approximately 12 to 17% improvement of surface roughness with the application of MQL as compared to dry and wet conditions. However, the authors stated that the dominant factors that influences surface roughness is due to the geometry of the cutting tool and not the cutting conditions. Shokrani et al. (2017) combined MQL and cryogenic cooling to improve the machinability of Inconel 718. They concluded that the hybrid machining method improved the tool life by double and also surface roughness by 18% which shows a significant improvement of machinability.

2.2.2 The Influences of Cutting Tool Material, Coating and Geometry on the Tool Wear Mechanism

Short tool life is one of the major problems faced in machining process of Inconel 718. The selection of cutting tool is crucial to avoid premature tool wear and prolong tool life. The cutting tool used in machining of Inconel 718 generally requires the following properties: (1) excellent wear resistance, (2) high strength and toughness at elevated temperatures, (3) good thermal shock properties, (4) high chemical stability at elevated temperatures, and (5) adequate oxidation resistance (Pervaiz et al. 2014).

In general, the tool material used in machining process of Inconel 718 are carbides, ceramics, high speed steel (HSS), cubic boron nitride (CBN), and polycrystalline-diamond (PCD). All of the tools are susceptible to failure mechanism during the machining process, namely, abrasive wear, adhesive wear, diffusion wear, oxidation wear or combinations of above (Zhu et al. 2013). Many research have been conducted by considering different tool materials, geometries and coatings to study the wear mechanism in the machining process of Inconel 718.

Ng et al. (2000) studied the influences of coated carbide tool on tool life. The coating used are Chromium Nitride (CrN), Titanium Aluminium Nitride (TiAlN) and Titanium Aluminium Chromium Nitride (TiAlCrN). They observed that TiAlN coating perform better than CrN coating due to the formal having better oxidation resistance and higher hardness, a similar result also shown by Kim et al. (2000). On the other hand, TiAlCrN coated tool was preferred over TiAlN due to significantly high tool life observed. Chen and Liao (2003) reported that frictional forces was the main factor that caused breakage of tool edge when TiAIN coated carbide tool was adopted in the milling process of Inconel 718. Jawaid et al. (2001) compared the performance of PVD Titanium Nitride (TiN) coated tool and uncoated tool when machining Inconel 718. The authors found that PVD TiN Coated tool perform better at cutting speed of 50m/min and feed rate of 0.08mm/z due to the high wear resistance and low thermal conductivity of the coating.

Li et al. (2006) performed experimental study on end milling process of Inconel 718 with coated carbide insert. The results show rapid propagation of flank wear significantly shorten the tool life which caused high cutting temperatures. Liao

et al. (2008) investigated the milling process of Inconel 718 using K10 carbide tool. The study observed that the high cutting temperatures causes difficulty of chip removal when machine under high cutting speed. The authors recommended the cutting speed from 90m/min to 110m/min can improve tool life in high speed machining. Kuo et al. (2010) developed a tool life equation based on the experimental data when milling Inconel 718 with uncoated carbide tool, TiN coated carbide tool and TiCN coated carbide tool. They concluded that flank wear is dominant at low cutting speeds while crater or notch wear are the main wear mechanism at higher cutting speeds. They also indicated that TiCN coated carbide tool outperform TiN coated and uncoated tool in term of surface integrity as well as tool life.

Bhatt et al. (2010) evaluated the performance of uncoated carbide tool, single layer (TiAlN) PVD coated carbide tool and triple layer (TiCN/Al_2O_3/TiN) CVD coated carbide tool in machining of Inconel 718. The results showed that uncoated tool performed better in low cutting speed (50m/min), single layer coated tool has longer tool life at medium cutting speed (75m/min), and triple layer coated tool exhibits highest resistance at high cutting speed (100m/min). Junxue et al. (2014) investigated the effect of passivated (with light coating) cutting tool on the cutting force and tool life. The passivated cutting tool used was tungsten carbide with the edge radius in the range 0µm to 16µm. The results showed that cutting force with passivated tool was slightly higher due to frictional force induced by the light coating. They concluded that passivated cutting tool with edge radius of 7.9µm prolonged tool life by 80% compared to the cutting tool without passivation.

Costes et al. (2007) studied the effect of Cubic Boron Nitride (CBN) content and grain size in machining of Inconel 718. According to their observations, longer tool life was achieved with CBN content of 45% to 60%. The dominant wear mechanism observed was adhesive and diffusion wear due to the chemical affinity between elements from Inconel 718 and CBN tools. Uhlmann et al. (2009) developed CBN coated cutting tool to machine Inconel 718, it exhibited a hardness twice as high compared to the conventional coatings, and it also possessed higher chemical and oxidation stability. The results showed that tool life of CBN coated cutting tool are able to improve tool life and better surface quality.

Bushlya et al. (2012) employed coated and uncoated Polycrystalline Cubic Boron Nitride (PCBN) tool to investigate the machinability performance in machining of Inconel 718. The finding shows that ability of coating to resist wear faded when cutting speed exceed 300m/min and the tool life was found highly sensitive to the cutting speed; the tool life decreases by 250% when the cutting speed increased from 250m/min to 350m/min. Khan et al. (2012) adopted Taguchi method to evaluate the effect of cutting geometry (round, C-type), tool edge preparation (extra honed, chamfered and honed), lubrication supply pressure (10 and 100 bar), tool coating (uncoated and coated) and cutting parameters on the tool life using PCBN tools. The authors revealed that flank wear was the dominant wear mode and round cutting tool performed significantly better than C-type cutting tools. However, at high cutting speed, the tool life for round and C-type cutting are similar.

Altin et al. (2007) evaluated the tool life and tool wear in machining process of Inconel 718 with Sialon based ceramics and Silicon Carbide whisker reinforced alumina tool. According to the authors, diffusion wears such as notch, adhesion and crater wear were dominant at high cutting speeds. The research found 250m/min as the optimum cutting speed for longer tool life. On the other hand, Zheng et al. (2016) investigated the ultra-high speed milling of Inconel 718 with ceramics tool. Micro cracking, chipping, abrasion and adhesion were observed as the tool wear mechanism in their research.

Akhtar et al. (2016) compared coated carbide and ceramic tool by evaluate the surface integrity of Inconel 718. The research showed that coated carbide tool produced better surface roughness as compared to ceramics tool. Although the productivity of ceramics tool was recorded higher, very high tensile residual stresses and poor surface finish were observed due to the adhered material debris. Xavior et al. (2017) compared the tool life of ceramic, coated carbide, and CBN tools in the machining process of Inconel 718, they concluded that the influencing parameters on tool wear was tool material and followed by cutting speed based on ANOVA. In general, Polycrystalline Diamond (PCD) tool was not recommended in machining process of Inconel 718 due to the chemical reaction of nickel elements with PCD tool (Pervaiz et al. 2014).

The design of cutting tool geometry play an important role in machining process of Inconel 718. The geometrical shape of the cutting edge can be either sharp shape ***Fig. 2.2 (a)*** or honed shape ***Fig. 2.2 (b)***. Research shows that honed shaped cutting tool is able to distribute the thermal load across the corner radius during the cutting process and therefore improves tool life (Endres and Kountanya 2002).

Fig. 2.2: Publication has been removed due to copyright restrictions

Nalbant et al. (2007) compared round and square honed ceramics insert in machining of Inconel 718, the result showed that the minimum cutting forces obtained was 812N when it is machined under cutting speed of 250m/min with square honed insert. Pawade et al. (2008) adopted carbide tool with honed edge to evaluate the surface integrity of Inconel 718, they concluded that the combination of highest cutting speed, lowest feed rate and moderate depth of cut coupled with honed cutting edge can ensure low compressive residual stress in the machined surfaces. Zetek et al. (2014) monitored and analysed the effect of polished tool edge radius in machining process of Inconel 718, they observed that the increase of tool edge radius increases the tool life. Besides that, Yusoff et al. (2010) revealed that cutting edge radius is able to increase process damping performance which results in more stable machining process.

2.2.3 The Influences of Milling Mode in the Machinability of Inconel 718

Milling process consists of up milling and down milling. In up milling mode, the rotation of cutter is opposite to the direction of feed and vice versa for down milling mode. Therefore, for down milling mode, the chip thickness is maximum at the beginning of the cut and minimum during exit of the cut (vice versa for up milling mode). The kinematics of milling process has shown that the milling mode will affect the stress distribution during the material removal process and also the cutting performance (Bouzakis et al. 2008).

In regard to milling of Inconel 718, Alauddin et al. (1995) performed up and down milling process under dry cutting condition to evaluate the tool life. The authors concluded that down milling mode sustain longer tool life compared to up milling mode. The authors also further explained that the rubbing action in the beginning of the cut in up milling mode causes the cutting edge to dull faster than down milling process. Li et al. (2006) also reported that the development of flank wear in up milling mode is more rapid than down milling and therefore, the cutting force experiences gradual increase in each successive cutting pass. Moreover, Hadi et al. (2013) revealed that the tool wear propagation in up milling mode is significantly faster than the down milling mode. In term of chip morphology, up milling mode produces typical saw-tooth shape while down milling produces serrated chip. The discussion above shows that down milling mode is more preferable in term of tool life. However, Zheng et al. (2016) observed that the flank wear development in down milling mode was more severe than up milling mode, even so, the surface roughness produced for down milling mode is lower. They explained that the surface roughness for up milling mode is higher due to the entry of the cutting tool with maximum chip thickness caused high frictional force and damaged to the machined surface. Nevertheless, most of the researchers considered down milling mode when machine Inconel 718 which able to provide good machinability (Cai et al. 2014; Krain et al. 2007; Kasim et al. 2013; Le Coz and Dudzinski 2014).

2.3 Chatter Vibration

Conventional machining process is a dynamic process and it is difficult to control in high precision level especially in the milling process. This is due to the presence of instability in the machining process known as mechanical vibration. In general, there are three types of vibration namely, free vibration, force vibration and self-excited vibration. These vibration arise due to the lack of dynamic stiffness which can be referred to the machine structure, machine-tool, the tool holder, the cutting tool, the workpiece material, or combination of elements. When the mechanical system is displaced from the equilibrium, the systems tend to vibrate freely which known as free vibration. On the other hand, forced vibration occurs when the mechanical systems are triggered by external excitation (spindle head). For free and forced vibration, they can be avoided when the sources of vibration are identified. However, self-excitation vibration is a complex phenomenon and it is difficult to address in machining. Self-excitation vibration occurs in the metal cutting process which is due to the frictional force, wavy surface and the discontinuous cutting process.

Self-excitation vibration is referred as chatter vibration, it can be classified into the primary chatter and secondary chatter (Wiercigroch and Budak 2001). The primary chatter is caused by the frictional force, thermo-mechanical effect or by mode coupling. While, the secondary chatter is caused by regenerative effect. In milling process, the regenerative effect is illustrated in ***Fig. 2.3***. When milling, the cutting tooth enters and exits periodically and creates a wavy surface on each cut. The next cutting tooth attacks on the same wavy surface left by the previous cutting tooth is the source of vibration amplification which is popularly known as regenerative effect. It also creates a dynamic chip thickness that varies depending on the rotational orientation of the cutting tooth. The variation of chip thickness creates a phase difference between the chip thickness and the wavy surface, when the phase difference is maximum, the intensity of the vibration is higher. This phenomenon amplifies the regenerative chatter at a particular frequency which is undesired.

Fig. 2.3: Publication has been removed due to copyright restrictions

Chatter vibration can cause huge impact on machinability because of the negative effects: (1) poor surface quality, (2) excessive noise, (3) fast tool wear, (4) high cutting force, and (5) increased production cost. Therefore, by addressing the chatter vibration, the quality of machinability will be improved. The advancement of science and technology has made the diagnosis of chatter vibration possible, there are multiple methods to monitor the vibrations in the machining process. The commonly used methods to diagnosis the chatter vibration are measuring cutting force, acceleration, and acoustic emission (Quintana and Ciurana 2011). With the appropriate measurement of chatter vibration using the above measurements, stability lobe diagram can be developed in order to predict the stable region and unstable region as a function of cutting parameters. Besides, the behaviour of the system in terms of cutting dynamics can be modified in order to mitigate chatter vibration.

2.3.1 Stability Lobe Diagram

The stable region (i.e no chatter) and the unstable region (i.e chatter) are identified by using stability lobe diagram in term of axial depth of cut as a function of the spindle speed as shown in ***Fig. 2.4***. This diagram serves as a guideline to seek the combination of cutting parameters within the stable region (below the lobe) depending on the end user requirement. At low cutting speed, the stability of the machining process is higher due to process damping effect. While at higher cutting speed, the stabilization effect of damping process reduces and therefore the machining process is more prone to regenerative chatter.

Fig. 2.4: Publication has been removed due to copyright restrictions

The initial development of stability lobe diagram begin in 1950s, the mathematical models in the form of delay differential equations (DDEs) was presented by Tobias and Fishwick (1958) and Tlusty and Polacek (1963). Following that, Merrit (1965) added a feedback system into the model that described the interaction between structural dynamics and the cutting process in a closed-loop system. Minis et al. (1990) proposed a general mathematical model that represents the milling dynamics to predict the maximum depth of cut under stable conditions. An analytical method to predict the stability in milling process was presented by Altintaş and Budak (1995) which uses zeroth order approximation, a reasonable accuracy prediction of stability lobe was achieved. Later, Altintas (2001) improved the analytical method from two dimensional model to three dimensional model. Insperger and Stépán (2004) attempted to predict the stability lobe diagram by adopting semi-discretization method which convert the delay differential equations to ordinary differential equations. Gradišek et al. (2005) compared the stability boundaries predicted by semi-discretization method and zeroth order approximation, the results showed that both methods obtain similar prediction. Henninger and Eberhard (2008) improved the computational efficiency of semi-discretization method by reducing the computational time and increasing the accuracy of the results. Altintas et al. (2008) presented a new dynamic cutting force model which includes the damping coefficient for better prediction on the stability at low cutting speed. Budak and Tunc (2010) developed an process damping model where damping coefficient can be identified from chatter tests, the effect of parameters (clearance

angle, edge radius, chatter frequency, chip thickness, helix angle and number of cutting edge) can be predicted using the process damping model. Gurdal et al. (2016) focused on development of process damping model for flat end milling, the effect of tool vibration and tool geometry was expressed as a function of vibration wavelength. However, the authors stated that more experimental data are required to test for the reliability of the models.

Besides modelling approach, Quintana et al. (2008) presented an experimental method for stability lobe diagram identification in the milling process. The authors used the advantages of incline surface that provides a gradual increase in depth of cut to estimate the stability lobe. Later on, Quintana et al. (2009) introduced a sound mapping technique for stability lobe diagram identification in milling process. However, the method requires large amount of time and experiments in order to identify the stability lobe diagram. Recently, Friedrich et al. (2017) adopted continuous learning algorithms to estimate stability lobe diagram in milling process based on experimental data, the method consists of two approach which are support learning machine and neural network. They concluded that the learning algorithms can reproduce the analytical results very well. Friedrich et al. (2018) developed an online learning algorithms which calculate the stability lobe diagram during the milling process, the algorithms achieved high accuracy on identifying the stability of the milling process.

2.3.2 Strategies for Chatter Vibration Mitigation

Apart from identifying the stability lobe diagram to ensure stable machining process, the other strategies such as in-process monitoring to avoid chatter vibration, changing the behaviour of the system (active damping technique, spindle speed tuning, increase stiffness) or improving the design of the machine tool (passive damping technique, special tool for chatter suppression) are widely studied. Rahman and Ito (1986) proposed an online chatter detection by measuring horizontal deflection of the workpiece, chatter vibration can be identified when the horizontal deflection is at maximum. Liao and Young (1996) presented an online spindle speed regulation strategy to control chatter vibration, the method is to regulate the spindle speed based on the cutting force signal during the machining process. Tsai et al. (2010) utilized a real-time feedback system by recording the acoustic cutting signal, when the magnitude of the acoustic signal increases, an algorithm will compute the new spindle speed to avoid excessive chatter vibration. Eppel et al. (2010) attempted to measure and record the vibration in milling process by utilizing optical device, the optical device able to differentiate between stable milling and unstable milling.

Active damping technique is a type of feedback system to identify and control chatter vibration, the system is based on the measurement and analysis of vibration response which carried out simultaneously during the machining process. Depending on the analysis of vibration response, a controlled force signal is then introduced to control the chatter vibration instantaneously by means of an actuator. Chung et al. (1997) evaluated the feasibility on the implementation of active damping system, the system uses electromagnetic actuator to reduce the vibration of a high speed machine tool based on the feedback on acceleration signal. The authors concluded that the system are able to improve the stability of the machining process significantly. Dohner et al. (2004) documented the experimental validation of an active control approach for chatter reduction in the milling process, the active control approach has successfully increased the stability of the process at higher material removal rate. Yao et al. (2010) employed a chatter recognition system based on wavelet transform and support vector machine, the system is able to detect chatter vibration at its infancy stage which allow implementation of chatter suppression method to take place.

Munoa et al. (2013) developed a biaxial active actuator damping system to control the chatter vibration in the milling process, they reported that the productivity of the machining process has been increased by double with the integrated actuator to the system. Sallese et al. (2017) focused on the active fixtures design which detect chatter vibration and counter it with external excitation in real time, the effectiveness of the active fixture system showed convincing results in mitigating chatter vibrations.

In the milling process of thin-walled structures, chatter vibration are difficult to control due to high flexibility of the workpiece, Fei et al. (2017) utilised moving damper to control the chatter vibration during the process. The moving damper supports the workpiece at its back side which strengthen the stiffness of the workpiece, they concluded that the moving damper are able to increase the stability of the process dramatically. Ma et al. (2017) developed an active sliding mode controller which only require the measurement of displacement on the cutting tool, they indicated that the controller is able to rectify the machining process to chatter free condition successfully.

Besides active damping technique, variation of spindle speed during the machining process is able to disrupt the regenerative chatter by interrupting the constant chip modulation that lead to vibrations build up (Takemura et al. 1975). Al-Regib et al. (2003) adopted sinusoidal spindle speed variation method to reduce chatter vibration, the spindle speed increase and decrease reflected to the sinusoidal wave behaviour, they concluded that the method is able to avoid chatter vibration when the specific chatter frequency are known. Otto et al. (2011) studied the chatter stability of variation spindle speed in turning and milling process, they focused on determining the minimum and maximum of spindle speed range in order to stabilize the machining process. The method is able to optimize the variation of spindle speed to achieve high stability in machining process. Seguy et al. (2010) investigated the adaptability of variation spindle speed in high speed machining, they computed the optimal amplitudes and frequencies of the speed modulation with semi-discretization method. The results showed that the method can effectively suppress the chatter vibration. However, in practice, the application of variation spindle speed is not an easy task. In some cases, selecting the cutting parameters within the working limit of the cutting tool will not guarantee a stable machining process and also variation in spindle speed may cause inconsistency of surface finish.

The concept of variation of spindle speed also can be adapted to special geometries for helical tool, they possess features such as variable helix tool, variable pitch tool, variable helix and pitch tool, serrated edge tool and honed edge tool which are able to mitigate chatter vibration in milling process. These features induces irregular intervals between cutting edges in a complete cutting cycle, and therefore the regenerative chatter can be disrupted. ***Fig. 2.5*** shows a schematic identifying the variable helix angle (β_1 and β_2) and the variable pitch angle (φ_1, φ_2, φ_3 and φ_4) in a cutting tool. A conventional tool would have only one helix angle and also equal pitch angle distributed between the cutting flutes. The initial development of variable pitch tool was proposed by Hahn (1951). Slavicek (1965) analysed the effect of variable pitch tool in milling process and revealed that the maximum depth of cut can be doubled as compared to the conventional cutters. Opitz (1966) carried out an experimental study by adopting variable pitch tool, a similar finding was observed where the stability of the machining process had improved. Altıntaş et al. (1999) presented an analytical model for stability prediction on milling process with variable pitch cutting tool. The proposed method is used to predict the stability lobe diagram on a specific setup, they concluded that variable pitch cutting tool design is suitable for eliminating the regenerative vibrations.

Fig. 2.5: Publication has been removed due to copyright restrictions

Huang et al. (2012) analysed the performance of variable pitch tool in milling process of titanium alloy, they concluded that during unstable milling, the milling forces increased by 67% and surface roughness increased by 40% compared with stable milling process. On the other hand, due to lack of attention of variable helix tool, Turner et al. (2007) explored the potential of variable pitch tool, they compared the chatter stability performance of the variable pitch, variable helix and standard tool. The results showed that variable pitch and variable helix tool perform better as compared to standard tool in term machining stability. However, they did not study whether variable helix tool or variable pitch tool are able to perform better. Sims et al. (2008) proposed three methods to predict the stability of variable helix tool and variable pitch tool: (1) using semi-discretisation to predict the stability of variable pitch or variable helix tool at low or high radial immersion. (2) using time-average semi discretisation method to predict the stability on variable helix tool at high radial

immersion. (3) using temporal-finite element method to predict the stability on variable pitch tools with a constant helix angle.

Yusoff and Sims (2011) optimised the geometry of conventional tool, variable pitch with uniform helix tool, variable helix with uniform pitch and combination of variable helix and pitch tool. They developed the optimisation procedure to improve chatter stability based on variation of custom geometry. They reported fivefold of improvement in chatter stability when variable helix tool was employed compared to conventional tool. Huang et al. (2014) compared the performance between uniform helix tool and variable helix tool in milling process of thin-wall titanium alloy, the experimental data showed that the vibration responses of variable helix tool is significantly lower as compared to uniform helix tool. Wang et al. (2015) analysed the machining stability of conventional tool and variable helix and pitch cutting tool, they concluded that variable helix and pitch tool are an effective way for chatter mitigation.

In addition, tool edge geometry also play an important role in mitigation of chatter vibration specifically at process damping region. Research shows that cutting edge with radius or honed edge can cause more process damping behaviour which increases the stability at low cutting speed (Tunç and Budak 2012). Yusoff et al. (2010) investigated the role of tool geometry at low cutting speed, they revealed that variable helix/pitch tool play most significant role in increasing performance at process damping region when compared to edge radius, rake angle, relief angle and feed rate. However, the increase of cutting edge radius also increase the process damping ability to a significant extent. Therefore, the authors commented that cutting edge radius may improve the machinability of difficult-to-cut material.

2.4 Summary

Based on the literatures discussed above, the machinability aspect of Inconel 718 has been investigated in multiple areas such as, cutting parameters, cutting conditions, tool wear, tool life, tool material, tool coating, tool geometry, cutting force, surface integrity, cutting temperatures and chips morphology. However, there are limited number of studies that considers the chatter vibration aspect in milling process of Inconel 718. Chatter vibration can be monitored, controlled, avoided and mitigated in different ways such as online chatter monitoring, construction of stability lobe diagram, and application of active damping device as discussed above. Among the discussed methods, the variable helix and pitch angle cutting tool may have the potential to increase the stability in machining process of Inconel 718 which is rarely discussed in the literatures.

Based on the review above, it provides the necessary background theories to aid in the understanding and comprehending the problem statement of the current research which may lead to develop the hypothesis towards utilizing variable helix and pitch cutting tool for improvement of the machinability of Inconel 718 in the milling process.

Chapter 3: Experimental methods and materials

This chapter provides a detail description of the experimental workpiece and cutting tool used to perform the experiments. It also covers the methodology of measurement on vibration response and surface roughness. In this study, two phases of experiment were carried out, the phase I of the experiment to achieve objective 1 and 2, while the phase II of the experiment to achieve objective 3. The detailed of the experimental procedure was discussed and a summary is presented in the end of the chapter.

3.1 Inconel 718

Inconel 718 is one of Nickel based superalloys which is extensively used in various high temperature applications such as gas turbine blade, aerospace components, and chemical plant reactor. Inconel 718 has a number of unique properties which make it an excellent choice for the applications above, it can maintain high strength at elevated temperatures, excellent chemical wear resistance, exceptional high corrosion resistance and high strength to weight ratio. However, it causes machining problems such as high tendency of work hardening, high cutting temperatures, short tool life and ultimately low productivity. Therefore, Inconel 718 is a difficult-to-cut material. The current research investigated the machinability of Inconel 718 in terms of vibration responses, surface roughness as well as tool wear progression.

In this study, Inconel 718 block as shown in ***Fig. 3.1*** was used. The dimension of the workpiece is 240 length ×104 width ×18 height (mm). The material chemical composition and mechanical properties are listed in ***Table 3.1*** and ***Table 3.2***.

Fig. 3.1: Nickel-based superalloy Inconel 718

Table 3.1: Chemical composition of Inconel 718 (Fan et al. 2013)

Material	Chemical composition (W_t) %									
	Ni	Cr	Nb	Mo	Ti	C	Si	Mn	B	Fe
Inconel 718	51.75	17	5.15	2.93	1.07	0.042	0.21	0.03	0.006	Last

Table 3.2: Mechanical properties of Inconel 718 (Ma et al. 2014)

Material	Tensile strength	Yield Strength	Elongation	Hardness
Inconel 718	1,447 MPa	1,207 MPa	22%	42 HRC

3.2 Cutting Tool and Tool Holder

In the milling process of Inconel 718, the selection of cutting tool material and geometry play an important role as it affects the productivity, surface roughness, tool life and manufacturing cost. Therefore, Supernova helical tool (S09 and S10) was chosen and purchased from AMAYA Company. They are made of solid carbide with submicrograin size of 0.2 µm, 12% of cobalt content with four flutes and diameters of 10mm. The small submicrograin size and cobalt content are able to enhance the heat resistance of the tool which is important in machining difficult-to-cut material.

Furthermore, the Supernova milling cutter are PVD coated with better resistance to wear off as well as better heat stability. However, the tool manufacturer did not release the actual contain of the coating due to it is labelled as private and confidential. In addition, S09 and S10 milling cutters have the unique features of

variable helix angle of 35° and 38° and variable pitch angle of 87º, 89º, 91º, and 93º distributed among the four flutes. The variable helix and pitch angle are expected to mitigate chatter vibration during the milling process. ***Fig. 3.2*** shows the dimension labelling of S09 and S10 milling cutters with the description of symbol. Based on the figures, S09 and S10 are the same type of milling cutters in terms of material and features except S10 is equipped with corner radius. The corner radius can be visualized in ***Fig. 3.3***, S09 is labelled as sharp corner, S10 is labelled as radius corner with 0.5mm and 1.0mm radius. All the cutting tools were purchased in a single order to prevent any inconsistency of the cutting tools. In addition, the cutting tools were pre-checked under microscope to prevent any defect before the experiments.

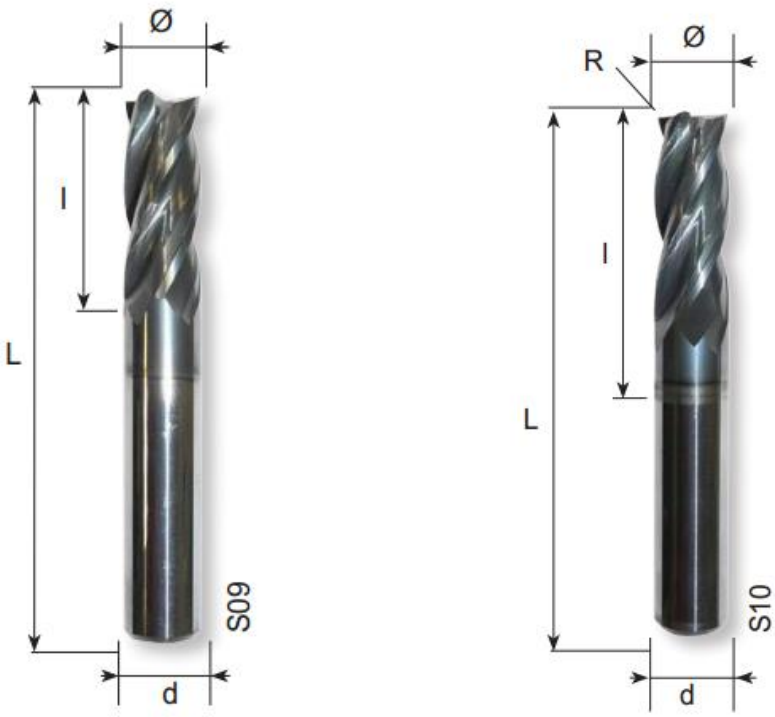

(a) (b)

Fig. 3.2: (a) S09 milling cutter (b) S10 milling cutter

Symbol	Description	Value
Ø	Tool Tip Diameter (mm)	10
L	Total Tool Length (mm)	72
l	Machining Length (mm)	22
d	Tool Diameter (mm)	10
R	Corner Radius (mm)	0, 0.5, 1.0

(a) (b) (c)

Fig. 3.3: (a) Sharp corner (b) corner radius of 0.5mm (c) corner radius of 1.0mm

In order to ensure consistent clamping force on the cutting tool, a new C-type precision power milling (***Fig. 3.4***) chucks made by Acrow Machinery, one of the leading manufacturers specialized in CNC tooling system. The C-type precision power milling chucks is designed to perform heavy and precision milling process, the tool holder able to apply maximum clamping force to the end mill cutters during the milling process to avoid run-out. The dimensions and their numerical values are shown in ***Fig. 3.5*** and ***Table 3.3*** respectively.

Fig. 3.4: C-Type Precision Power Milling Chucks

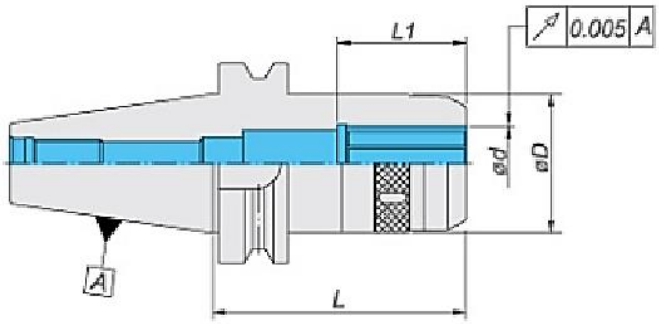

Fig. 3.5: Schematic view of C-type precision power milling chucks

Table 3.3: Dimension value of C-Type Precision power milling chucks

Part. No	Ød (mm)	ØD (mm)	L (mm)	L1 (mm)
BT 40-C20 -090	20	57	90	60

3.3 Vibration Responses Measurement

In the current study, the chatter vibration of the milling process was measured by using piezoelectric accelerometer. It is a sensor that measures the vibration by recording the acceleration on the vibrating surface. The tri-axial accelerometer was adhesively mounted on top of the workpiece to measure the vibration intensity, similar method has been adapted in the literature (Zhong et al. 2010). The overall size of the accelerometer (***Fig. 3.6***) is around 6.35mm^3 and it is very light (the value around 1 gram). Since the accelerometers is significantly lighter compared to the workpiece, the vibration responses will not be affected by the accelerometers. ***Table 3.4*** shows the value of sensitivity at x-axis, y-axis, and z-axis. The sampling rate of the accelerometer was deduced at 5000Hz.

Fig. 3.6: Triaxial ICP Accelerometer

Table 3.4: Sensitivity value for different axis of the accelerometer

Axis	Sensitivity (mV/g)
X-axis	4.84
Y-axis	4.95
Z-axis	5.10

In this experimentation, the accelerometer was mounted on top of the workpiece. The accelerometer was then connected to the data acquisition board to convert the signal from analog to digital and amplify the signal before the signal are logged by data logging system. The setup is illustrated in ***Fig. 3.7*** and ***Fig. 3.8*** . The signal recoreded from the sensor will then logged by the software known as Signal Express.

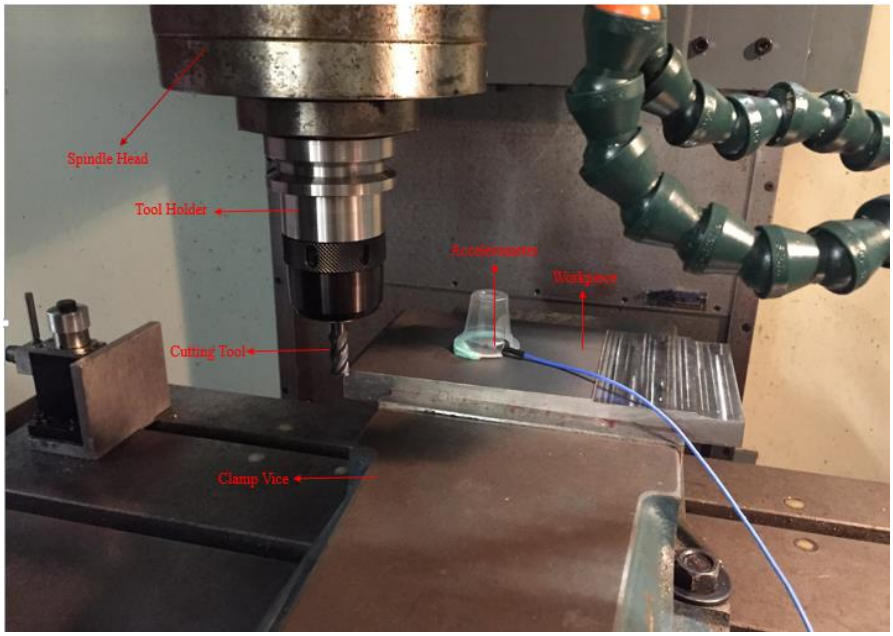

Fig. 3.7: Accelerometer setup

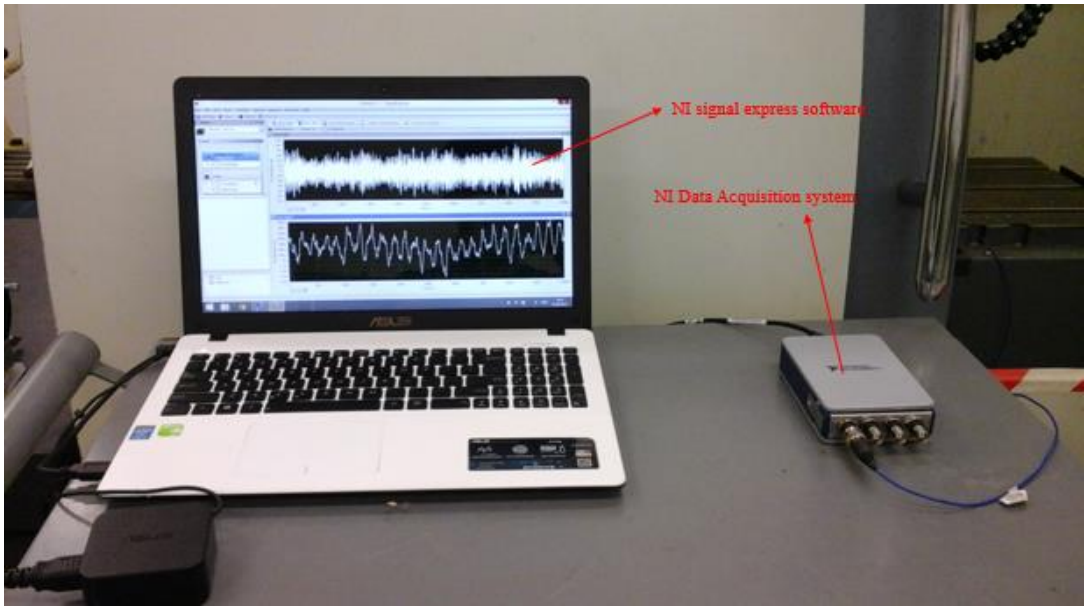

Fig. 3.8: Data acquisition board and the data logging system setup

In order to assure the comparability among the tests, the vibration responses were sampled at same position at which the accelerometer was approximately in the middle of every cutting pass and 50mm away from the direction of feed as illustrated in ***Fig. 3.9.*** The direction of feed is the y-axis, x-axis is perpendicular to the direction of feed, while z-axis is parallel to the cutting tool as shown in the figure.

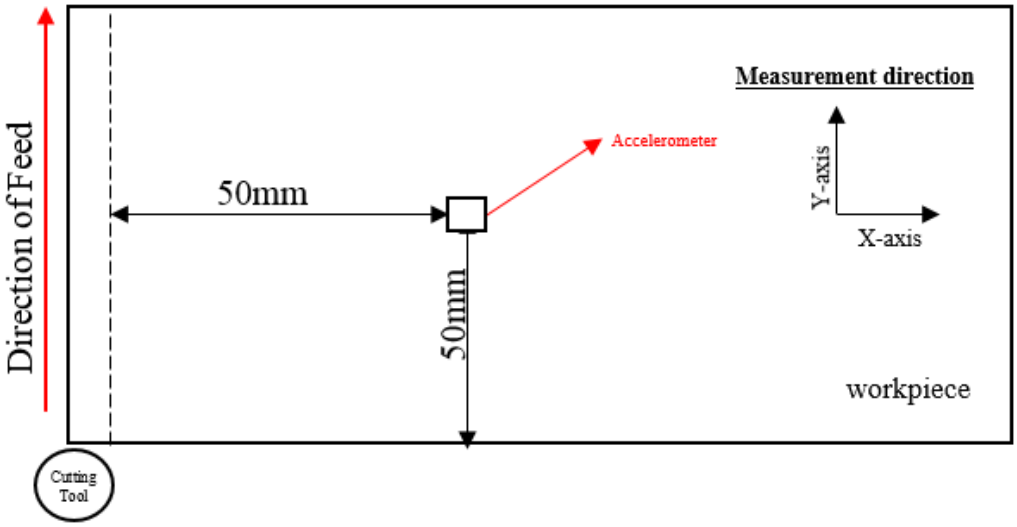

Fig. 3.9: Location of the accelerometer

3.4 Surface Roughness Measurement

The quality of machined surface is described by surface roughness which is quantified by the deviation in the direction of the normal vector of a real surface from its ideal form and denoted as R_a with the unit of micrometres (μm). Surface roughness is affected by the cutting parameters, cutting environment as well as the development of tool wear. Surface roughness is also one of the main indicators of machinability, the lower the value of surface roughness indicate better machinability.

SJ-301 portable surface roughness tester by Mitutoyo is used to measure the surface roughness of the machined surface. The device consists of display unit, drive unit and the detector as shown in ***Fig. 3.10***. The measurement result will be displayed from the display unit, the detector will perform the measurement with the assistance of the drive unit. The device is conforming to various standards such as JIS, ISO, DIN and ANSI standards.

Fig. 3.10: Mitutoyo SJ-301 portable surface roughness tester

On each cutting pass, the surface roughness will be measured on three locations as shown in ***Fig. 3.11***. The location is described as the beginning of the cutting pass, middle of the cutting pass and end of the cutting pass. The mean value of the three locations will be recorded in the end of the milling process.

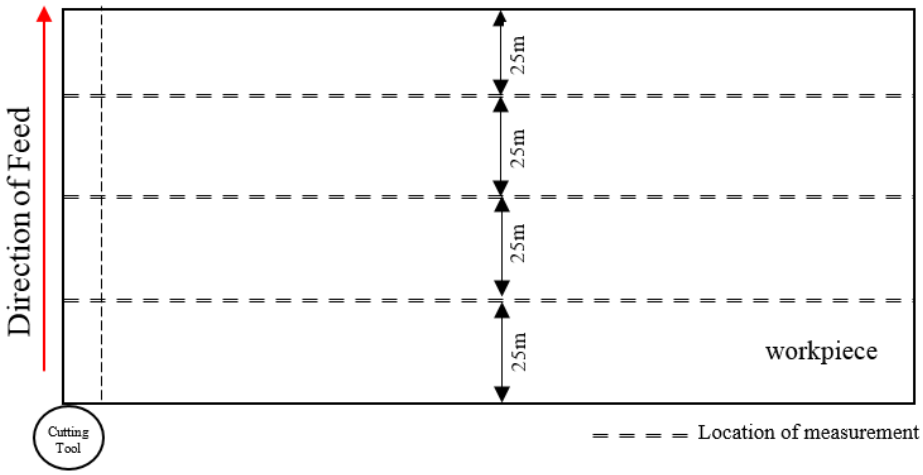

Fig. 3.11: Location of the surface roughness measurement

3.5 Tool Wear Observation

In machining process, the development of tool wear can be monitored by qualitatively using optical microscope. Leica EZ4E optical microscope was employed to observe the development of the tool wear. The optical microscope has the ability to observe three dimensional sample which provide sufficient space for large sample which is the variable helix and pitch cutting tool. The optical microscope offers up to 500 times magnification. In addition, the build in camera of the microscope is able to capture image in high definition, therefore, comparison of tool wear are possible.

3.6 Experimental Procedure

The experimentation were carried out in two phases as illustrated in ***Fig. 3.12***. The Phase I of the experiment investigated the performance of the variable helix and pitch cutting tool with sharp corner and radius corner. The vibration responses and surface roughness were recorded. Based on the experimental results, the best combination of cutting parameters were identified. Phase I of the experiments are designed to fulfil the objectives 1 and 2 by studying the behaviour of vibration responses and surface quality.

The phase II of the experimentation was carried out with the best combination of cutting parameters (obtained from phase I) to evaluate the progression of tool wear and vibration responses on selective tools such as sharp corner cutting tool, 0.5mm corner radius cutting tool and 1.0mm corner radius cutting tool. Phase II of the experimentation was employed to achieve the objective 3.

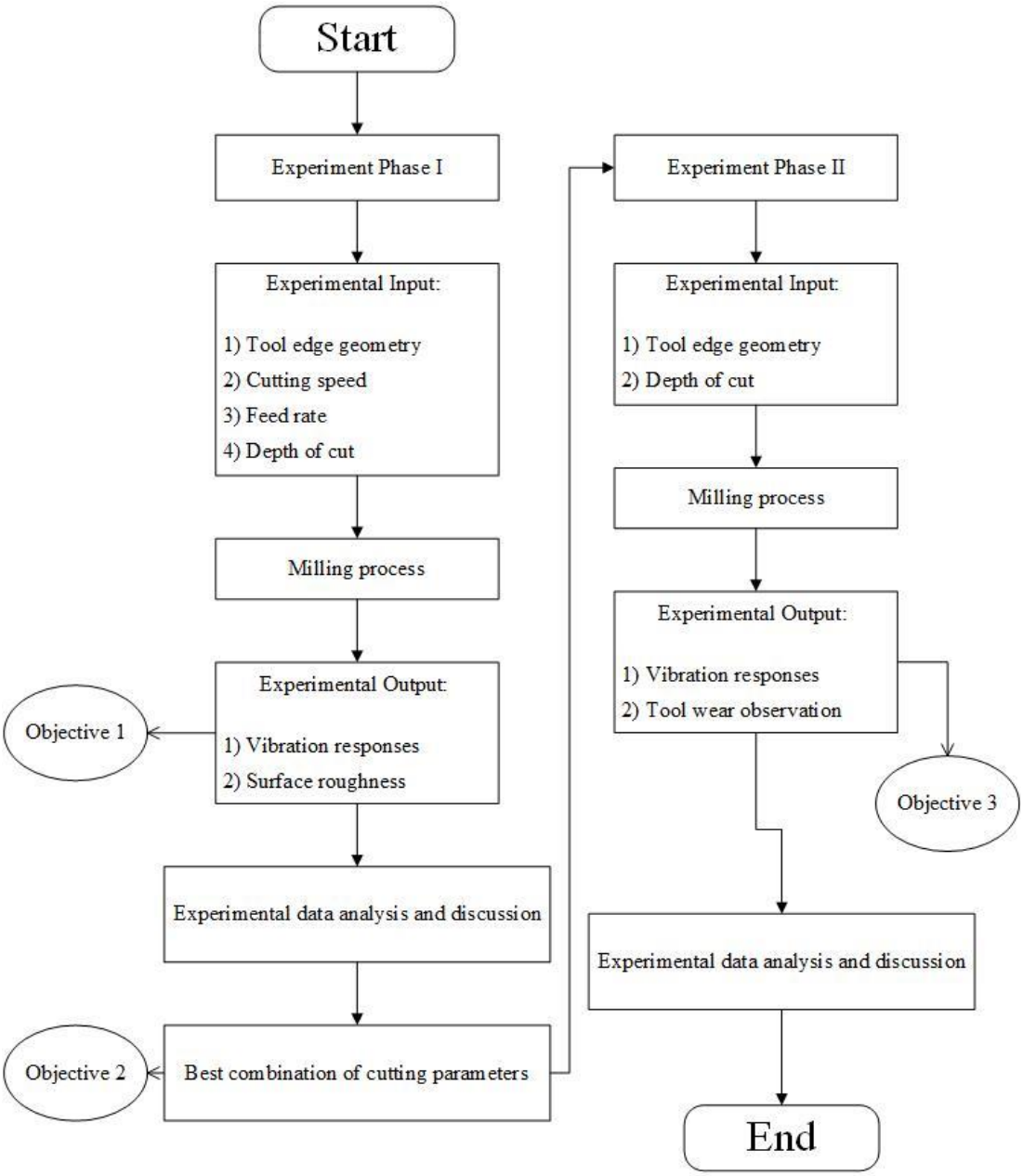

Fig. 3.12 Experimental procedure flow chart

3.6.1 Modal analysis

Before the experiments, the frequency response function (FRF) of the machine-tool was determined during the preliminary test, the purpose of finding the FRF of the machine-tool system is to ensure that the operating frequency will not trigger the resonance point of the system. The standardize procedure in obtaining the FRF of the system is followed based on the reference of Yusoff et al. (2010).

The impact test was carried out using a PCB-352C23 medium size steel-tip impact hammer and also PCB-352C03 ceramic shear ICP accelerometer. Both of the sensor data were collected by NI-USB 9234 4-channel data acquisition module. The result of the FRF is shown in ***Fig. 3.13***.The first and second mode of the system are 860 Hz and 1280 Hz respectively. Since the maximum operating frequency for the current experiment is around 233.4 Hz. Therefore, it should not trigger the resonance point of the machine-tool system.

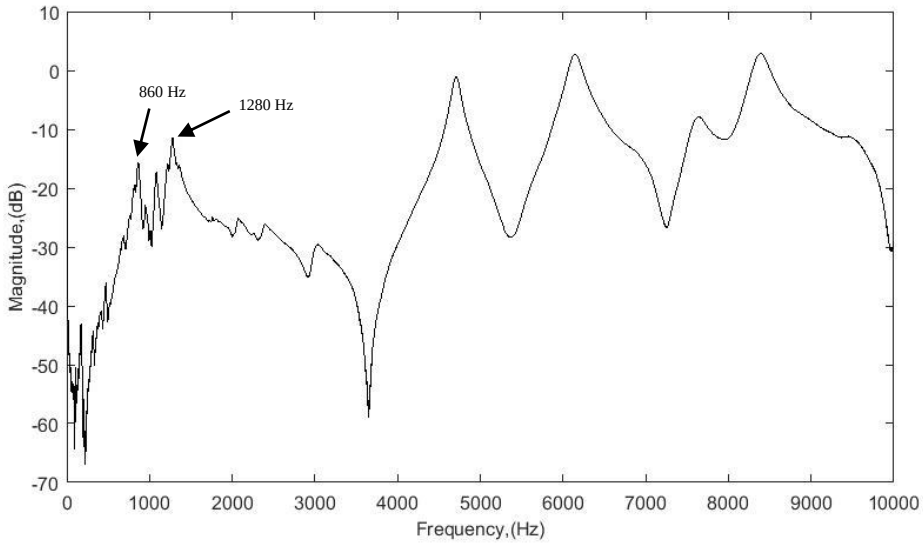

Fig. 3.13: FRF of the machine tool

3.6.2 Experiments Test and Parameters

The experimental tests were carried out on Leadwell V-30 vertical CNC machine as shown in ***Fig. 3.14***. The spindle head of the machine is capable of rotating up to 8000 revolutions per minute. However, it is wise to only use up 80% of the maximum capacity to avoid damage to the spindle head bearing and as well as the motor.

Fig. 3.14: Leadwell V-30 vertical CNC machine

In the phase I of the experimentation, four controlled inputs: cutting speed, feed rate, depth of cut and tool corner geometry were selected. These input can be manipulated to obtain the output in the form of vibration responses and surface roughness which were recorded in the experimental tests. ***Table 3.5*** summarise the parameters in the experiments. There are 5 levels of cutting speed, 3 levels of feed rate, 3 types of corner radius and under finishing conditions (low depth of cut). The two level of depth of cut was chosen to observe the performance of the cutting tool when milling Inconel 718 under finishing conditions. Each combination of parameters (full factorial) were carried out with new cutting tool to avoid the influences of tool wear on the vibrations response and surface roughness. All the experimental tests were carried out under dry cutting condition (without coolant/lubrication) in down milling mode.

The phase II of the experimentation was carried out with selected cutting parameters, a manipulated inputs: tool corner geometry was investigated to observe the behaviour of vibration responses and tool wear progression in consecutive cutting process. A total of 50 consecutive cutting passes were carried out. The vibration responses and tool wear were measured at five regular intervals with an increment of 10 cutting passes.

Table 3.5: Parameters in the Phase I of the experimentation

Type of parameters	Item	Value
Investigated parameter	Cutting speed, *V* (m/min)	30, 50, 70, 90, 110
Investigated parameter	Feed rate, *f* (mm/z)	0.02, 0.04, 0.06
Investigated parameter	Axial depth of cut, DoC_a (mm)	0.1, 0.3
Investigated parameter	Corner radius, R (mm)	0*, 0.5, 1.0
Constant parameter	Machining conditions	Dry
Constant parameter	Immersion rate, DoC_R (%),	30
Responsive parameter	Vibration responses	-
Responsive parameter	Surface roughness, R (µm)	-
Responsive parameter	Tool wear progression	-

*sharp corner

3.6.3 Experimental Analysis

The post processing of the vibration response involves time domain analysis and frequency domain analysis. In time domain analysis, the commonly used method is to find the root mean square (RMS) of the signal. After the signal was logged by the Signal Express software. The signal was exported to Matlab for further processing. The static component of the raw acceleration signal was filtered by Butterworth bandpass filter. After the static component of the signal was filtered, the calculation of RMS values was computed with the filtered signal by using ***Equation 3.1***. The computed RMS acceleration value represents the chatter vibration intensity which were presented in graphical method for discussion.

$$X_{rms} = \sqrt{\frac{1}{N}\sum_{n=1}^{N} |X|_n^{\,2}} \qquad \textit{Equation 3.1}$$

On the other hand, Fast Fourier Transform known as FFT are widely used in transforming time domain signal to frequency domain signal. The filtered time-domain

signal was converted to frequency domain by using ***Equation 3.2***. In frequency domain, the magnitude of the FFT represents the vibration magnitude at a particular frequency. In milling process, the magnitude of the spectrum should appear at its tooth pass frequency and the harmonics. The tooth pass frequency is multiplication of the number of tooth (Z) and the spindle frequency as shown in ***Equation 3.3***. The spindle frequency can be computed by dividing spindle speed (N) over 60 as shown in ***Equation 3.4***.

$$Y(k)=\sum_{j=1}^{n} X(j)e^{(\frac{-2\pi i}{n})(j-1)(k-1)} \qquad \textbf{\textit{Equation 3.2}}$$

$$\text{Tooth pass frequecy (Hz)}=Z\times\text{Spindle frequency} \qquad \textbf{\textit{Equation 3.3}}$$

$$\text{Spindle frequency (Hz)}=\frac{N}{60} \qquad \textbf{\textit{Equation 3.4}}$$

3.7 Summary

As a summary, the current study used Inconel 718 as the experimental workpiece, there are three types of end mill cutters used: (1) S09 Variable helix and pitch cutting tool with sharp corner, (2) S10 variable helix and pitch cutting tool with corner radius of 0.5mm, and (3) S10 variable helix and pitch cutting tool with corner radius of 1.0mm. The vibration responses was measured by using tri-axial piezoelectric accelerometer. The surface roughness of the machined surface was measured by surface roughness tester. The tool wear were observed using optical microscope. The milling process of Inconel 718 was carried out on vertical CNC centre.

There are two phases of experiment carried out in this study, the Phase I of the experiments was carried out to determine the vibration response and surface roughness. Based on the experimental results, an optimal cutting parameters was recommended. Phase I of the experiment was design to achieve objective 1 and 2.

The Phase II of the experimental study was to determine the tool wear progression and vibration response under consecutive cutting pass. The tool wear progression and vibration responses when machine with sharp corner tool and corner radius corner tool was compared under selected cutting parameters.

Chapter 4: Results and Discussion

The aim of the chapter is to examine the performance of the end milling process of Inconel 718 by using variable helix and pitch cutting tools with different corner radii. For the ease of discussion, the cutting tool with sharp corner is denoted with cutting tool A, cutting tool with corner radius of 0.5mm is denoted as cutting tool B, and cutting tool with corner radius of 1.0mm is denoted as cutting tool C. This chapter discusses the vibration responses and surface roughness generated by the milling process of Inconel 718. The vibration responses are analysed in time-domain and frequency domain. In the Phase I of the experiments, the investigated parameters are cutting speed, feed rate, tool corner geometry of the cutting tools and under different finishing conditions (low depth of cut). The vibration responses of three of the cutting tools are compared and evaluated. The optimum combination of cutting parameters are recommended. In the Phase II of the experimental study, the wear progression for all of the cutting tools were observed.

4.1 Vibration Responses for Sharp Corner and Radius Corner

The vibration responses for cutting tool A, B, and C under cutting speed of 30m/min, axial depth of cut of 0.1mm and feed rate of 0.02mm/z are shown in ***Fig. 4.2*** (x-axis direction) and ***Fig. 4.3*** (y-axis direction). The x-axis direction represent the cutting direction while the y-axis direction represent the feed direction which are illustrated in ***Fig. 4.2***. In the current study, the vibration on z-axis was not discussed, it is because the cutting direction and feed direction are the dominant forces in the milling process (Liao et al. 2008; Ítalo Sette Antonialli et al. 2010; Wang and Liu 2016).

Based on the observation, cutting tool A generates higher peak to peak value (0.30g) as compared to cutting B (0.20g) and cutting tool C (0.15g) in x-axis direction. While in y-axis direction, the peak to peak value are estimated at around (0.19g) for cutting tool A, (0.16g) for cutting tool B and (0.14g) for cutting tool C. In overall, cutting tool A shows high peak to peak value in x and y direction under same combination of cutting parameters.

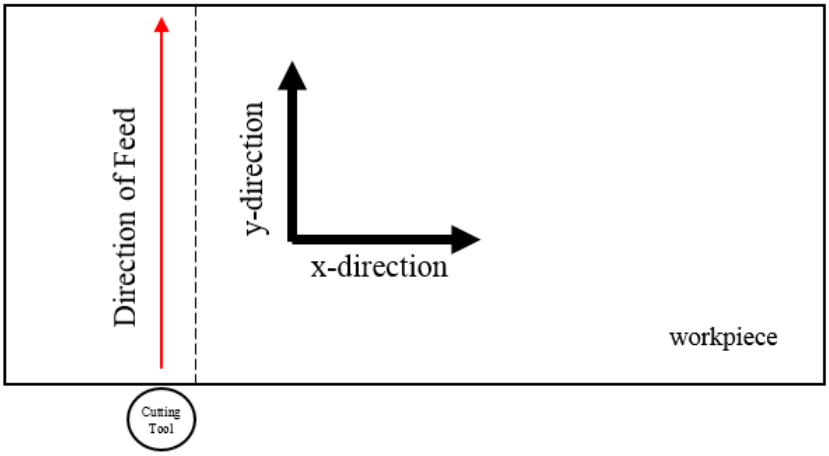

Fig. 4.1: Indication of x-axis and y-axis direction

The high peak to peak value observed in cutting tool A shows that the sharp corner tool affect the vibration responses in the milling process of Inconel 718. This generally due to the sharp corner has very small contact area between the tool and the workpiece. This small area generates higher forces during the cutting process (Denkena and Biermann 2014). Following the Newton's Second Law of Motion, the increase in force will subsequently increases the vibrations responses as evident by the equation: $m\ddot{x}+c\dot{x}+kx=F$. In addition, the increase in forces will eventually increases the pressure due to high forces over the small contact area between the cutting tool corner and the workpiece. Based on the vibration responses in x-axis and y-axis direction, a general observation is that smaller corner radius will exhibits higher cutting force on the tool.

In order to further evaluate the vibration responses under different cutting parameters as well as the performance of different cutting tool, the root mean square (RMS) value of the vibration responses will be evaluated to show the vibration responses during the milling process. In time domain signal analysis, RMS value is often regarded as a meaningful parameter in quantifying the responses, it is a method that have used by many authors in the research. (Zhong et al. 2010; Bonifacio and Diniz 1994; Lauro et al. 2014).

(a)

(b)

(c)

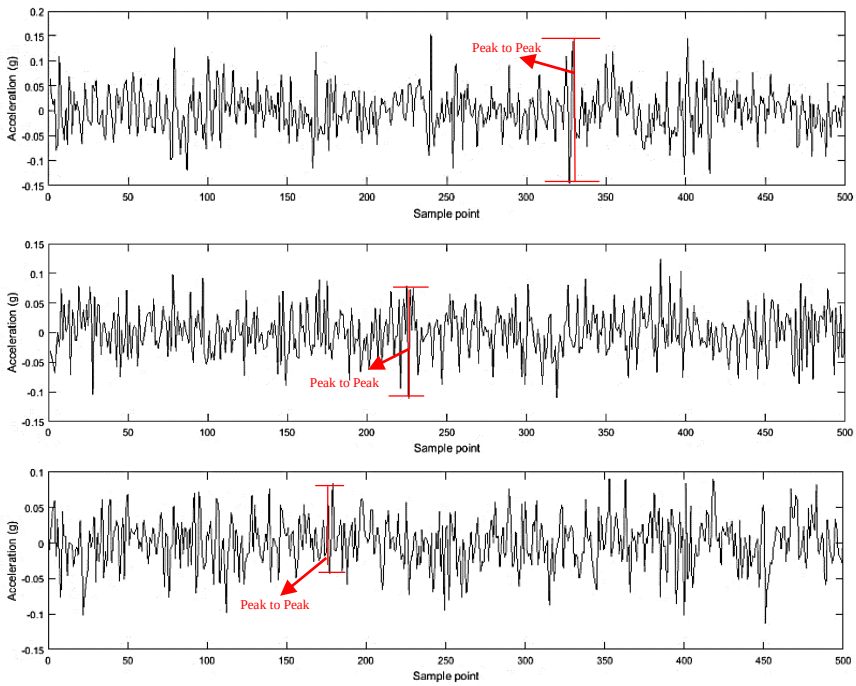

Fig. 4.2: Vibration responses in x-axis (a) Cutting tool A (b) Cutting tool B (c) Cutting tool C

(a)

(b)

(c)

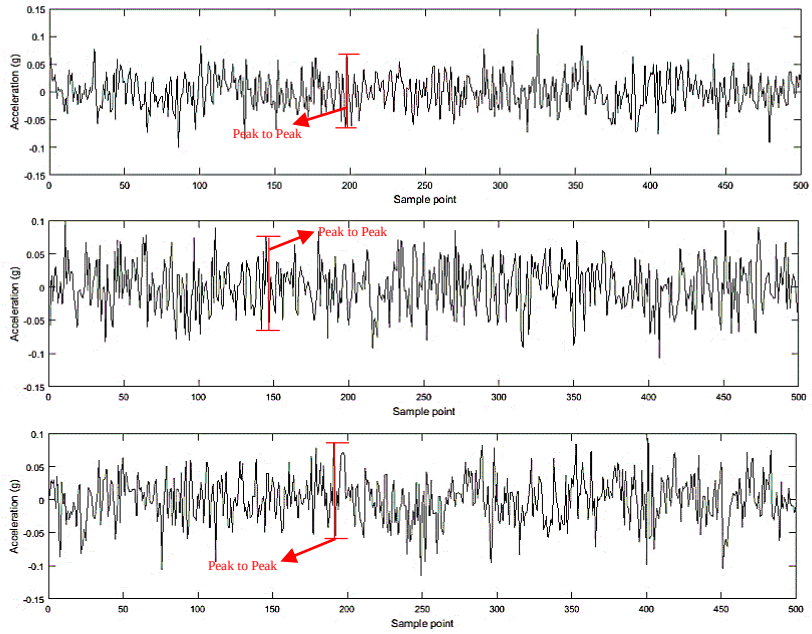

Fig. 4.3: Vibration responses in y-axis (a) Cutting tool A (b) Cutting tool B (c) Cutting tool C

The following section *(**4.2** to **4.4*** provide a detailed discussion and comparison between cutting tool A, B, and C on the performance of milling process on Inconel 718 in term of vibration responses and surface roughness. The process are carried out under dry conditions, down milling mode and constant depth of cut.

4.2 Results of Experiments Conducted on Cutting tool A

Cutting tool A is S09 variable helix and pitch cutting tool with sharp corner. The vibration responses and surface roughness under two finishing condition which are depth of cut of 0.1mm and 0.3mm are analysed and discussed in the following.

4.2.1 Vibration Responses and Surface Roughness when Machined Under Constant Depth of Cut of 0.1mm

The milling process are carried out under axial depth of cut of 0.1mm, cutting speed of 30m/s to 110m/s (interval of 20m/s) and feed rate of 0.02mm/z to 0.06mm/z (interval of 0.02mm/z) with cutting tool A. ***Fig. 4.4*** presents the RMS acceleration values under the above cutting conditions in x-axis direction (cutting direction). From the figure, it can be seen that the RMS acceleration values in the x-axis direction are mostly below 1m/s^2 except for the combination of parameters at (V=90m/s, f =0.06mm/z), (V= 110m/s, f =0.02mm/z), (V= 110m/s, f =0.04mm/z), and (V= 110m/s, f =0.06mm/z). It is noted that the RMS acceleration value reaches above or close to 1m/s^2 are either at high cutting speed or high feed rate or combination of both. In addition, extremely high value of RMS acceleration value observed at cutting speed of 110m/s, and feed rate of 0.06mm/z are likely due to the instability or chattering of the milling process. (Quintana and Ciurana 2011).

On the other hand, it also note that the RMS acceleration values increases when the feed rate increase, it is due to the increase of chip load on the cutting tool corner, which increases the vibration responses. However, at low cutting speed of 30m/s, the influences of feed rate are insignificant to the increase of feed rate. At cutting speed of 30m/s, it is observed that RMS acceleration decreases slightly from 0.42m/s^2 to 0.39m/s^2 when feed rate increases from 0.02mm/z to 0.04mm/z and then, the RMS acceleration further reduces to 0.32m/s^2 when feed rate increases to 0.06mm/z. This phenomena might due to the process damping effect at low cutting speed which the stability of the milling process are high and therefore, low vibration responses are generated (Yusoff et al. 2010).

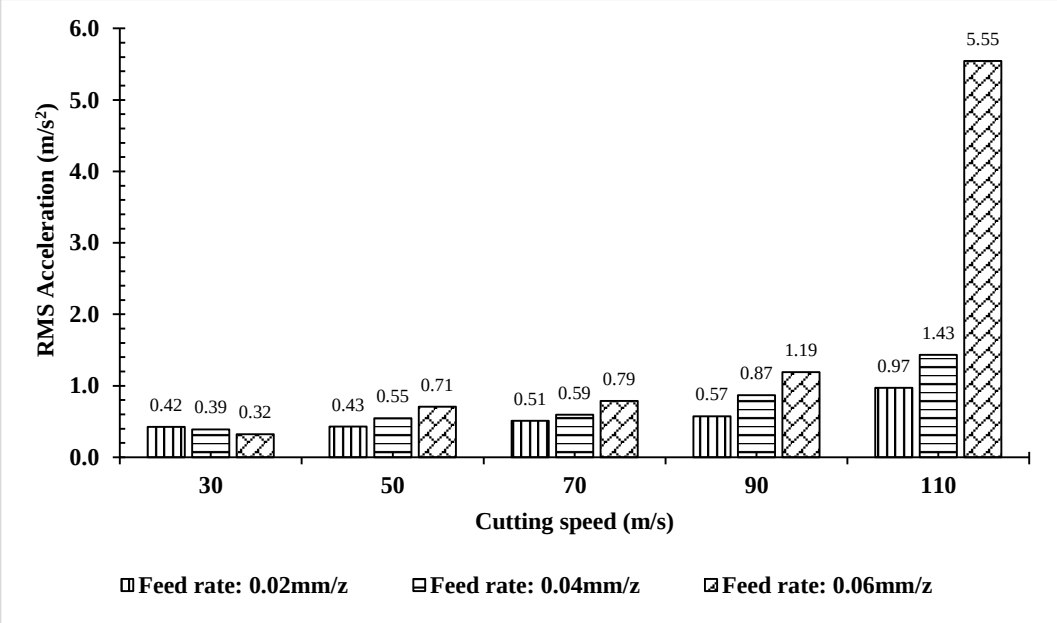

Fig. 4.4: RMS acceleration values against cutting speed in x-axis direction (cutting tool A, DoC_a: 0.1mm)

In y-axis direction, which is the feed direction, ***Fig. 4.5*** presents the RMS acceleration values under combinations of cutting speed and feed rate. The results show that all the RMS acceleration values in y-axis direction are generally lower than the RMS acceleration values in x-axis direction. The RMS acceleration values are fluctuating from 0.1m/s^2 to 0.42m/s^2 for all of the cutting conditions except at the combination of cutting speed at 110m/s^2 and feed rate of 0.06mm/z. The RMS acceleration values increase significantly up to 1.37m/s^2 at the highest cutting speed and feed rate, in which, a similar trend also observed in x-axis direction. It might due to the work hardening properties of the material when it is machined under high cutting parameters which causes high cutting temperatures and softening of the cutting tool which causes instability of the milling process (Le Coz and Dudzinski 2014). In addition, the RMS acceleration in y-axis direction are observed at minimal when the combination of cutting parameters are (V=30m/s, f =0.06mm/z), (V= 50m/s, f =0.02mm/z), (V= 50m/s, f =0.04mm/z) and (V= 70m/s, f=0.04mm/z).

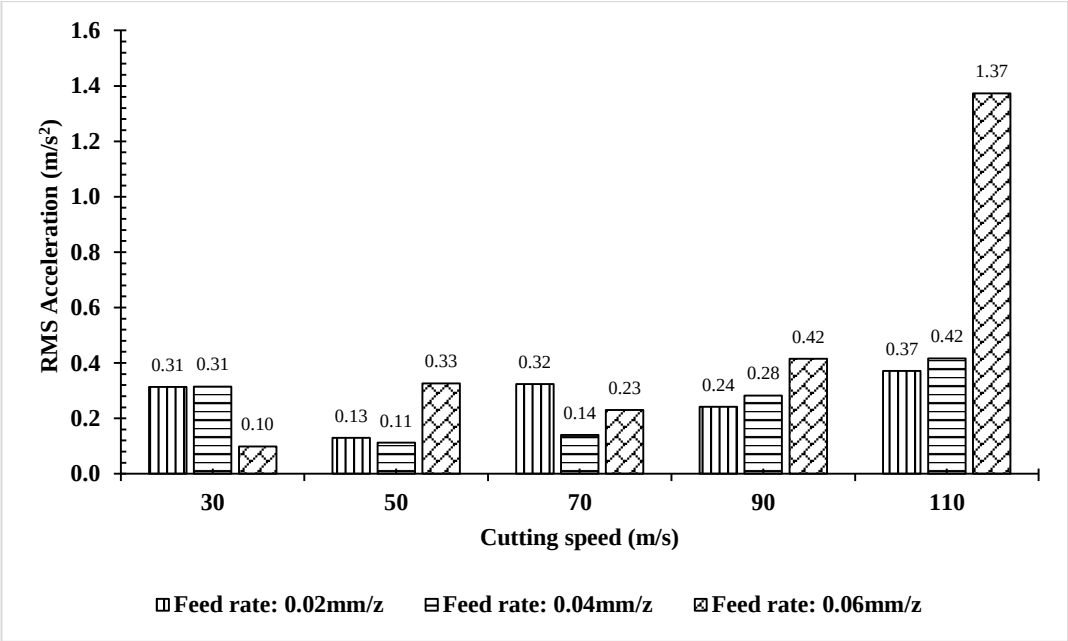

Fig. 4.5: RMS acceleration values against cutting speed in y-axis direction (cutting tool A, DoC$_a$: 0.1mm)

The surface roughness produced by cutting tool A under depth of cut of 0.1mm are presented in ***Fig. 4.6***. The trend shows a steady increment of the surface roughness from cutting speed 30m/s to 110m/s. At cutting speed of 30m/s, the surface roughness achieved at feed rate of 0.02mm/z is 0.21µm, while at feed rate of 0.04mm/z is 0.20µm, and at feed rate of 0.06mm/z is 0.22µm. It can be seen that the increment of feed rate at cutting speed of 30m/s is almost insignificant to the surface roughness. Similarly, the increment of feed rate at cutting speed of 50m/s, 70m/s and 90m/s only has little influences on the surface roughness. By relating back to the RMS acceleration value in x-axis and y-axis direction, the RMS values difference between feed rates of 0.02mm/z, 0.04mm/z and 0.06mm/z are small as well. Further into the experimental data, it is found that the surface roughness increase for about 15% due to the increase of cutting speed from 30m/s to 90m/s regardless of feed rate. However, there is a high increment of surface roughness at cutting parameters (V= 110m/s, f= 0.02mm/z and V=110m/s, f= 0.06mm/z) which increase up to 30% of surface roughness values.

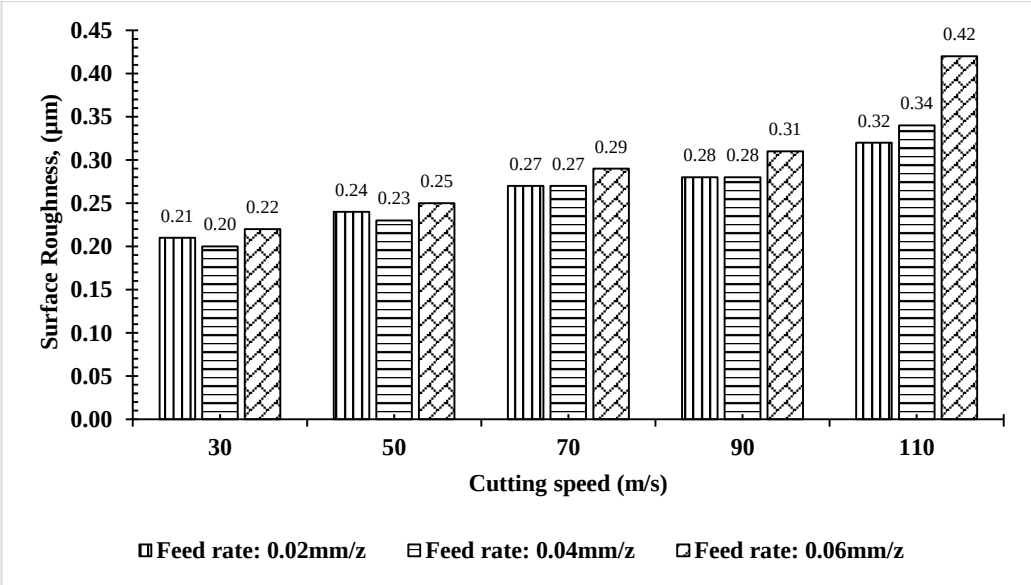

Fig. 4.6: Surface roughness against different cutting speed (Cutting tool A, DoC$_a$: 0.1mm)

As a summary, the performance of the cutting tool A under axial depth of cut of 0.1mm are summarise as below:

- The range of RMS acceleration value in x-direction under cutting speed of 30m/s to 110m/s are as follow:
    - Feed rate of 0.02mm/z: RMS value from 0.42m/s^2 to 0.97m/s^2
    - Feed rate of 0.04mm/z: RMS value from 0.39m/s^2 to 1.43m/s^2
    - Feed rate of 0.06mm/z: RMS value from 0.32m/s^2 to 5.55m/s^2
- The range of RMS acceleration value in y-direction under cutting speed of 30m/s to 110m/s are as follow:
    - Feed rate of 0.02mm/z: RMS value from 0.13m/s^2 to 0.37m/s^2
    - Feed rate of 0.04mm/z: RMS value from 0.11m/s^2 to 0.42m/s^2
    - Feed rate of 0.06mm/z: RMS value from 0.10m/s^2 to 1.37m/s^2
- The range of surface roughness achieved under different cutting speed are as follows:
    - Feed rate of 0.02mm/z: 0.21µm to 0.32 µm
    - Feed rate of 0.04mm/z: 0.20µm to 0.34 µm
    - Feed rate of 0.06mm/z: 0.22µm to 0.42 µm

Based on the experimental data above, it is noted that the vibration in x-axis direction (cutting direction) exhibits higher vibration than the y-axis direction (feed direction). This might due x-axis direction is the entry of the cutting edge which exhibits higher cutting force while y-axis direction is the trailing point of the cutting

process and therefore, the force in y-axis varies based on the force generated in x-axis direction.

4.2.2 Vibration Responses and Surface Roughness when Machined Under Constant Depth of Cut of 0.3mm

Fig. 4.7 shows the RMS acceleration values in x-axis direction at depth of cut of 0.3mm. As compared to ***Fig. 4.4*** which is the RMS acceleration values of x-axis direction at depth of cut 0.1mm, it can be seen that there is a substantial increase in RMS acceleration values with an increase of axial depth of cut by 0.2mm. Generally, the RMS acceleration values for cutting tool A in x-axis direction under depth of cut (0.3mm) are almost double of the RMS acceleration values at depth of cut (0.1mm).

Based on ***Fig. 4.7***, the RMS acceleration values at cutting speed of 30m/s and feed rate of 0.02mm/z is 0.46m/s^2, the values increases almost by 100% at cutting speed of 50m/s with the RMS acceleration value of 0.80m/s^2, the RMS acceleration value increases to 1.10m/s^2 at 70m/s, the RMS acceleration value is 2.21m/s^2 at 90m/s, and the RMS acceleration value is 2.47m/s^2 at 110m/s. A similar trend are observed for feed rate 0.04mm/z, the RMS acceleration value is 0.48m/s^2 at cutting speed of 30m/s, the RMS acceleration value increases up to 0.94m/s^2 at cutting speed of 50m/s, the RMS acceleration value is 1.29m/s^2 at 70m/s, the RMS acceleration value increases to 2.44m/s^2 at 90m/s, and the RMS acceleration value reached its maximum with the value of 3.07m/s^2 at cutting speed of 110m/s.

As for feed rate of 0.06mm/z, the RMS acceleration increase almost linearly at cutting speed of 30m/s to 70m/s from 0.67m/s^2 to 2.66m/s^2. Then, the RMS acceleration increases substantially at cutting speed of 90m/s with the value of 6.29m/s^2. At cutting speed of 110m/s, the RMS acceleration is highest with the value of 9.79m/s. In overall, feed rate of 0.06mm/z exhibits higher vibration responses as compared to feed rate of 0.02mm/z and 0.04mm/z especially at high cutting speeds.

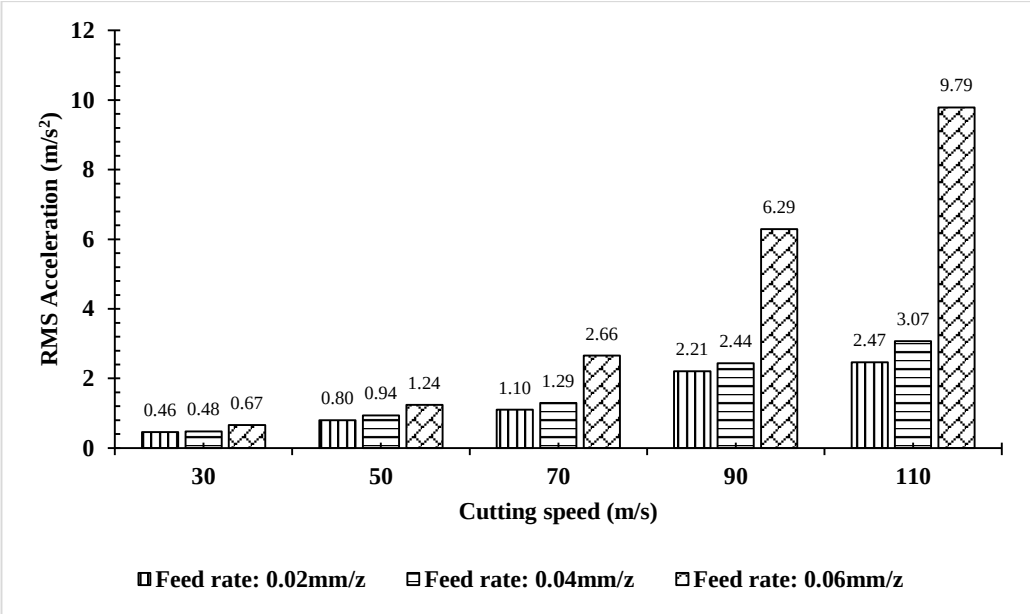

Fig. 4.7: RMS acceleration value against cutting speed in x-axis direction (cutting tool A, DoC$_a$: 0.3mm)

Fig. 4.8 presents the RMS acceleration values in y-direction at depth of cut of 0.3mm. At feed rate of 0.02mm/z, the RMS acceleration value at cutting speed of 30m/s is 0.35m/s^2, the RMS acceleration increase slightly to 0.36m/s^2 at cutting speed of 50m/s, the RMS acceleration value increase up to 0.41m/s^2 at cutting speed of 70m/s. In contrast, there are significant increase in RMS acceleration value at cutting speed of 90m/s with the RMS acceleration value at 1.47m/s^2. Then, a slight decrease of RMS acceleration value are observed at cutting speed of 110m/s with value of 1.12m/s^2.

At feed rate of 0.04mm/z, the RMS acceleration value at cutting speed of 30m/s is 0.33m/s^2, it increases slightly to 0.36m/s^2 at cutting speed of 50m/s, the RMS acceleration value is 0.41m/s^2 at cutting speed of 70m/s. Then, the RMS acceleration value increases drastically at cutting speed of 90m/s with the value of 1.72m/s^2 and decreases slightly to 1.50m/s^2 at cutting speed of 110m/s.

When milling process is carried out with highest feed rate of 0.06mm/z, the RMS acceleration value at cutting speed of 30m/s is 0.38m/s^2 and the value increases to 0.41m/s^2 at cutting speed of 50m/s, the RMS acceleration is doubled at cutting speed of 70m/s^2 with the value of 0.86m/s^2. Similar to the feed rate of 0.02mm/z and 0.04mm/z, the sudden increase of RMS acceleration value at cutting speed of 90m/s also observed in the feed rate of 0.06mm/z with the RMS acceleration value of

3.30m/s^2. The RMS acceleration value is maximum at cutting speed of 110m/s with the value of 3.59m/s^2.

The RMS acceleration values in y-direction are at its minimal at cutting speed of 30m/s and 50m/s regardless of feed rate and also the combination of parameters (*V*= 70m/s, *f*= 0.02mm/z) and (*V*=70m/s, *f*= 0.04mm/z) which is similar to the trend shows in the x-direction. It noted that at cutting speed of 90m/s and feed rate of 0.06mm/z, there is significant increase in the RMS acceleration value which indicate high vibration responses during the milling process.

As compared to the y-axis direction for depth of cut 0.1mm, the vibration responses are generally higher at depth of cut of 0.3mm, especially in high cutting speed and high feed rate. It is due to high contact area between the tool and workpiece surface as a result of increase in depth of cut. Therefore, more material have to be removed which induce high vibration responses are observed.

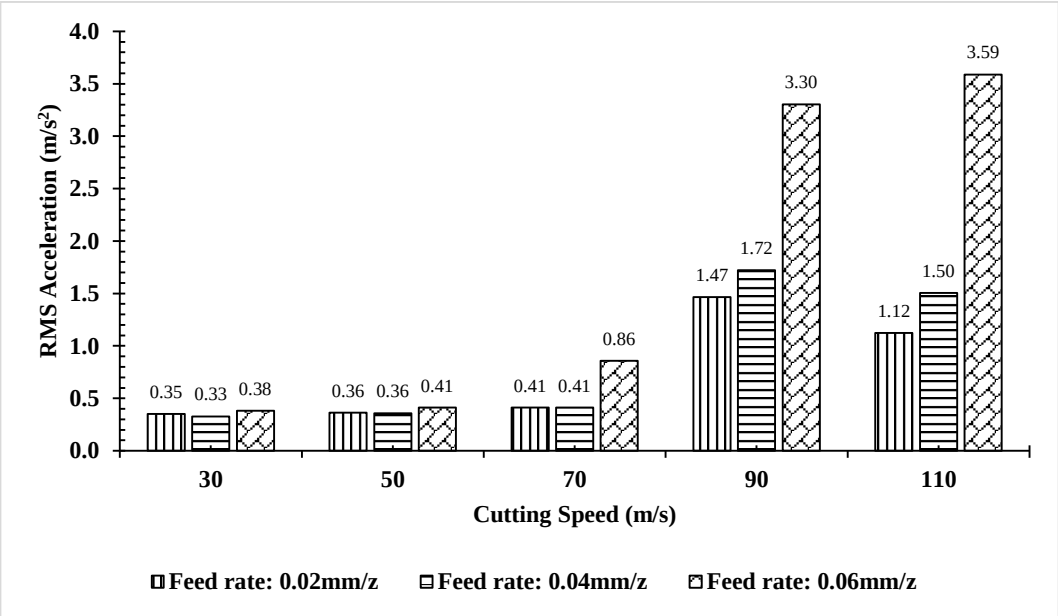

Fig. 4.8: RMS acceleration value against cutting speed in y-axis direction (cutting tool A, DoC$_a$: 0.3mm)

Fig. 4.9 presents the surface roughness value under depth of cut of 0.3mm when machined with cutting tool A. At feed rate of 0.02mm/z, the value increases almost linear with respect to the cutting speeds, the surface roughness are recorded at 0.24µm at cutting speed of 30m/s, 0.28µm at cutting speed of 50m/s, 0.29µm at cutting speed of 70m/s, 0.31µm at cutting speed of 90m/s, and 0.37µm at cutting speed of 110m/s.

On the other hand, at the feed rate of 0.04mm/z, the surface roughness is 0.23µm at cutting speed of 30m/s, 0.26µm at cutting speed of 50m/s, 0.30µm at cutting speed of 70m/s, 0.32µm at cutting speed of 90m/s and increase up to 0.36µm at 110m/s.

As for feed rate of 0.06mm/z, the surface roughness is initially recorded as 0.24µm at cutting speed of 30m/s, and then increases to 0.28µm at 50m/s, the surface roughness value is 0.31µm at cutting speed of 70m/s, the surface roughness is 0.39µm at cutting speed of 90m/s and peaked at 0.46µm at cutting speed of 110m/s.

Based on the figure, it seem like that the increase of the surface roughness is more sensitive to the increase of feed rate as compared to cutting speed. In addition, the surface roughness value are recorded slightly higher as compared to the surface roughness obtained from milling process at depth of cut (0.1mm). Furthermore, it is also note that the high vibration responses at the combination of parameters (*V*= 90m/s, *f*= 0.06mm/z) and (*V*=110m/s, *f*= 0.06mm/z) which causes higher value of surface roughness.

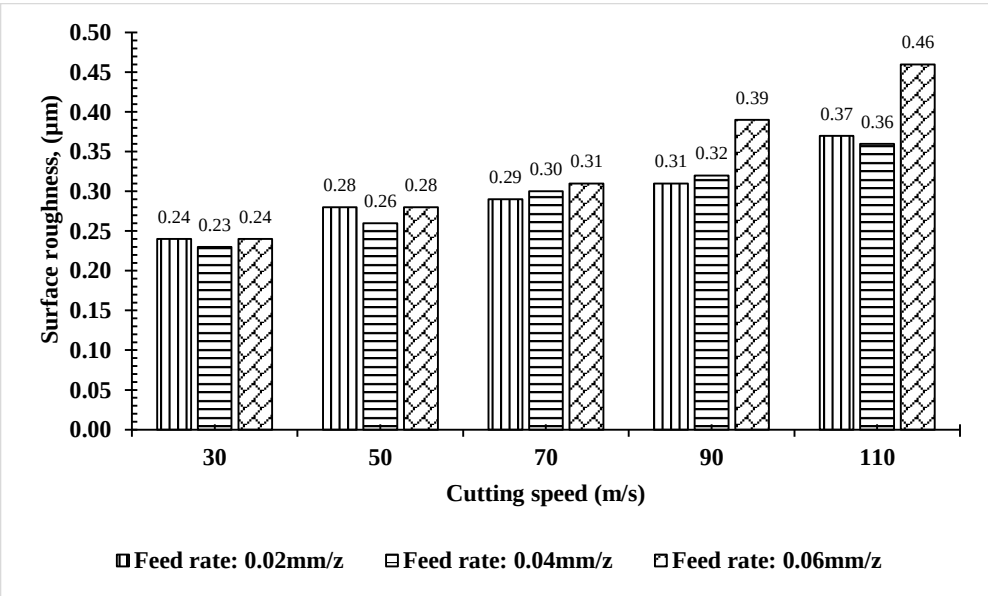

Fig. 4.9: Surface roughness against different cutting speed (Cutting tool A, DoC$_a$: 0.3mm)

In summary, the performance of the cutting tool A under axial depth of cut of 0.3mm can be summarize as below:

- The range of RMS acceleration value in x-direction under cutting speed of 30m/s to 110m/s are as follow:
    - Feed rate of 0.02mm/z: RMS value from 0.46m/s^2 to 2.47m/s^2
    - Feed rate of 0.04mm/z: RMS value from 0.48m/s^2 to 3.07m/s^2

    - Feed rate of 0.06mm/z: RMS value from 0.67m/s^2 to 9.79m/s^2
- The range of RMS acceleration value in y-direction under cutting speed of 30m/s to 110m/s are as follow:
    - Feed rate of 0.02mm/z: RMS value from 0.35m/s^2 to 1.47m/s^2
    - Feed rate of 0.04mm/z: RMS value from 0.33m/s^2 to 1.72m/s^2
    - Feed rate of 0.06mm/z: RMS value from 0.38m/s^2 to 3.59m/s^2
- The range of surface roughness achieved under different cutting speed are as below:
    - Feed rate of 0.02mm/z: 0.24µm to 0.37 µm
    - Feed rate of 0.04mm/z: 0.23µm to 0.36 µm
    - Feed rate of 0.06mm/z: 0.24µm to 0.46 µm

4.3 Results of Experiments Conducted on Cutting tool B

Cutting tool B is S10 variable helix and pitch cutting tool with corner radius of 0.5mm. The vibration responses and surface roughness under depth of cut of 0.1mm and 0.3mm are presented and discussed in the following.

4.3.1 Comparison of Vibration Responses and Surface Roughness of Cutting tool B to Cutting tool A when Machined under Constant Depth of Cut of 0.1mm

In the previous section, the performance of cutting tool A was discussed with respect to the vibration responses and surface roughness. In the following, the performance of cutting tool B are discussed and compared to the cutting tool A.

Fig. 4.10 presents the RMS acceleration value in x-direction for cutting tool B under axial depth of cut of 0.1mm. In overall, it shows that the RMS acceleration values of cutting tool B are slightly lower as compared to cutting tool A at low cutting speed (30m/s to 70m/s) and significantly lower at higher cutting speed (90m/s and 110m/s). From the ***Fig. 4.4*** and ***Fig. 4.10*** , it can be seen that the maximum RMS acceleration value is 0.85m/s^2 and the minimum RMS acceleration value is 0.36m/s^2 for cutting tool B, while the maximum RMS acceleration value for cutting tool A is 5.55m/s^2 and the minimum RMS acceleration value is 0.32m/s^2. The difference

between the maximum and minimum value of RMS acceleration values for cutting tool A is much higher compared to cutting tool B, this signifies that the milling process of cutting tool B is more stable as compared to cutting tool A.

At low cutting speed, the RMS acceleration values of cutting tool A and cutting tool B are almost similar with the RMS acceleration values ranging from 0.32m/s^2 to 0.42m/s^2 regardless of feed rate value. For cutting tool B, the RMS acceleration values at feed rate of 0.04mm/z are lowest as compared to feed rate of 0.02mm/z and 0.06mm/z regardless of cutting speed. However, this phenomena is not shown for cutting tool A. Nevertheless, cutting tool A still shows a higher RMS acceleration values in general especially at high cutting parameters. Therefore, it indicate that the corner radius of cutting tool B reduces the vibration responses at high cutting speed which is evident at cutting speed of 90m/s and 110m/s.

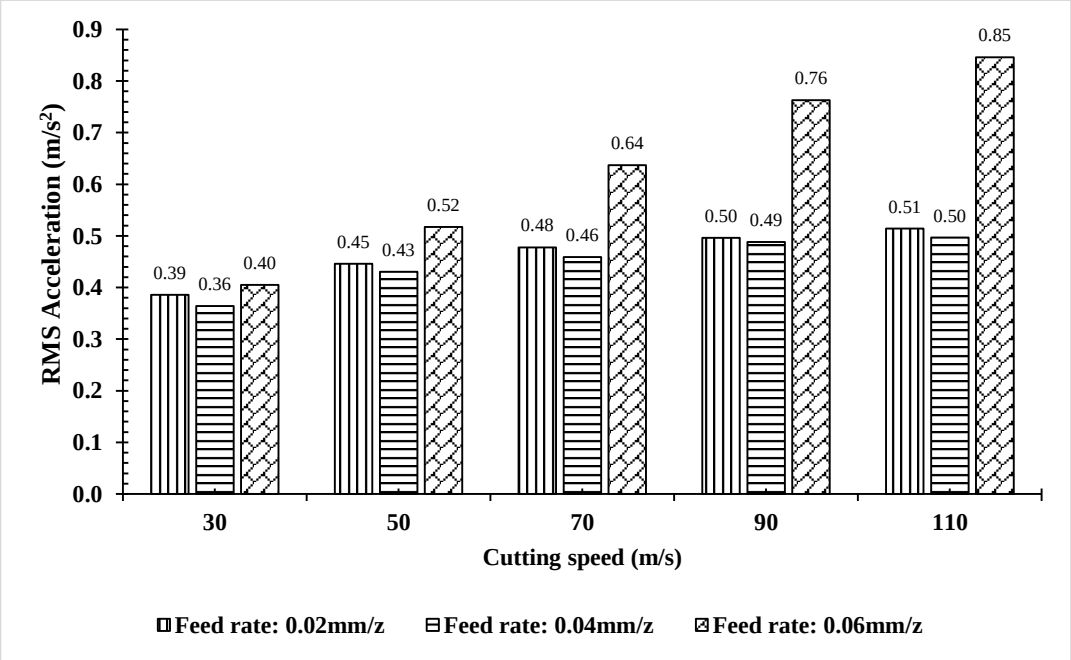

Fig. 4.10: RMS acceleration value against cutting speed in x-axis direction (cutting tool B, DoC$_a$: 0.1mm)

Fig. 4.11 present the RMS acceleration value in the y-axis direction for cutting tool B. Based on the figure, the RMS acceleration values increases and decreases within the range of 0.33m/s^2 to 0.42m/s^2 for all the combination of cutting speed and feed rate. Therefore, it indicated that the influences of cutting speed and feed rates on the vibration responses in y-axis direction are minimal. It might due to

the stabilizing factor induced by the corner radius, it can be seen that the vibration in y-axis direction for cutting tool B are much more stabilized as compared to the vibration response in y-axis direction for cutting tool A (***Fig. 4.5***). This phenomenon shows that the feed force on cutting tool B are smaller as compared to cutting tool A at higher cutting speed, which imply that cutting tool B are able to cut smoother than cutting tool A. On the other hand, it also noted that the RMS acceleration at feed rate of 0.04mm/z are the lowest as compared to the feed rate of 0.02mm/z and 0.06mm/z.

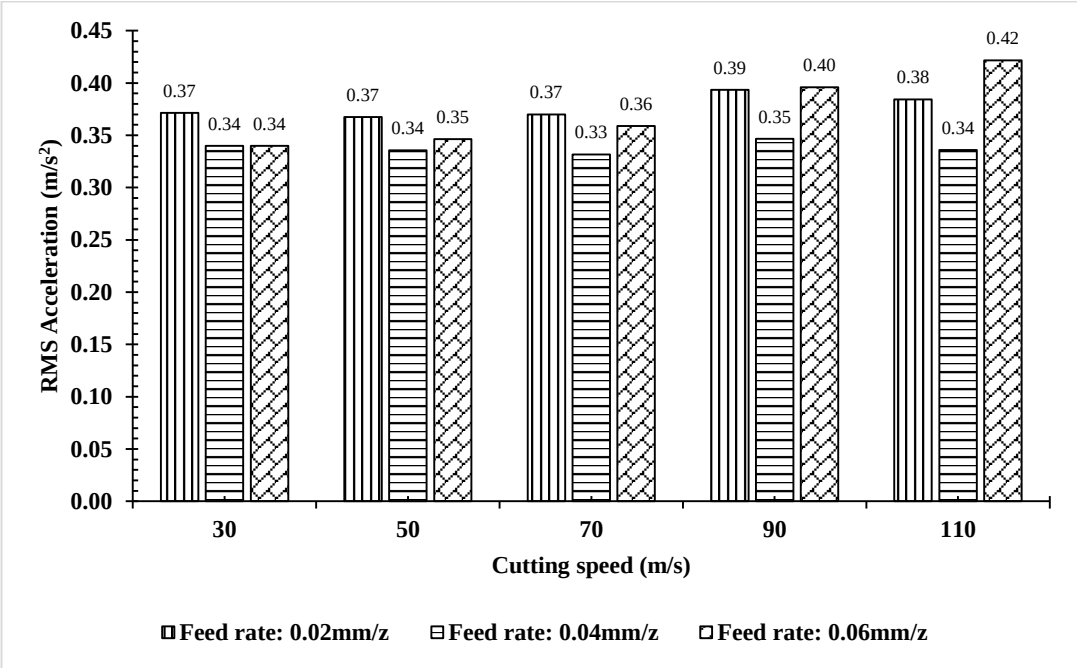

Fig. 4.11: RMS acceleration value against cutting speed in y-axis direction (cutting tool B, DoC$_a$: 0.1mm)

The surface roughness produced in the milling process of Inconel 718 with cutting tool B under depth of cut of 0.1mm are given in ***Fig. 4.12***. Based on the figure, the surface roughness value for cutting tool B is slightly lower compared to cutting tool A. The surface roughness are compared at cutting speed of 30m/s, the surface roughness produced by cutting tool B improve up to 19% as compared to cutting tool A. As for cutting speed of 50m/s and 70m/s, the surface quality improve for up to 26%. For cutting speed of 90m/s, the surface quality improve up to 18% and for cutting speed of 110m/s, the surface quality improve by 20%. It can be seen that for every combination of cutting parameters, the improvement of surface quality for cutting tool B is increase at least 22% on average,

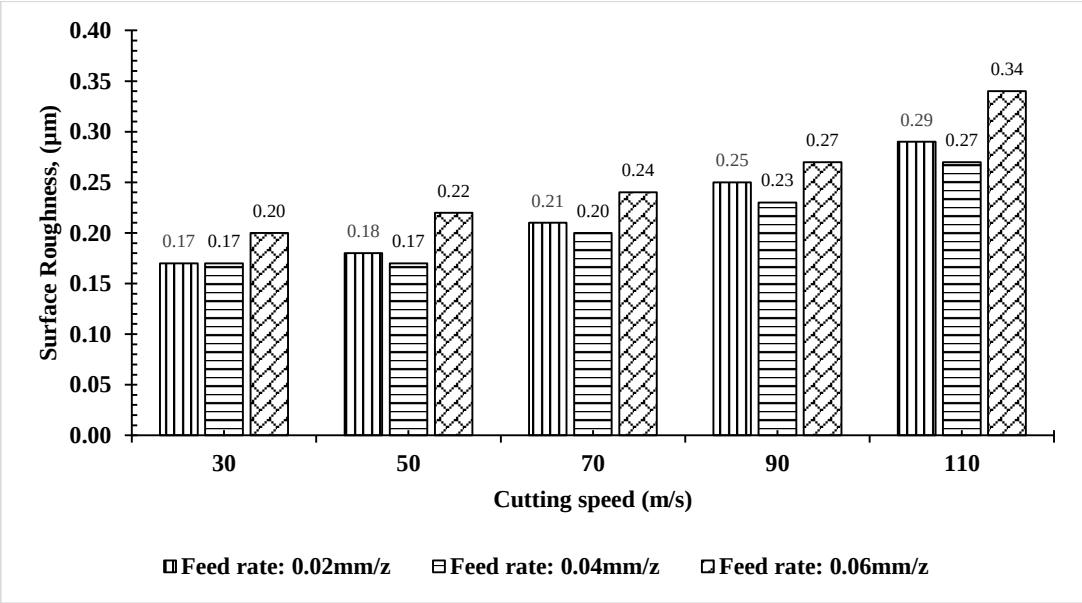

Fig. 4.12: Surface roughness against different cutting speed (Cutting tool B, DoC$_a$: 0.1mm)

4.3.2 Comparison of Vibration Responses and Surface Roughness of Cutting tool B to Cutting tool A when Machined under Constant Depth of Cut of 0.3mm

The performance of cutting tool B under depth of cut 0.3mm are discussed and compared to cutting tool A. ***Fig. 4.13*** shows the RMS acceleration values in the x-axis direction for cutting tool B. At feed rate of 0.02mm/z, a steady increment of RMS acceleration values are observed, the RMS acceleration values increases about 0.1m/s^2 for every increment in cutting speeds. For feed rate of 0.04mm/z, the RMS acceleration increases with a slightly higher gradient as compared to the trend at feed rate of 0.02mm/z. Similarly, the increment of RMS acceleration at every interval of cutting speed at feed rate of 0.06 are much higher as compared to feed rate of 0.04mm/z. For cutting tool B, the results shows that there are about 10% to 30% increase of RMS acceleration values at cutting speed of 30m/s when the depth of cut increases from 0.1mm to 0.3mm. It is due to the increase of contract area and therefore more forces are required to remove the material. Hence, the vibration responses increases with the increase of depth of cut.

As compared to cutting tool A (***Fig. 4.7***) under same parameters, the vibration responses are generally lower for cutting tool B. It is observed that at the combination

of parameters (V=110m/s, f= 0.06mm/z), the RMS acceleration are reduced by about 78%. It might be due to reduction of thermal and mechanical stress sustain by the corner radius tool as oppose to the sharp corner tool.

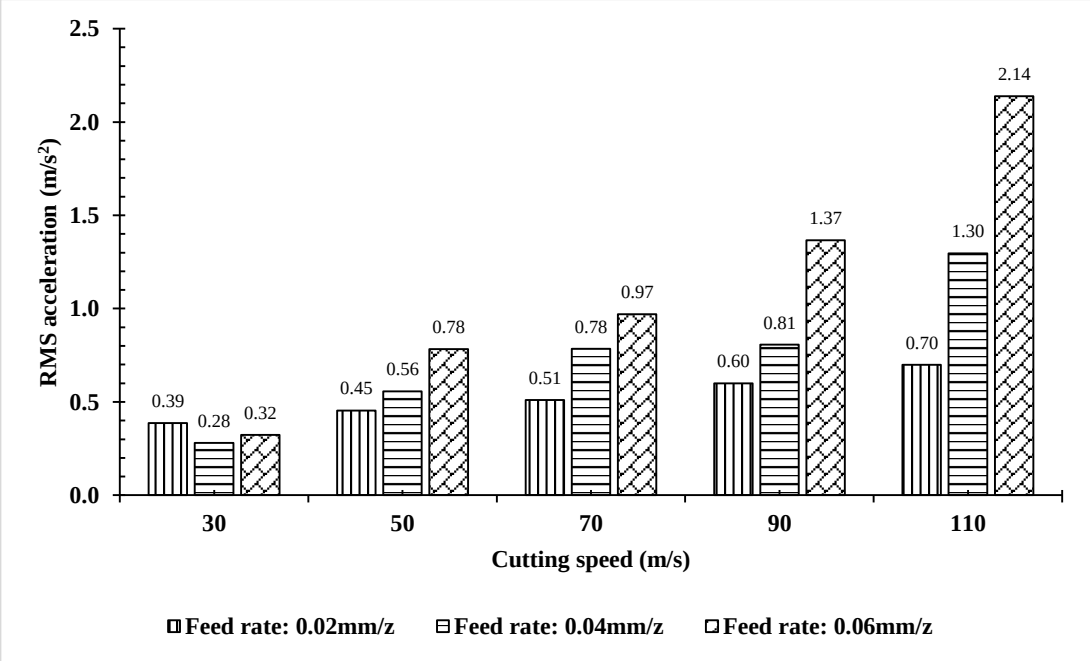

Fig. 4.13: RMS acceleration value against cutting speed in x-axis direction (cutting tool B, DoC$_a$: 0.3mm)

Fig. 4.14 presents the RMS acceleration values at y-axis direction of cutting tool B under depth of cut of 0.3mm, it is shows that the vibration responses increase and decrease with the increase of cutting speed and feed rate. When cutting tool B are machined under depth of cut of 0.1mm, the vibration responses varies between 0.33m/s^2 to 0.42m/s^2 , in which, the vibration responses are consistent in y-axis direction. However, it shows otherwise when the depth of cut increases to 0.3mm, the RMS acceleration values increases drastically at cutting speed of 110m/s and feed rate of 0.06mm/z. Nevertheless, variation of RMS acceleration in the y-axis direction at depth of cut 0.3mm are quite similar to the trend of cutting tool B when it is perform under depth of cut 0.1mm except the vibration responses are slightly higher values.

On the other hand, when the performance of cutting tool B are compared with cutting tool A under depth of cut of 0.3mm, the RMS acceleration values obtained by cutting tool B are much lower as compared to the RMS acceleration values obtained

by cutting A. There is a significant reduction of RMS acceleration values at the combination of (V=110m/s, f =0.06mm/z) which the reduction yield about 80%. In general cutting tool B exhibits lower vibration responses as compared to cutting tool A in y-axis direction.

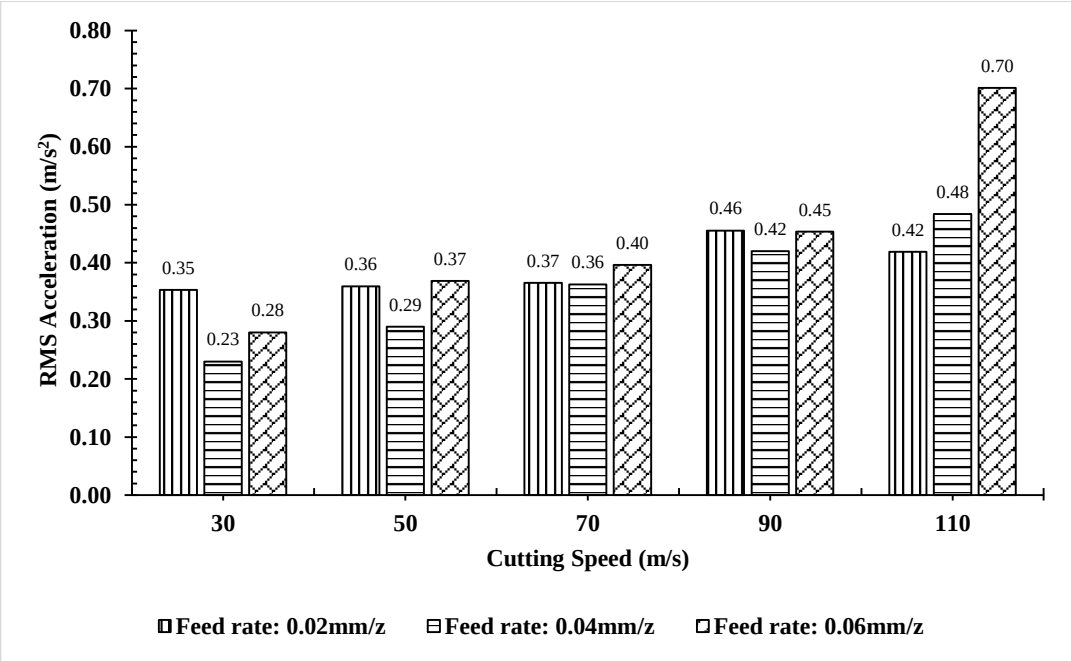

Fig. 4.14: RMS acceleration value against cutting speed in y-axis direction (cutting tool B, DoC$_a$: 0.3mm)

Fig. 4.15 shows the surface roughness produced by cutting tool B under depth of cut of 0.3mm. Based on the figure, the surface roughness values for cutting tool B is slightly lower compared to cutting tool A. At cutting speed of 30m/s, the surface roughness is improve by 4% as compared to cutting tool A. As for cutting speed of 50m/s, the surface quality improve for about 10%. For cutting speed of 70m/s, the surface quality improve by 10%. For cutting speed of 90m/s, the surface quality improve by 15% and for cutting speed of 110m/s, the surface quality improve by 24%. In overall, cutting tool B produced better surface roughness as compared to cutting tool A with the improvement ranging from 4% to 24%

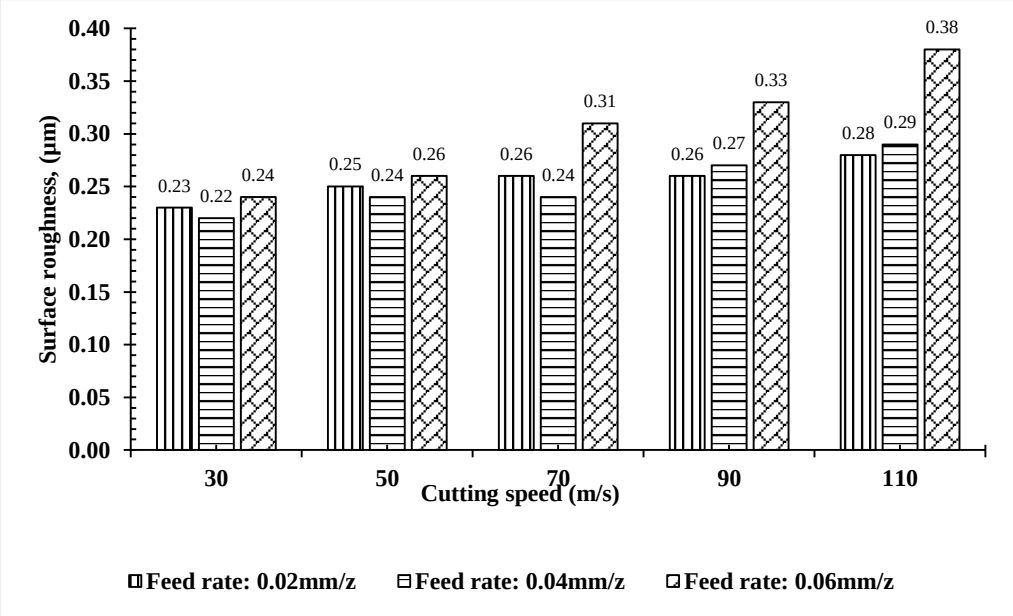

Fig. 4.15: Surface roughness against different cutting speed (Cutting tool B, DoC$_a$: 0.3mm)

4.4 Results of Experiments Conducted on Cutting tool C

Cutting tool C is S10 variable helix and pitch cutting tool with corner radius of 1.0 mm. The vibration responses and surface roughness are presented, discussed and compared with cutting tool A and B in the following.

4.4.1 Comparison of Vibration Responses and Surface Roughness of Cutting tool C to Cutting tool A and B when Machined under Constant Depth of Cut of 0.1mm

As a recap on previous discussion, generally cutting tool B has lower RMS acceleration values and better surface roughness as compared to cutting tool A.

Fig. 4.16 shows the RMS acceleration values in x-axis direction of cutting tool C under depth of cut of 0.1mm. The figures shows a steady increment of vibration responses at feed rate of 0.02mm/z. Similarly, at feed rate of 0.04mm/z, the RMS acceleration values increases steadily with a slight higher gradient and value as compared to feed rate of 0.02mm/z. At feed rate of 0.06mm/z, the increment of RMS acceleration values are at much higher gradient (almost exponentially) as compared to feed rate of 0.02mm/z and 0.04mm/z.

Based on the RMS acceleration value obtained for cutting tool C under depth of cut 0.1mm, the RMS acceleration values at x-axis direction of cutting tool C are lower as compared to the vibration responses of cutting tool A. The most significant reduction in vibration responses are observed at high cutting speed and high feed rate (*V*= 110m/s, *f*= 0.06mm/z).

On the other hand, the vibration responses at low cutting speed (30m/s to 70m/s) are comparable between cutting tool C and cutting tool B, in which case, cutting tool C might be higher or lower. However, higher cutting speed (90m/s and 110m/s), the vibration response for cutting tool C are higher as compared to cutting tool B, it might due to the overcompensation of corner radius when it is increases from 0.5mm to 1.0mm. Therefore, the frictional force generated at high cutting speed are higher which result in high vibration responses.

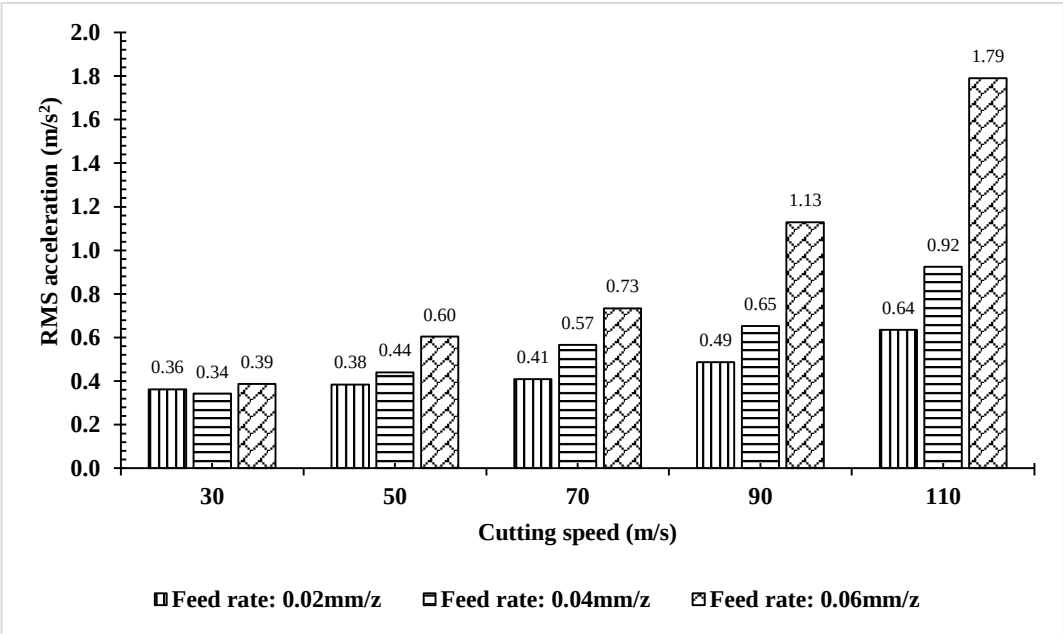

Fig. 4.16: RMS acceleration value against cutting speed in x-axis direction (cutting tool C, DoC_a: 0.1mm)

Fig. 4.17 presents the RMS acceleration value in y-axis direction for cutting tool C under axial depth of cut of 0.1mm. The RMS acceleration values at y-direction are mostly at the range of 0.35m/s^2 to 0.41m/s^2, it shows minimal RMS acceleration values at cutting speed (*V*= 30m/s, *f*= 0.02mm/z), (*V*= 50m/s, *f*= 0.04mm/z) and (*V*= 70m/s, *f*= 0.04mm/z), the highest RMS acceleration are observed at (*V*= 90m/s, *f*= 0.06mm/z) and (*V*= 110m/s, *f*= 0.06mm/z).

The RMS acceleration values in cutting tool C are comparable to cutting tool A except at highest cutting parameters (*V*= 110m/s, *f*= 0.06mm/z) which shows a clear reduction in RMS acceleration for cutting tool C. In some cases, the RMS acceleration of cutting tool C are higher while some of the cases the RMS acceleration values of cutting tool A are higher, it shows non-linear relationship. Nevertheless, better stability are shown by cutting tool C as compared to cutting tool A.

In general, the RMS acceleration values in y-axis direction for cutting tool B are very consist which already discussed in section ***4.3.1*** , as compared to cutting tool C, the stability of cutting tool C are wider in term of the range of RMS acceleration values. In addition, in most of the cases, the RMS acceleration values for cutting tool B and cutting tool C are similar except at the following combination of parameters (*V*= 30m/s, *f*= 0.04mm/z), (*V*= 50m/s, *f*= 0.04mm/z) ,(*V*= 70m/s, *f*= 0.04mm/z), (*V*= 90m/s, *f*= 0.06mm/z) , and (*V*= 110m/s, *f*= 0.04mm/z), in which, the cutting tool C exhibits slightly lower vibration responses. Therefore, it is evident that the vibration responses in y-axis direction for cutting tool B and C are similar.

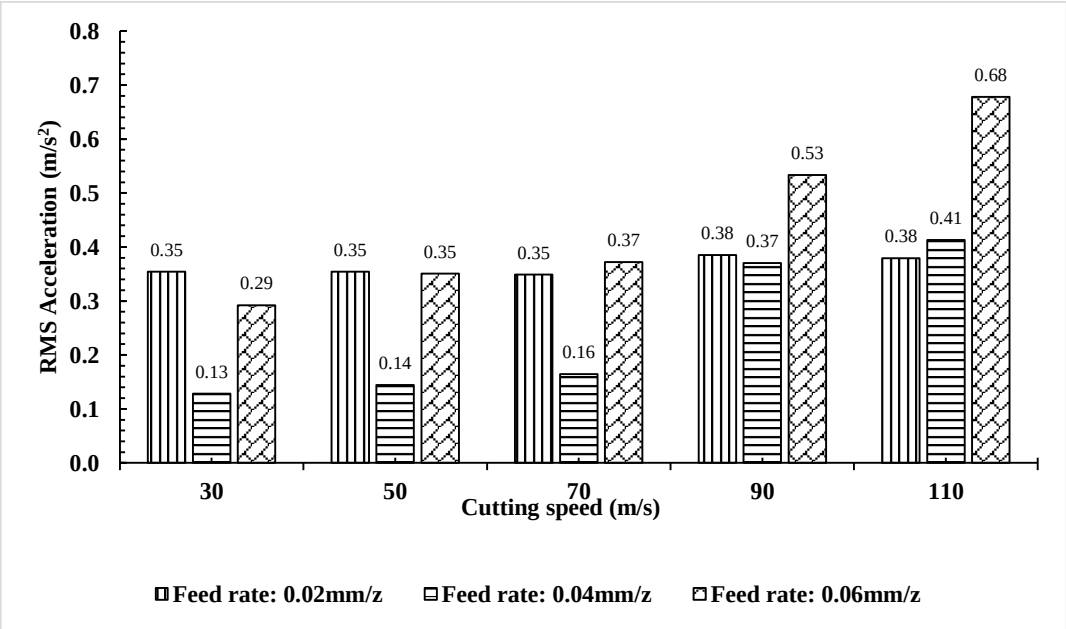

Fig. 4.17: RMS acceleration value against cutting speed in y-axis direction (cutting tool C, DoC$_a$: 0.1mm)

Fig. 4.18 shows the surface roughness of cutting tool C under depth of cut of 0.1m, the overall surface roughness values is ranging from 0.19µm to 0.38µm.

As compared to the surface roughness produced by cutting tool C and cutting tool A, cutting tool C gives slightly better surface roughness. At cutting speed of 30m/s, the surface roughness improves up to 5%. At cutting speed of 50m/s, the surface roughness improves up to 8%. At cutting speed of 70m/s, the surface roughness improves up to 22%. At cutting speed of 90m/s, the surface roughness increases up to 14% and at cutting speed of 110m/s, the surface roughness increases up to 21%.

On the other hand, when compare the surface roughness by cutting tool C and cutting tool B, the surface roughness of cutting tool C are slightly higher than cutting tool B in general. In overall, the surface roughness increases up 18%, 30%, 25%, 22%, and 11% with respect to cutting speed of 30m/s, 50,m/s, 70m/s, 90m/s and 110m/s.

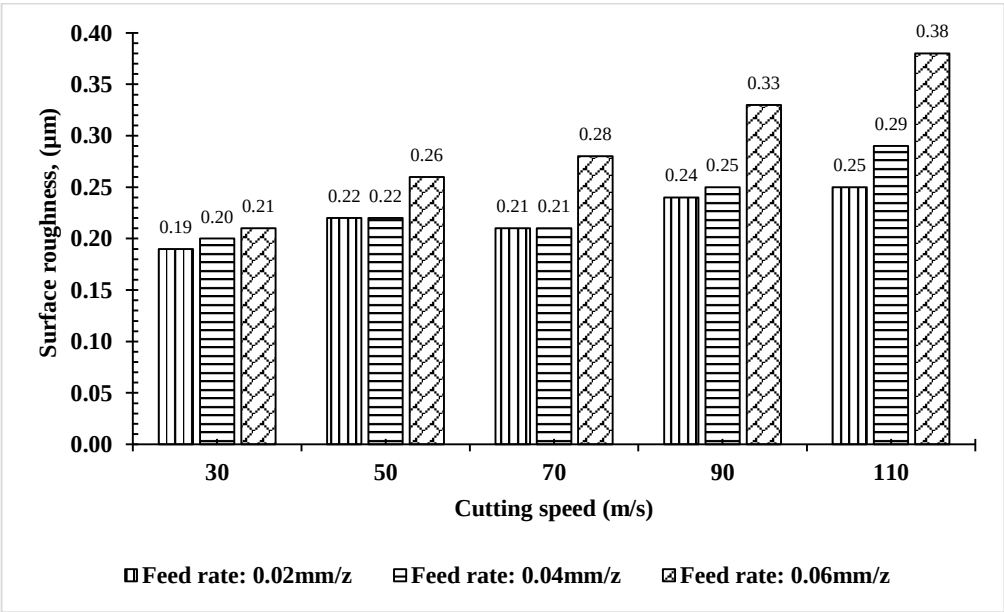

Fig. 4.18: Surface roughness against different cutting speed (Cutting tool C, DoC$_a$: 0.1mm)

4.4.2 Comparison of Vibration Responses and Surface Roughness of Cutting tool C to Cutting tool A and B when Machined under Constant Depth of Cut of 0.3mm

Fig. 4.19 shows the x-axis direction of RMS acceleration values recorded with cutting tool C under axial depth of cut of 0.3mm. A similar vibration responses trend are observed when cutting tool C is machine at depth of cut 0.1mm and depth of

cut at 0.3mm, but with slightly higher RMS acceleration value. The increment gradient are highest at feed rate of 0.06mm/z, follow by 0.04mm/z and 0.02mm/z.

As compared to cutting tool A, cutting tool C exhibits lower vibration responses at x-axis direction in all of the cases. On the other hand, the vibration responses obtained by cutting tool B and cutting tool C are comparable except at high cutting speed in which cutting tool C exhibits slightly higher vibration. In general, the vibration responses in x-axis direction are highest for cutting tool A, follow by cutting tool C and the least is cutting tool B.

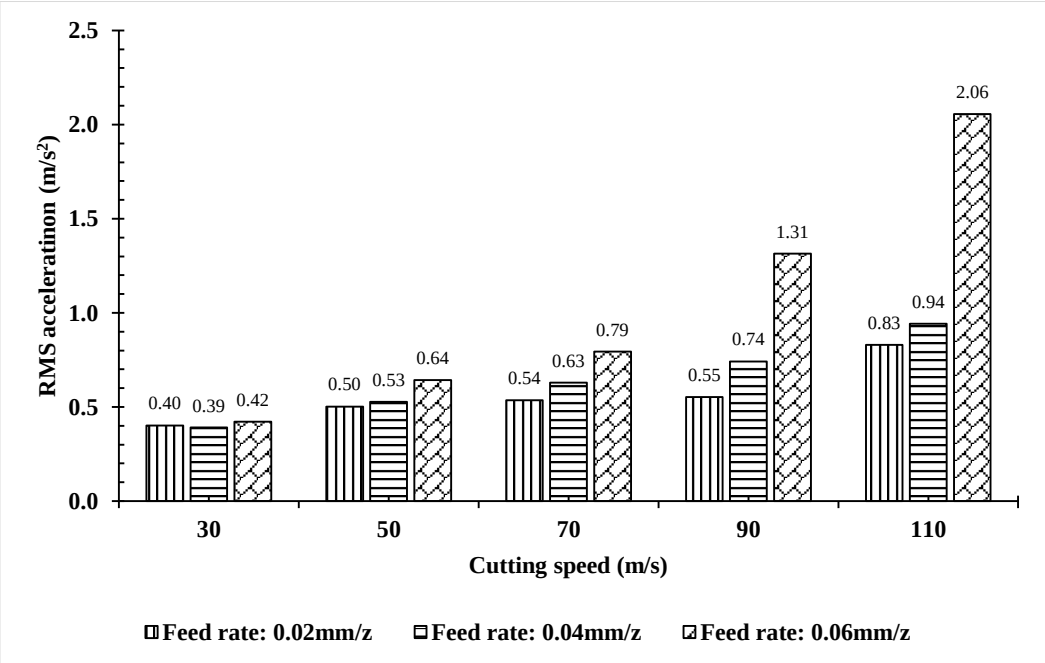

Fig. 4.19: RMS acceleration value against cutting speed in x-axis direction (cutting tool C, DoC$_a$: 0.3mm)

Fig. 4.20 presents the RMS acceleration value in y-axis direction under depth of cut 0.3mm. Based on the figures, the RMS acceleration values is ranging from 0.3m/s^2 to 0.87m/s^2 for cutting tool C. The highest RMS acceleration are observed at cutting parameters of (V= 110m/s, f= 0.06mm/z). While on the other cases, the vibration responses are increase and decreases slightly with the increase of cutting parameters.

In general, the comparison of vibration response in cutting tool A, B and C in y-axis direction shows that, the vibration responses in cutting tool A fluctuate the most with increases of cutting parameters while cutting tool B and C fluctuate the least. However, the vibration responses for cutting tool C are slightly higher as compare to cutting tool B.

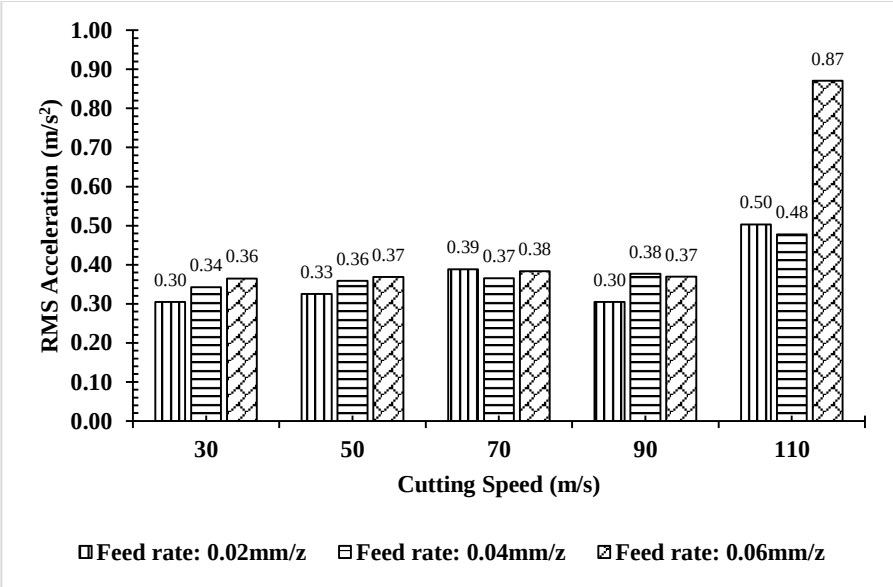

Fig. 4.20: RMS acceleration value against cutting speed in y-axis direction (cutting tool C, DoC$_a$: 0.3mm)

Fig. 4.21 shows the surface roughness of cutting tool C under depth of cut of 0.3mm. Based on the figure, it shows that the surface roughness values is ranging from 0.21µm to 0.36µm for cutting tool C. As compared to cutting tool A, in all of the cutting parameters, the surface roughness of cutting tool C are lower. On the other hand, the surface roughness for cutting tool B and cutting tool C are similar, in some cases, cutting tool B are higher than cutting tool C with a very small margin.

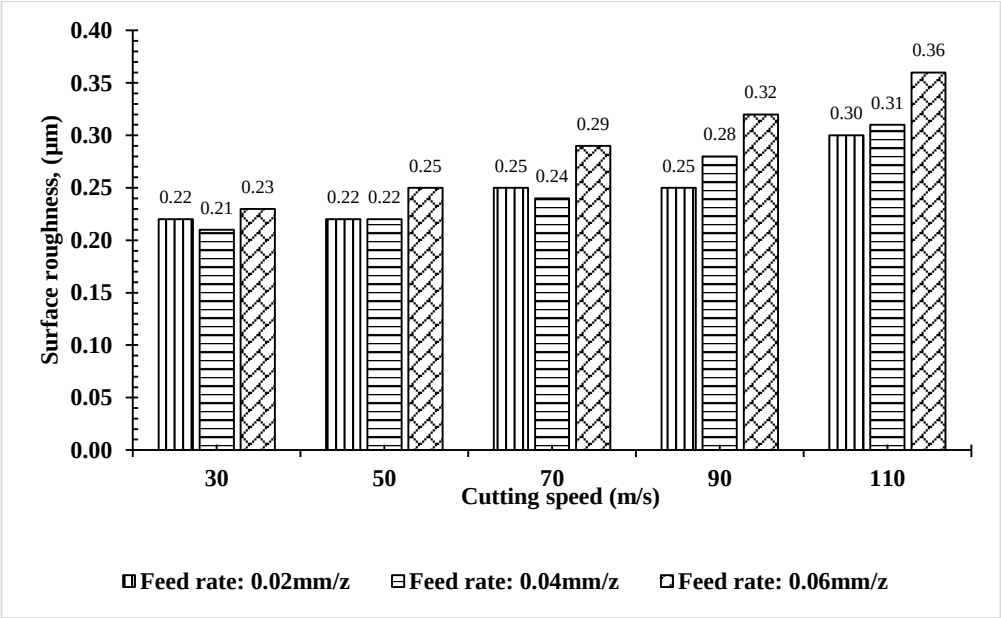

Fig. 4.21: Surface roughness against different cutting speed (Cutting tool C, DoC$_a$: 0.3mm)

4.5 Summary of Phase I Experimental Results on Vibration Responses and Surface Finish

Based on the experimental results which are discussed and compared in the previous section (***4.2*** to ***4.4***). It is observed that, the vibration responses are minimal at low cutting speed (30m/s to 50m/s) for all of cutting tools and the vibration responses increase significantly at high cutting speed (70m/s to 110m/s). Cutting tool A, B and C, show minimal vibration responses at low cutting speed might due to the process damping effect at low cutting speed region (Tunç and Budak 2012). Process damping occur due to the changing of actual clearance or relief angle of the tool edge while cutting on the micro wavy surface (Taylor et al. 2011). The indentation of the cutting tool into the machined surface is the source of damping forces. For illustration purposes, ***Fig. 4.22*** shows the variation of actual clearance angle on the wavy surface, from point A to point B, the indentation of the tool on the negative slope generates a ploughing force which is the source of damping force that oppose the cutting motion, therefore, reduces the vibration. From point B to point C, the transition of negative slope to positive slope subsequently induces a resistance force to the cutting motion which further reduces the vibration. In other words, the variation of phase shift between point A to C, and C to D creates a damping effect to the cutting process. This effects are enhanced when the slope of the wavy surface are steeper and therefore,

process damping effect will be increased. Furthermore, it is believed that the process damping effect will be greater with small relief angles on the cutting tool. In the current experiments, the measurement of the relief and clearance are not possible. Therefore, based on the experimental results, it can be assume that sharp corner tool has larger relief or clearance angle as compare to radius corner tool. Therefore, the vibration responses for sharp corner tool are higher as compared to corner radius tool. In addition, the variable helix and pitch features of the cutting tool also play a significant role in process damping, the regenerative effect is minimised by the feature of the tool. Therefore, the experimental results show high stability of milling process at low cutting speeds.

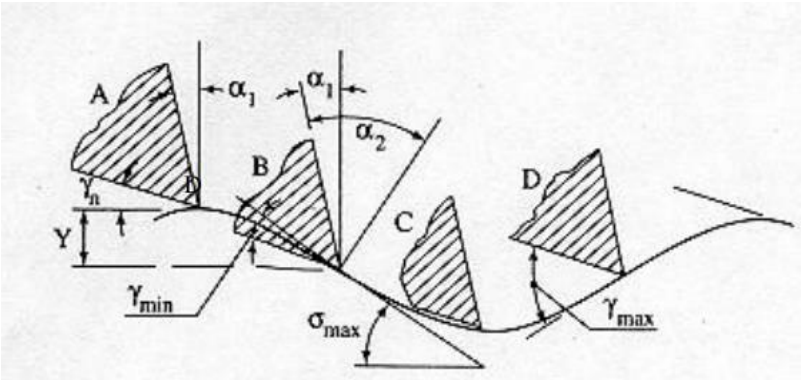

Fig. 4.22: Process damping mechanism illustration (Sam 2011)

On the other hand, the process damping effect diminished with the increase of cutting speed. Therefore, the milling process are more prone to chatter vibration. Cutting tool A exhibits the characteristic of severe chatter vibration in which excessive noise was heard, high vibration responses was obtained, and high surface roughness value was observed at high cutting parameters. As a comparison between slight chatter and severe chatter conditions, ***Fig. 4.23*** (a) and (c) show the Fast Fourier Transform diagram of cutting tool B under high cutting parameters. In the frequency band from 1.5k Hz to 2k Hz, it can be seen that the magnitude of FFT are around 500 to 1000. On the other hand, ***Fig. 4.23*** (b) and (d) show the FFT diagram of cutting tool A under the same cutting parameters, it can be seen that the magnitude at frequency band from 1.5k Hz to 2k Hz increases drastically. Therefore, it indicate that cutting tool A exhibits sever chatter vibrations at high cutting parameters as shown in ***Fig. 4.23*** (b) and (d).

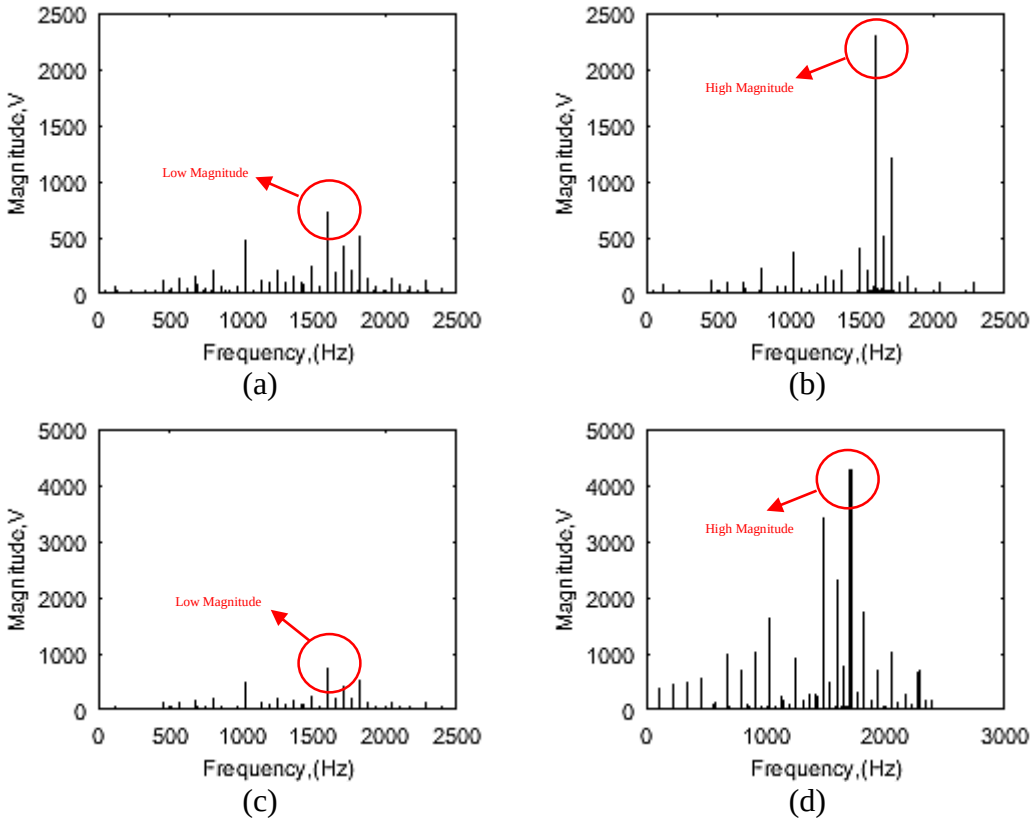

Fig. 4.23: FFT diagram (a) Slight chatter on cutting tool B (DoC$_a$: 0.1mm) (b) Severe chatter on cutting tool A (DoC$_a$: 0.1mm) (c) Slight chatter on cutting tool B (DoC$_a$: 0.3mm) (d) severe chatter on cutting tool A (DoC$_a$:0.3mm)

Based on the experimental results, the performance of cutting tools in term of stability of the process can be observed by considering the range of minimum and maximum values of RMS acceleration. ***Table 4.1*** shows the minimum and maximum RMS acceleration values for cutting tool A, B and C under cutting speed ranging from 30m/s to 110m/s and depth of cut of 0.1mm. It shows that cutting tool A, B, C have similar minimum RMS acceleration values in x-axis direction and y-axis direction which are between 0.32m/s^2 to 0.42m/s^2 at x-axis and 0.1m/s^2 to 0.37m/s^2 respectively. However, the maximum RMS acceleration values are not similar. For cutting tool A, the maximum value at x-axis direction are ranging from 0.97m/s^2 up to 5.55m/s^2, as for cutting tool B, the maximum RMS acceleration values are ranging from 0.50m/s^2 to 0.85m/s^2, while for cutting tool C, the maximum RMS acceleration values are ranging from 0.64m/s^2 to 1.79m/s^2. As for maximum RMS acceleration values in y-axis direction, the RMS acceleration values are ranging from 0.37m/s^2 to 1.37m/s^2, while cutting tool B ranging from 0.39m/s^2 to 0.42m/s^2, and cutting tool C ranging from 0.38m/s^2 to 0.68m/s^2. Based on the discussion above, it shows that cutting tool A generate the highest vibration and follow by cutting tool C and the least vibration

generated is cutting tool C under depth of cut of 0.1mm. In term of stability in milling process, cutting tool B are the most stable, follow by cutting tool C and least stable are cutting tool A. Similarly, ***Table 4.2*** shows the minimum and maximum RMS acceleration values for cutting tool A, B and C under cutting speed ranging from 30m/s to 110m/s and depth of cut of 0.3mm. The range of maximum and minimum RMS acceleration also suggested that cutting tool A exhibits highest vibration, follow by cutting tool C and least by cutting tool B.

Table 4.1: Minimum and maximum RMS acceleration value under depth of cut of 0.1mm

Cutting tool	Feed rate, (mm/z)	X-axis RMS value, (m/s^2)		Y-axis RMS value, (m/s^2)	
		Minimum	Maximum	Minimum	Maximum
A	0.02	0.42	0.97	0.13	0.37
	0.04	0.39	1.43	0.11	0.42
	0.06	0.32	5.55	0.10	1.37
B	0.02	0.39	0.51	0.37	0.39
	0.04	0.36	0.50	0.33	0.35
	0.06	0.40	0.85	0.34	0.42
C	0.02	0.36	0.64	0.35	0.38
	0.04	0.34	0.92	0.13	0.41
	0.06	0.39	1.79	0.29	0.68

***T*able 4.2: Maximum and minimum RMS acceleration value under depth of cut of 0.3mm**

Cutting tool	Feed rate, (mm/z)	X-axis RMS value, (m/s^2)		Y-axis RMS value, (m/s^2)	
		Minimum	Maximum	Minimum	Maximum
A	0.02	0.46	2.47	0.35	1.47
	0.04	0.48	3.07	0.33	1.72
	0.06	0.67	9.79	0.38	3.59
B	0.02	0.39	0.70	0.35	0.42
	0.04	0.28	1.30	0.23	0.48
	0.06	0.32	2.14	0.28	0.70
C	0.02	0.40	0.83	0.30	0.50
	0.04	0.39	0.94	0.34	0.48
	0.06	0.42	2.06	0.36	0.87

Table 4.3 shows the overall performance of variable helix cutting tools in term of surface roughness generated under cutting speed ranging from 30m/s to 110m/s and depth of cut (0.1mm and 0.3mm).

At depth of cut 0.1mm, cutting tool B achieve the best surface roughness at 0.17µm, follow by cutting tool C with surface roughness value of 0.19µm and lastly is cutting tool A with the surface roughness of 0.20 µm. The difference between the surface roughness produced by cutting tool A, B and C are only differ by 1µm. However, the worst surface roughness generated by cutting tool A, B and C are slightly higher margin. The highest surface roughness by cutting tool A is 0.42µm, follow by

cutting tool C with the value of 0.38µm and lastly cutting tool B with the value 0.34 µm. This signify that cutting tool B provides the best surface roughness quality and follow by cutting tool C and lastly is cutting tool A. At depth of cut of 0.3mm, similar trend are observed, in which cutting tool B outperform cutting tool C and cutting tool A.

In overall, the minimal surface roughness obtained in the current study are varies from 0.17 to 0.24µm. As a comparison to the recent literatures, Kumar et al. (2017) obtained surface roughness ranging from 0.8µm to 1.8µm when milling Inconel 718, D'Addona et al. (2017) obtained surface roughness ranging from 0.3 to 5.1µm and Mehta et al. (2018) obtained surface roughness ranging from 0.5µm to 0.6µm. Therefore, as compared to current study, there is an improvement of surface roughness.

Table 4.3: Minimum and maximum surface roughness under depth of cut 0.1mm and 0.3mm

Cutting tool	Feed rate, (mm/z)	Surface roughness, (µm) DoC_a= 0.1mm		Surface roughness, (µm) DoC_a=0.3mm	
		Minimum	Maximum	Minimum	Maximum
A	0.02	0.21	0.32	0.24	0.37
	0.04	0.20	0.34	0.23	0.36
	0.06	0.22	0.42	0.24	0.46
B	0.02	0.17	0.29	0.23	0.28
	0.04	0.17	0.27	0.22	0.29
	0.06	0.20	0.34	0.24	0.38
C	0.02	0.19	0.25	0.22	0.30
	0.04	0.20	0.29	0.21	0.31
	0.06	0.21	0.38	0.23	0.36

4.6 Parameters Evaluation

Based on the discussion in section ***4.5*** , it is clear that cutting tool B outperformed cutting tool A and perform slightly better than cutting tool C. In the following, the influences of each controlled parameters are discussed and evaluated to recommend the optimal combination of parameters which the vibration responses are as low as possible and also good surface quality for each of the cutting tool.

4.6.1 The Influences of Feed Rate on Vibration Responses and Surface Roughness

Based on the discussion from section ***4.2*** to ***4.4*** , it is evident that feed rate is one of the significant parameter that influences the vibration responses and also surface roughness. It is well documented that feed per tooth signify the constant loading on

the each of the cutting edge in the milling process. In order to maintain the constant feed per tooth with the increment of cutting speed, the table feed have to make an adjustment based cutting speed value. Therefore, the changes made on the table feed are directly influences the vibration responses and the surface roughness. In order to illustrate the effect of table feed, ***Fig. 4.24*** shows the table feed (mm/min) value at different No. of experiment. From experiment No.1 to No.5, the feed per tooth value is 0.02mm/z under cutting speed range of 30m/s to 110m/s, while the for experiment No.6 to No.10, the feed per tooth value is 0.04mm/z, lastly for experiment No.11 to No.15, the feed per tooth value is 0.06mm/z. Based on the figure, it can be seen that the table feed increase linearly from cutting speed of 30m/s to 110m/s. As the feed per tooth value increases, the gradient of the table feed become steeper. This explained that, in the current experiments, it is observed that little influences on the vibration responses and surface roughness when the feed per tooth value is 0.02mm/z. However, when the feed per tooth value increases to 0.06mm/z, it is observed that the vibration responses and surface roughness increases drastically especially at high cutting speed which is due to the increase of table feed. Table feed has a direct impact on the productivity, the higher the value of table feed, the time taken for a complete cutting process will be shorter. However, the increases of table feed causes high frictional force especially during the milling process of Inconel 718 which result in high vibration responses which are observed in the current experiments. Therefore, based on the current experimental results, it is recommended that the feed per tooth of 0.04mm/z is the optimal value, which in most of the cases, low vibration responses and adequate surface roughness value can be achieved for all of the cutting tools.

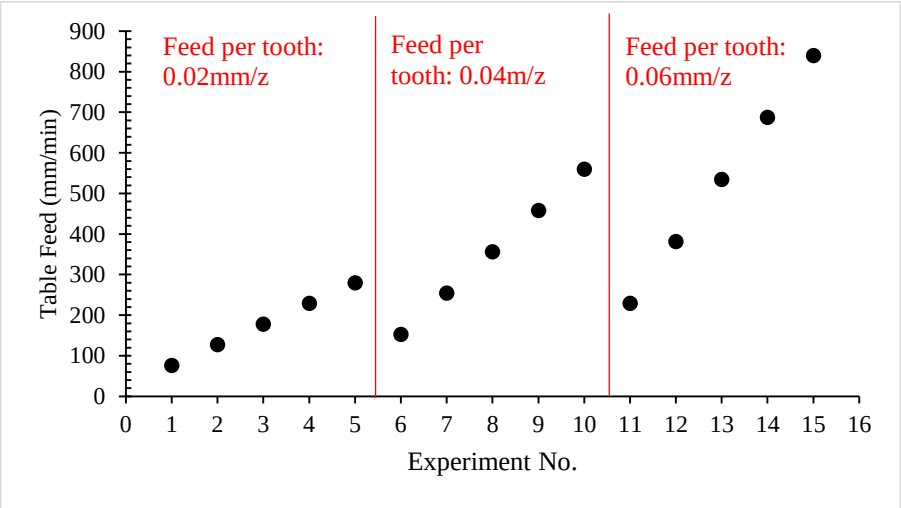

Fig. 4.24: The effect of feed rate on table feed at cutting speed varies from 30m/s to 110m/s

4.6.2 The Influences of Cutting Speed on Vibration responses and Surface Roughness

In the current study, the cutting speed covers from 30m/s to 110m/s in the milling process of Inconel 718. The range of cutting speed are consider from low cutting speed to high cutting speed region which defined by (Schulz and Moriwaki 1992). Based on the experimental results which have been discussed in section ***4.2*** to ***4.4*** , at most of the cases, the vibration responses are minimal at cutting range of 30m/s to 50m/s, while at high cutting speed (70m/s to 110m/s), vibration responses increases significantly.

In machining process of Inconel 718, the tendency of work hardening of the material often due to high cutting temperatures at high cutting speed (Liu et al. 2015). Therefore, the vibration responses increases drastically during high cutting speed. In some cases, the chip are welded on the workpiece after the cutting process. Based on the observation in the experiments, it is found that cutting tool A (sharp corner) are tend to produced welded chip on the workpiece as illustrated at ***Fig. 4.25***, which (a) illustrated the serrated shape chip welded on workpiece, and (b) a small portion of the chip was welded on the workpiece. This phenomena mostly occured for cutting tool A and least on cutting tool B and C when machine in high cutting parameters. This phenomena will impose a resistance to the cutting process during consecutive cutting which will decrease the performance of machinability including high vibration responses and bad surface roughness.

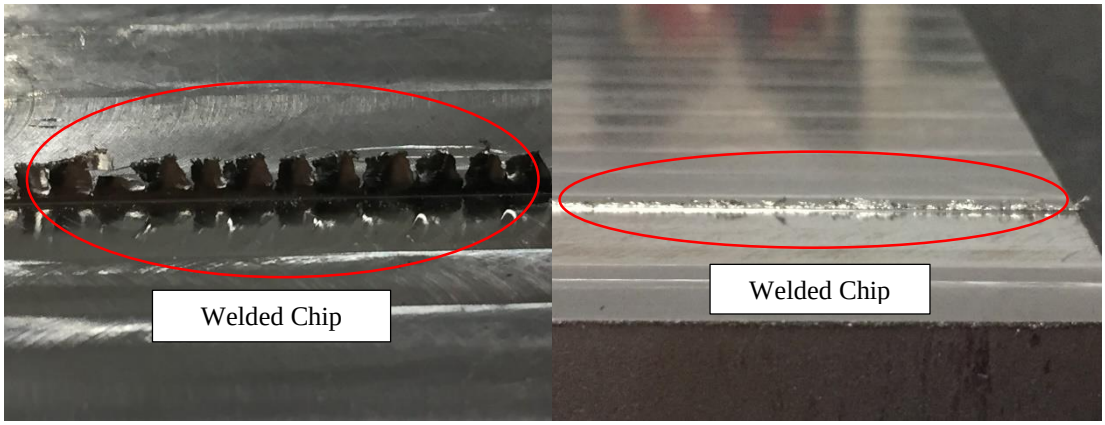

(a) (b)

Fig. 4.25: Welded chip on the workpiece (a) Extreme case (b) Mild case

Based on the investigated parameters, the suitable feed rate for the current scope of study is 0.04mm/z which have been discussed in section ***4.6.1*** . Therefore, a moderate cutting speed (50m/s) are recommended to avoid high cutting temperatures and chatter vibration, and to achieve good surface roughness for cutting tool A, B and C. ***Fig. 4.26*** to ***Fig. 4.28*** show the minimal vibration responses and low surface roughness achieve when cutting tool A, B and C are performed under cutting speed of 50m/s. The optimal vibration response and minimal surface roughness for cutting tool A is 0.55m/s^2 and surface roughness of 0.23µm. As for cutting tool B, the RMS acceleration value is 0.43m/s^2 and surface roughness of 0.17µm. For cutting tool C, the RMS acceleration responses is 0.44m/s^2 and surface roughness of 0.22µm.

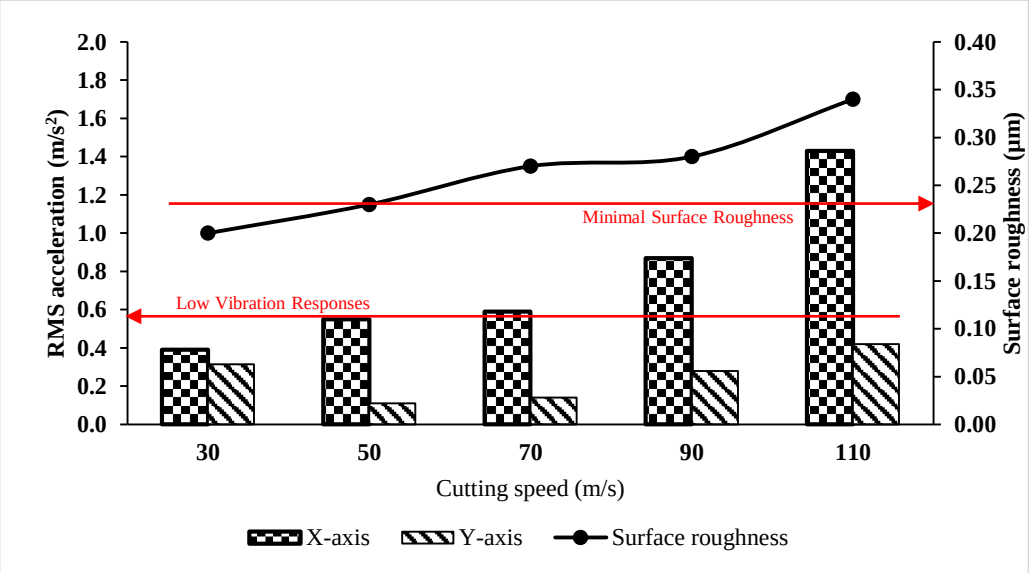

Fig. 4.26: RMS acceleration and surface roughness under constant feed rate of 0.04mm/z and depth of cut 0.1mm (Cutting tool A)

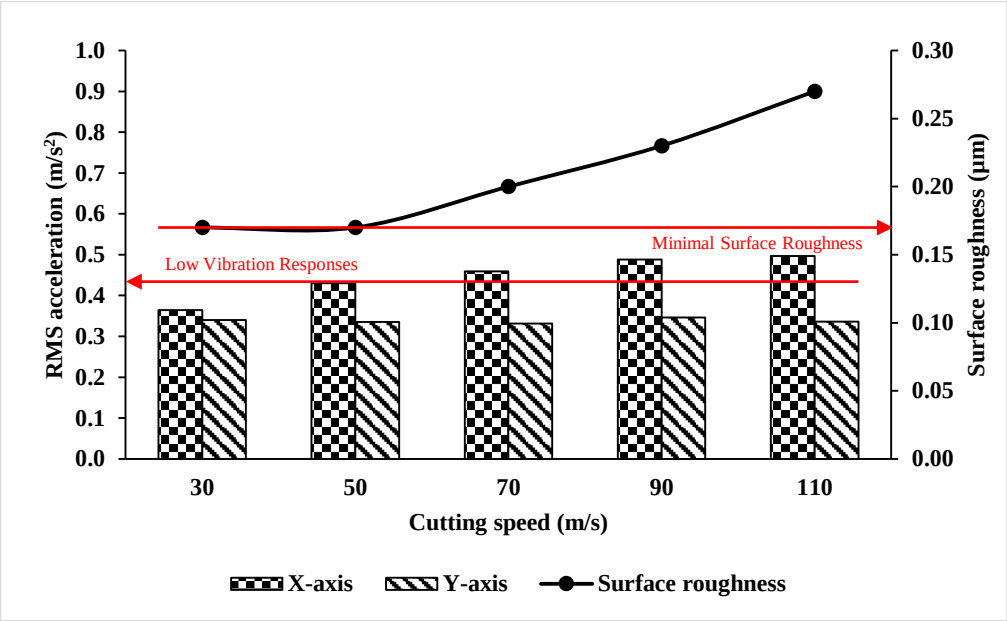

Fig. 4.27: RMS acceleration and surface roughness under constant feed rate of 0.04mm/z and depth of cut 0.1mm (Cutting tool B)

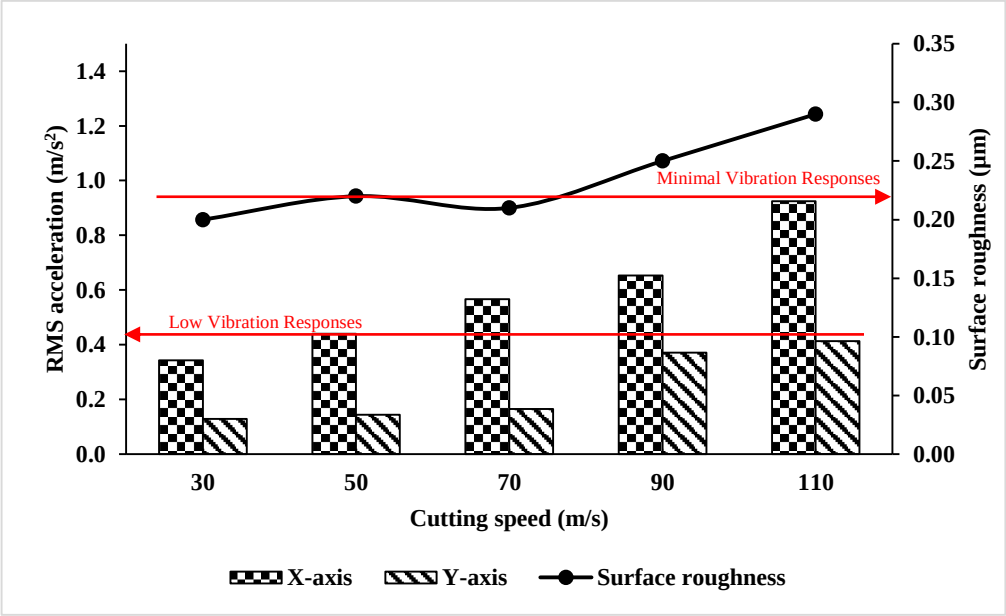

Fig. 4.28: RMS acceleration and surface roughness under constant feed rate of 0.04mm/z and depth of cut 0.1mm (Cutting tool C)

4.6.3 The Influences of Depth of Cut on Vibration Responses and Surface Roughness

Depending on the end user, varying depth of cut is useful to increase the productivity, avoid chatter vibration or to achieve a desire shape of the product by specifically selecting the depth of cut. In the current study, there are two level depth of cut (0.1mm, and 0.3mm), it is consider as very low depth of cut which usually focused on surface finishing process. Form this experiments, it is observed that the increase of depth of cut will increase the vibration intensity as well as a slight increase in surface roughness. However, there are little influences on the surface roughness at low cutting speed due process damping effect. In addition, increasing depth of cut at high cutting speed and feed rate will adversely affect the surface roughness and vibration intensity. Therefore, the increase of depth of cut at low cutting parameters are viable for all of the cutting tool to achieve low vibration responses and adequate surface roughness.

4.7 Best Combination of Parameters for All Cutting Tool

Below is the suggestion and recommendation on the cutting parameters used to machine Inconel 718 for cutting tool A, B and C. The recommendation are based on the experimental data observed and discussed from section ***4.1*** to ***4.6*** The milling process are carried out under dry conditions, down milling mode and constant radial depth of cut. The recommended cutting parameters are to achieve surface roughness within 0.17µm to 0.25µm as well as low vibration responses with adequate productivity.

Cutting tool A, B and C:

Cutting speed: 50m/s, Feed rate: 0.04mm/z, Depth of cut: 0.1mm

Cutting tool A:

i) Cutting speed: 30m/s, Feed rate: 0.06mm/z, Depth of cut: 0.1mm

ii) Cutting speed: 30ms, Feed rate: 0.04mm/z, Depth of cut: 0.3mm

Cutting tool B:

i) Cutting speed: 50m/s, Feed rate: 0.04mm/z, Depth of cut: 0.1mm

ii) Cutting speed: 50ms, Feed rate: 0.04mm/z, Depth of cut: 0.3mm

Cutting tool C:

i) Cutting speed: 50m/s, Feed rate: 0.04mm/z, Depth of cut: 0.1mm

ii) Cutting speed: 50ms, Feed rate: 0.04mm/z, Depth of cut: 0.3mm

4.8 Tool Wear Progression and Vibration Responses based on Optimal Cutting Parameters

In order to evaluate the tool wear progression during the milling process of Inconel 718, experiments are carried out to qualitatively observe the progression of tool wear and to the vibration responses on different cutting passes. Cutting tool A, B and C undergo the optimal cutting parameters (cutting speed: 50m/s, Feed rate: 0.04mm/z, Depth of cut: 0.1mm) for 50 cutting passes. The milling process are carried out under dry conditions, down milling mode as well as constant radial depth of cut. The tool wear progression at every 10 interval of cutting pass can be referred to APPENDIX I.

Fig. 4.29 and ***Fig. 4.30*** present the vibration responses at increasing number of cutting passes under depth of cut of 0.1mm and 0.3mm respectively. It is observed that the RMS acceleration values increases with the increase of cutting passes which is due to the development of tool wear. The vibration responses for depth of cut 0.3mm are generally higher than 0.1mm. On the other hand, among cutting tool A, B, and C, cutting tool A exhibits higher RMS acceleration values with the increase of cutting passes. Meanwhile, cutting tool B and cutting tool C exhibits similar vibration responses in which one may higher or lower than another. Therefore, it further proven that the corner radius cutting tool outperform sharp corner tool.

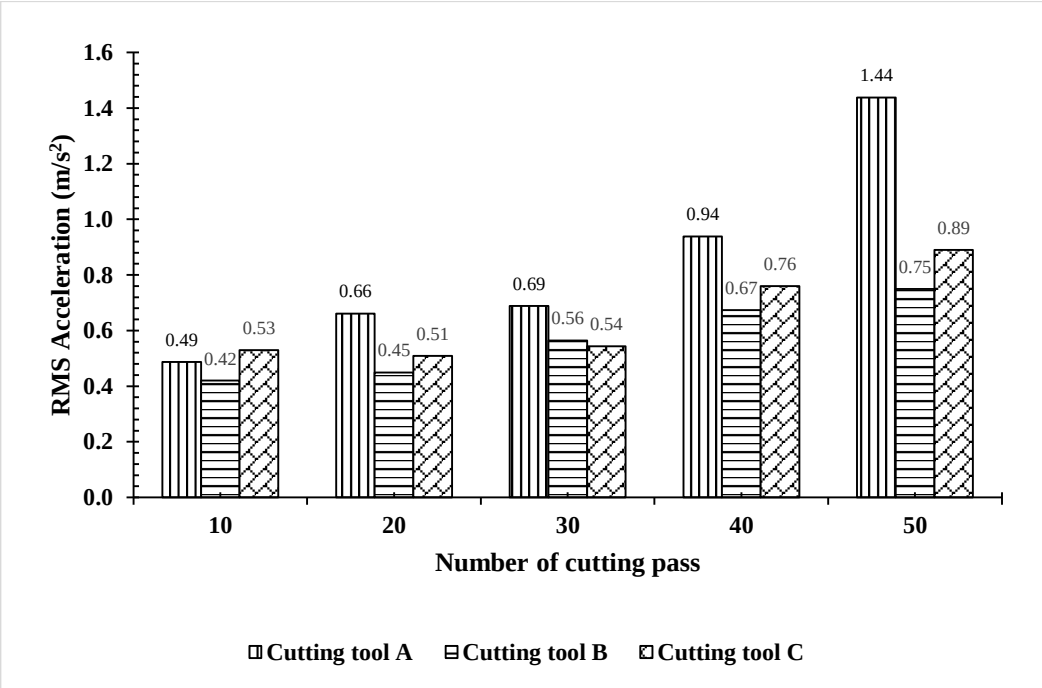

Fig. 4.29: RMS Acceleration value at different number of cutting pass for depth of cut 0.1mm

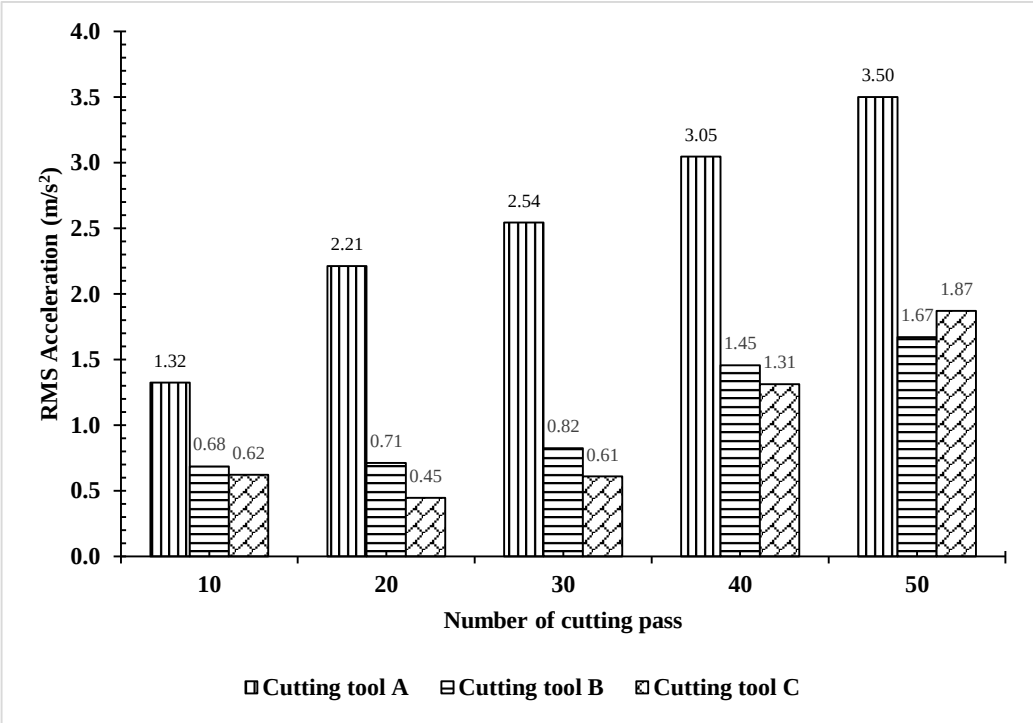

Fig. 4.30: RMS Acceleration value at different number of cutting pass for depth of cut 0.3mm

Fig. 4.31 and ***Fig. 4.32*** shows the development of tool wear on the 50 cutting passes and also the corresponding frequency spectrum plot at depth of cut of 0.1mm and 0.3mm respectively. Based on ***Fig. 4.31***, it is observed that cutting tool A yield the highest wear rate and follow by cutting tool C and least by cutting tool B. In the

frequency spectrum, it is noted that the magnitude of the frequency spectrum the tooth pass frequency are highest for cutting tool A with the value of 266, follow by cutting tool C with value of 132 and the least by cutting tool B with the magnitude of 97. The magnitude of the frequency spectrum plot implies the vibration intensity at the tooth pass frequency during the machining process. Therefore, it shows that, at 50 cutting passes, cutting tool A has the highest development of tool wear and also higher vibration responses and the least is cutting tool B.

Meanwhile, ***Fig. 4.32*** shows the vibration responses and the tool wear progression on 50 cutting passes under depth of cut of 0.3mm. The vibration responses increases about double as compared to the vibration responses obtained in depth of cut of 0.1mm. For cutting tool A, a severe deformation of cutting tool edge was observed which lead to the magnitude of 468 at its tooth pass frequency shown in the frequency spectrum plot. As for cutting tool B, the progression of tool wear are less severe compared to cutting tool A, the frequency spectrum plot shows the magnitude of 225 at the tooth pass frequency which the intensity almost half of cutting tool A. Similarly, the tool wear observed on cutting tool C are not as severe as cutting tool A, the frequency spectrum plot shows a magnitude of 265 at the tooth pass frequency. Therefore, cutting tool B outperform cutting tool A and perform slightly better than cutting tool C.

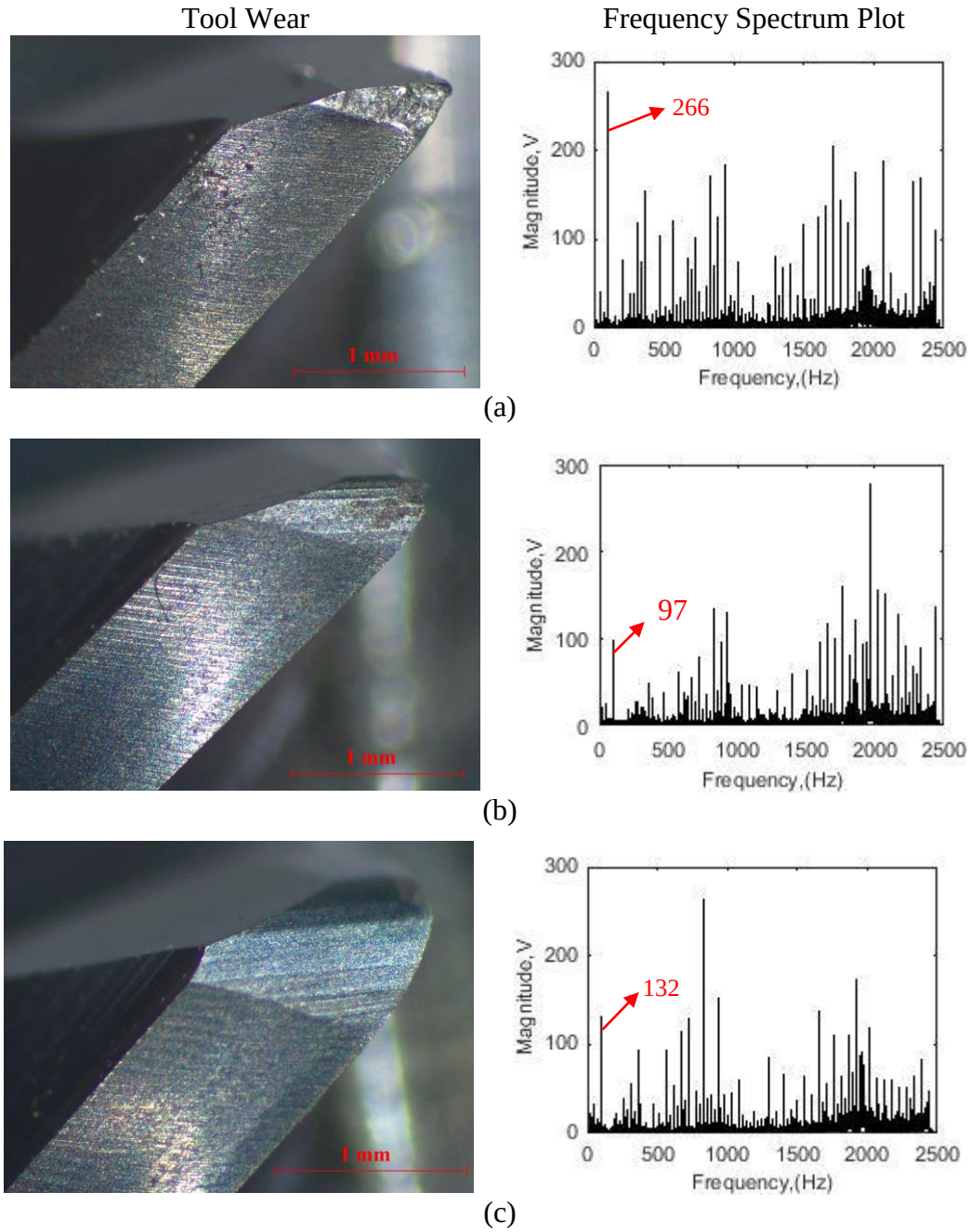

Fig. 4.31: Tool wear and FFT diagram at 50 cutting passes under DoCa : 0.1mm (a) Cutting tool (b) Cutting tool B (c) Cutting tool C

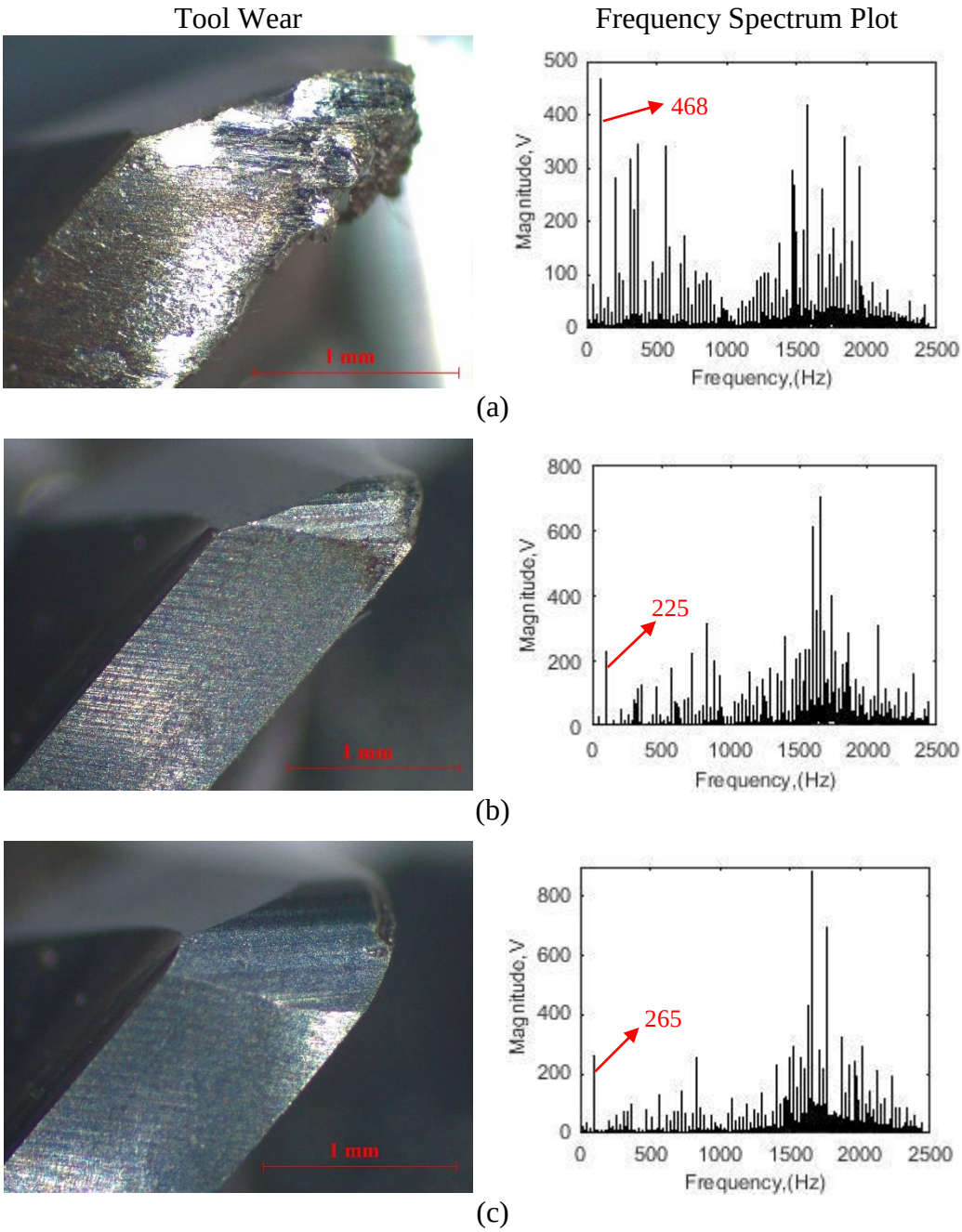

Fig. 4.32: Tool wear and FFT diagram at 50 cutting passes under DoCa: 0.3mm (a) Cutting tool (b) Cutting tool B (c) Cutting tool C

Chapter 5: Conclusion and Recommendation

This chapter summarises the key findings on the performance in the end milling process of Inconel 718 by using variable helix and pitch cutting tools with or without corner radius. It also provides the recommendations for future research in this area.

5.1 General Discussion

The productivity of machining process often hindered by the chatter vibration especially in the milling process of difficult-to-cut material: Inconel 718. The recent developed cutting tool known as variable helix and pitch cutting tool are able to reduce chatter vibration which was well documented in the literatures. In the current research work, the performance of variable helix and pitch cutting tool with sharp corner and radius corner are investigated and analysed experimentally in the milling process of Inconel 718.

Based on the initial observation on the vibration responses in time-domain signal, sharp corner tool (cutting tool A) shows the highest peak to peak value follow by 1.0mm corner radius tool (cutting tool C) and least by 0.5mm corner radius tool (cutting tool B). The RMS acceleration values and surface roughness were computed for further discussion and analysis. Based on the comparison of RMS acceleration values and surface roughness generated by all the cutting tools, the general trend observed is that the vibration responses amplitude retained at minimal at low cutting speed (30m/s to 50m/s) which shows only a little influence to the surface roughness. In addition, variable helix and pitch cutting tool with corner radius shows even lower vibration responses and better surface roughness at low cutting speeds which could be due to the corner radius tool having a lower relief angle as compared to sharp corner tool, as a results, the stability of process damping effect increases. However, at high cutting speed (70m/s to 110m/s), the vibration responses for sharp corner tool increases significantly while the vibration responses for 0.5mm corner radius tool and 1.0mm corner radius cutting tool increase gradually. This could be due to the increase of thermal stress sustained by the sharp corner which causes high cutting temperature and welded chip on the workpiece. Based on the observation in the experiments, the feed

rate influences the vibration responses and surface roughness exponentially at high cutting speed. Therefore, moderate feed rate is the best option to suit the best productivity without compromising the machinability. In addition, sharp tool corner cutting tool show high cutting temperature which causes difficulties in chip disposal and welded onto the workpiece while this phenomena was not observed for cutting tool with corner radius, it also causes chatter vibration at high cutting speed and feed rate. Based on the observation of tool wear progression, the wear rate of cutting tool with radius corner are lower as compared to sharp corner. Therefore, cutting tool with corner radius are expected to preserve longer tool life.

5.2 Summary of Conclusions

As a conclusion, variable helix and pitch cutting tools show high stability in milling process of Inconel 718 at low cutting speed with good machinability. In addition, tool corner geometry plays a significant role in achieving even lower vibration responses and good surface roughness. In term of cutting tools performance in machinability of Inconel 718, cutting tool with corner radius of 0.5mm had performed better than cutting tool with corner radius of 1.0mm, and cutting tool with sharp corner performed the least.

The summary of conclusions are listed as follows:

One of the recent developed tools are the variable helix and pitch cutting tool. Three tool corner geometries are used: (1) sharp corner, (2) 0.5mm radius corner, and (3) 1.0mm radius corner in the milling process of Inconel 718. The performance of the cutting tools are evaluated based on the vibration responses and surface roughness which is one of the objective in this research work.

- Minimal vibration responses and low surface roughness (0.17µm to 0.24µm) are obtained by all cutting tools at low cutting speeds (30m/s to 50m/s) with moderate feed rate (0.04mm/z).
- At high cutting speed (70m/s to 110m/s) with feed rate (0.04mm/z and 0.06mm/z), variable helix and pitch cutting tool with corner radius exhibits much lower vibration responses as compared to variable helix and pitch cutting tool with sharp corner. Accordingly, the tool with corner radius reduces the

maximum surface roughness to 0.36µm as compared to cutting tool with sharp corner to 0.46 µm.

- The best combination of cutting parameters are identified as cutting speed (50m/s), feed rate (0.04mm/z), and under finishing conditions (low depth of cut) based on the experimental results to achieve low vibration responses and good surface roughness.
- The tool corner geometry has a significant effect on the vibration responses, surface roughness and tool wear in the milling process of Inconel 718. Corner radius tool exhibits much lower vibrations, lower tool wear, and better surface roughness as compared to sharp corner cutting tools. Therefore, based on the observation of tool wear progression, variable helix and pitch tool with corner radius are expected to preserve longer tool life.

In summary, variable helix and pitch cutting tools (with corner radius) show high stability in the milling process of Inconel 718 with good surface finish, lower tool wear, as well as minimal vibration responses at selective cutting parameters as a results of the improved stability region in process damping due to the lower relief angle of the tool.

5.3 Recommendation for Future Work

This research work has provided useful insight for the milling process of Inconel 718 with variable helix and pitch cutting tool in term of vibration responses and its machinability. The following recommendations are suggested for future studies:

- Performance of the variable helix and pitch cutting tool to manufacture complex geometry.
- Optimisation of corner radius with experimental and numerical method to address chatter vibration problem at high cutting speeds specifically on difficult-to-cut materials.
- Further experimental study can consider other parameters such as radial depth of cut, higher value of depth of cut, and other tool material with variable helix and pitch features.
- Comparison of conventional tool and variable helix/pitch tool on the performance of Inconel 718.

REFERENCE

Akhtar, Waseem, Jianfei Sun, and Wuyi Chen. 2016. "Effect of Machining Parameters on Surface Integrity in High Speed Milling of Super Alloy Gh4169/Inconel 718." *Materials and Manufacturing Processes* 31 (5): 620-627

Al-Regib, Emad, Jun Ni, and Soo-Hun Lee. 2003. "Programming Spindle Speed Variation for Machine Tool Chatter Suppression." *International Journal of Machine Tools and Manufacture* 43 (12): 1229-1240

Alauddin, M., M. A. El Baradie, and M. S. J. Hashmi. 1995. "Tool-Life Testing in the End Milling of Inconel 718." *Journal of Materials Processing Technology* 55 (3–4): 321-330

Alauddin, M., M. A. El Baradie, and M. S. J. Hashmi. 1996. "Modelling of Cutting Force in End Milling Inconel 718." *Journal of Materials Processing Technology* 58 (1): 100-108

Alauddin, M., M. A. Mazid, M. A. El Baradi, and M. S. J. Hashmi. 1998. "Cutting Forces in the End Milling of Inconel 718." *Journal of Materials Processing Technology* 77 (1–3): 153-159

Altin, A., M. Nalbant, and A. Taskesen. 2007. "The Effects of Cutting Speed on Tool Wear and Tool Life When Machining Inconel 718 with Ceramic Tools." *Materials & Design* 28 (9): 2518-2522

Altintaş, Y, and E Budak. 1995. "Analytical Prediction of Stability Lobes in Milling." *CIRP Annals-Manufacturing Technology* 44 (1): 357-362

Altıntaş, Y., S. Engin, and E. Budak. 1999. "Analytical Stability Prediction and Design of Variable Pitch Cutters." *Journal of Manufacturing Science and Engineering* 121 (2): 173-178

Altintas, Y., M. Eynian, and H. Onozuka. 2008. "Identification of Dynamic Cutting Force Coefficients and Chatter Stability with Process Damping." *CIRP Annals* 57 (1): 371-374

Altintas, Yusuf. 2001. "Analytical Prediction of Three Dimensional Chatter Stability in Milling." *JSME International Journal Series C Mechanical Systems, Machine Elements and Manufacturing* 44 (3): 717-723

Altintas, Yusuf. 2012. *Manufacturing Automation: Metal Cutting Mechanics, Machine Tool Vibrations, and Cnc Design*: Cambridge university press.

Anhai, Li, Zhao Jun, Zheng Guangming, and Pei Zhiqiang. 2011. "Machined Surface Roughness and Chip Morphology in High Speed Side Milling of Inconel 718" *Consumer Electronics, Communications and Networks (CECNet), 2011 International Conference on*, doi: 10.1109/CECNET.2011.5768874.

Aramcharoen, Ampara, and Shaw Kah Chuan. 2014. "An Experimental Investigation on Cryogenic Milling of Inconel 718 and Its Sustainability Assessment." *Procedia CIRP* 14: 529-534

Bhatt, Abhay, Helmi Attia, R. Vargas, and V. Thomson. 2010. "Wear Mechanisms of Wc Coated and Uncoated Tools in Finish Turning of Inconel 718." *Tribology International* 43 (5–6): 1113-1121

Bonifacio, M. E. R., and A. E. Diniz. 1994. "Correlating Tool Wear, Tool Life, Surface Roughness and Tool Vibration in Finish Turning with Coated Carbide Tools." *Wear* 173 (1–2): 137-144

Bouzakis, K. D., S. Gerardis, G. Katirtzoglou, S. Makrimallakis, N. Michailidis, and E. Lili. 2008. "Increasing Tool Life by Adjusting the Milling Cutting Conditions According to Pvd Films' Properties." *CIRP Annals* 57 (1): 105-108

Budak, E., and L. T. Tunc. 2010. "Identification and Modeling of Process Damping in Turning and Milling Using a New Approach." *CIRP Annals* 59 (1): 403-408

Bushlya, V., J. Zhou, and J. E. Ståhl. 2012. "Effect of Cutting Conditions on Machinability of Superalloy Inconel 718 During High Speed Turning with Coated and Uncoated Pcbn Tools." *Procedia CIRP* 3: 370-375

Cai, Xiaojiang, Sheng Qin, Junli Li, Qinglong An, and Ming Chen. 2014. "Experimental Investigation on Surface Integrity of End Milling Nickel-Based Alloy— Inconel 718." *Machining Science and Technology* 18 (1): 31-46

Chen, Y. C., and Y. S. Liao. 2003. "Study on Wear Mechanisms in Drilling of Inconel 718 Superalloy." *Journal of Materials Processing Technology* 140 (1): 269-273

Chung, B., S. Smith, and J. Tlusty. 1997. "Active Damping of Structural Modes in High-Speed Machine Tools." *Journal of Vibration and Control* 3 (3): 279-295

Costes, J. P., Y. Guillet, G. Poulachon, and M. Dessoly. 2007. "Tool-Life and Wear Mechanisms of Cbn Tools in Machining of Inconel 718." *International Journal of Machine Tools and Manufacture* 47 (7–8): 1081-1087

D'Addona, D. M., Sunil J. Raykar, and M. M. Narke. 2017. "High Speed Machining of Inconel 718: Tool Wear and Surface Roughness Analysis." *Procedia CIRP* 62: 269-274

Debnath, Sujan, Moola Mohan Reddy, and Qua Sok Yi. 2014. "Environmental Friendly Cutting Fluids and Cooling Techniques in Machining: A Review." *Journal of Cleaner Production* 83: 33-47

Denkena, B., and D. Biermann. 2014. "Cutting Edge Geometries." *CIRP Annals - Manufacturing Technology* 63 (2): 631-653

Devillez, A., G. Le Coz, S. Dominiak, and D. Dudzinski. 2011. "Dry Machining of Inconel 718, Workpiece Surface Integrity." *Journal of Materials Processing Technology* 211 (10): 1590-1598

Dohner, Jeffrey L., James P. Lauffer, Terry D. Hinnerichs, Natarajan Shankar, Mark Regelbrugge, Chi-Man Kwan, Roger Xu, Bill Winterbauer, and Keith Bridger. 2004. "Mitigation of Chatter Instabilities in Milling by Active Structural Control." *Journal of Sound and Vibration* 269 (1): 197-211

Endres, William J., and Raja K. Kountanya. 2002. "The Effects of Corner Radius and Edge Radius on Tool Flank Wear." *Journal of Manufacturing Processes* 4 (2): 89-96

Eppel, Andras, Eniko T. Enikov, Tamas Insperger, and Stepan Gabor. 2010. "Feasibility Study of Optical Detection of Chatter Vibration During Milling." *International Journal of Optomechatronics* 4 (2): 195-214

Ezugwu, E. O., J. Bonney, and Y. Yamane. 2003. "An Overview of the Machinability of Aeroengine Alloys." *Journal of Materials Processing Technology* 134 (2): 233-253

Fan, YiHang, ZhaoPeng Hao, MinLi Zheng, FengLian Sun, and ShuCai Yang. 2013. "Study of Surface Quality in Machining Nickel-Based Alloy Inconel 718." *The International Journal of Advanced Manufacturing Technology* 69 (9-12): 2659-2667

Fei, Jixiong, Bin Lin, Shuai Yan, Mei Ding, Juliang Xiao, Jin Zhang, Xiaofeng Zhang, Chunhui Ji, and Tianyi Sui. 2017. "Chatter Mitigation Using Moving Damper." *Journal of Sound and Vibration* 410: 49-63

Friedrich, Jens, Christoph Hinze, Anton Renner, Alexander Verl, and Armin Lechler. 2017. "Estimation of Stability Lobe Diagrams in Milling with Continuous

Learning Algorithms." *Robotics and Computer-Integrated Manufacturing* 43: 124-134

Friedrich, Jens, Jonas Torzewski, and Alexander Verl. 2018. "Online Learning of Stability Lobe Diagrams in Milling." *Procedia CIRP* 67: 278-283

Gradišek, Janez, Martin Kalveram, Tamás Insperger, Klaus Weinert, Gábor Stépán, Edvard Govekar, and Igor Grabec. 2005. "On Stability Prediction for Milling." *International Journal of Machine Tools and Manufacture* 45 (7): 769-781

Groover, Mikell P. 2007. *Fundamentals of Modern Manufacturing : Materials, Processes, and Systems*: Third edition. Hoboken, NJ : J. Wiley & Sons, [2007] ©2007.

Gurdal, Ozan, Erdem Ozturk, and Neil D. Sims. 2016. "Analysis of Process Damping in Milling." *Procedia CIRP* 55: 152-157

Hadi, M. A., J. A. Ghani, C. H. Che Haron, and M. S. Kasim. 2013. "Comparison between up-Milling and Down-Milling Operations on Tool Wear in Milling Inconel 718." *Procedia Engineering* 68: 647-653

Hahn, R. S. 1951. "Design of Lanchester Damper for Elimination of Metal Cutting Chatter." *Trans. ASME* 73: 331

Henninger, Christoph, and Peter Eberhard. 2008. "Improving the Computational Efficiency and Accuracy of the Semi-Discretization Method for Periodic Delay-Differential Equations." *European Journal of Mechanics - A/Solids* 27 (6): 975-985

Huang, Pan Ling, Jian Feng Li, Jie Sun, and Jun Zhou. 2014. "Study on Performance in Dry Milling Aeronautical Titanium Alloy Thin-Wall Components with Two Types of Tools." *Journal of Cleaner Production* 67: 258-264

Huang, Panling, Jianfeng Li, Jie Sun, and Maojie Ge. 2012. "Milling Force Vibration Analysis in High-Speed-Milling Titanium Alloy Using Variable Pitch Angle Mill." *The International Journal of Advanced Manufacturing Technology* 58 (1): 153-160

Huang, Panling, Jianfeng Li, Jie Sun, and Jun Zhou. 2013. "Study on Vibration Reduction Mechanism of Variable Pitch End Mill and Cutting Performance in Milling Titanium Alloy." *The International Journal of Advanced Manufacturing Technology* 67 (5): 1385-1391

Insperger, Tamás, and Gábor Stépán. 2004. "Updated Semi-Discretization Method for Periodic Delay-Differential Equations with Discrete Delay." *International Journal for Numerical Methods in Engineering* 61 (1): 117-141

Ítalo Sette Antonialli, Armando, Anselmo Eduardo Diniz, and Robson Pederiva. 2010. "Vibration Analysis of Cutting Force in Titanium Alloy Milling." *International Journal of Machine Tools and Manufacture* 50 (1): 65-74

Jawaid, A., S. Koksal, and S. Sharif. 2001. "Cutting Performance and Wear Characteristics of Pvd Coated and Uncoated Carbide Tools in Face Milling Inconel 718 Aerospace Alloy." *Journal of Materials Processing Technology* 116 (1): 2-9

Junxue, Ren, Xu Yingying, Liang Yongshou, Yao Changfeng, and Shao Guangpeng. 2014. "Cutting Forces, Tool Life, and Size Effect of Passivated Cutters in Milling of Inconel 718" *Innovative Design and Manufacturing (ICIDM), Proceedings of the 2014 International Conference on*, doi: 10.1109/IDAM.2014.6912686.

Kasim, M. S., C. H. Che Haron, J. A. Ghani, M. A. Sulaiman, and M. Z. A. Yazid. 2013. "Wear Mechanism and Notch Wear Location Prediction Model in Ball Nose End Milling of Inconel 718." *Wear* 302 (1–2): 1171-1179

Khan, S. A., S. L. Soo, D. K. Aspinwall, C. Sage, P. Harden, M. Fleming, A. White, and R. M'Saoubi. 2012. "Tool Wear/Life Evaluation When Finish Turning Inconel 718 Using Pcbn Tooling." *Procedia CIRP* 1: 283-288

Kim, S. K., T. H. Kim, J. Wöhle, and K. T. Rie. 2000. "Ticn Coatings on Aluminum Alloy Formed by Mo-Pacvd." *Surface and Coatings Technology* 131 (1): 121-126

Krain, H. R., A. R. C. Sharman, and K. Ridgway. 2007. "Optimisation of Tool Life and Productivity When End Milling Inconel 718tm." *Journal of Materials Processing Technology* 189 (1–3): 153-161

Kumar, Sunil, Dilbag Singh, and Nirmal S. Kalsi. 2017. "Experimental Investigations of Surface Roughness of Inconel 718 under Different Machining Conditions." *Materials Today: Proceedings* 4 (2, Part A): 1179-1185

Kuo, Chun‐Pao, Sen‐Chieh Su, and Shao‐Hsien Chen. 2010. "Tool Life and Surface Integrity When Milling Inconel 718 with Coated Cemented Carbide Tools." *Journal of the Chinese Institute of Engineers* 33 (6): 915-922

Lauro, C. H., L. C. Brandão, D. Baldo, R. A. Reis, and J. P. Davim. 2014. "Monitoring and Processing Signal Applied in Machining Processes – a Review." *Measurement* 58: 73-86

Le Coz, G., and D. Dudzinski. 2014. "Temperature Variation in the Workpiece and in the Cutting Tool When Dry Milling Inconel 718." *The International Journal of Advanced Manufacturing Technology* 74 (5-8): 1133-1139

Li, H. Z., H. Zeng, and X. Q. Chen. 2006. "An Experimental Study of Tool Wear and Cutting Force Variation in the End Milling of Inconel 718 with Coated Carbide Inserts." *Journal of Materials Processing Technology* 180 (1–3): 296-304

Li, W., Y. B. Guo, M. E. Barkey, and J. B. Jordon. 2014. "Effect Tool Wear During End Milling on the Surface Integrity and Fatigue Life of Inconel 718." *Procedia CIRP* 14: 546-551

Liao, Y. S., H. M. Lin, and J. H. Wang. 2008. "Behaviors of End Milling Inconel 718 Superalloy by Cemented Carbide Tools." *Journal of Materials Processing Technology* 201 (1–3): 460-465

Liao, Y. S., and Y. C. Young. 1996. "A New on-Line Spindle Speed Regulation Strategy for Chatter Control." *International Journal of Machine Tools and Manufacture* 36 (5): 651-660

Liu, Chang, Chengzu Ren, Guofeng Wang, Yinwei Yang, and Lu Zhang. 2015. "Study on Surface Defects in Milling Inconel 718 Super Alloy." *Journal of Mechanical Science and Technology* 29 (4): 1723-1730

Ma, Haifeng, Jianhua Wu, Liuqing Yang, and Zhenhua Xiong. 2017. "Active Chatter Suppression with Displacement-Only Measurement in Turning Process." *Journal of Sound and Vibration* 401: 255-267

Ma, Jian-wei, Fu-ji Wang, Zhen-yuan Jia, Qiang Xu, and Yan-yu Yang. 2014. "Study of Machining Parameter Optimization in High Speed Milling of Inconel 718 Curved Surface Based on Cutting Force." *The International Journal of Advanced Manufacturing Technology* 75 (1-4): 269-277

Mehta, A., S. Hemakumar, A. Patil, S. P. Khandke, P. Kuppan, R. Oyyaravelu, and A. S. S. Balan. 2018. "Influence of Sustainable Cutting Environments on Cutting Forces, Surface Roughness and Tool Wear in Turning of Inconel 718." *Materials Today: Proceedings* 5 (2, Part 2): 6746-6754

Merrit, H. E. 1965. "Theory of Self-Excited Machine-Tool Chatter: Contribution to Machine-Tool Chatter Research—." *Journal of Engineering for Industry* 87 (4): 447-454

Minis, Ioannis, Rafael Yanushevsky, Abel Tembo, and Robert Hocken. 1990. "Analysis of Linear and Nonlinear Chatter in Milling." *CIRP Annals* 39 (1): 459-462

Munoa, J., I. Mancisidor, N. Loix, L. G. Uriarte, R. Barcena, and M. Zatarain. 2013. "Chatter Suppression in Ram Type Travelling Column Milling Machines Using a Biaxial Inertial Actuator." *CIRP Annals* 62 (1): 407-410

Nalbant, Muammer, Abdullah Altın, and Hasan Gökkaya. 2007. "The Effect of Cutting Speed and Cutting Tool Geometry on Machinability Properties of Nickel-Base Inconel 718 Super Alloys." *Materials & Design* 28 (4): 1334-1338

Ng, E. G., D. W. Lee, A. R. C. Sharman, R. C. Dewes, D. K. Aspinwall, and J. Vigneau. 2000. "High Speed Ball Nose End Milling of Inconel 718." *CIRP Annals - Manufacturing Technology* 49 (1): 41-46

Opitz, H. 1966. "Improvement of the Dynamic Stability of the Milling Process by Irregular Tooth Pitch." *Proc. 7th Int. MTDR Conf.* 213:

Otto, Andreas, Gerhard Kehl, Michael Mayer, and Günter Radons. 2011. "Stability Analysis of Machining with Spindle Speed Variation." *Advanced Materials Research* 223: 600-609

Patil, N. G., Ameer Asem, R. S. Pawade, D. G. Thakur, and P. K. Brahmankar. 2014. "Comparative Study of High Speed Machining of Inconel 718 in Dry Condition and by Using Compressed Cold Carbon Dioxide Gas as Coolant." *Procedia CIRP* 24: 86-91

Pawade, R. S., Suhas S. Joshi, and P. K. Brahmankar. 2008. "Effect of Machining Parameters and Cutting Edge Geometry on Surface Integrity of High-Speed Turned Inconel 718." *International Journal of Machine Tools and Manufacture* 48 (1): 15-28

Pervaiz, Salman, Amir Rashid, Ibrahim Deiab, and Mihai Nicolescu. 2014. "Influence of Tool Materials on Machinability of Titanium- and Nickel-Based Alloys: A Review." *Materials and Manufacturing Processes* 29 (3): 219-252

Quintana, Guillem, and Joaquim Ciurana. 2011. "Chatter in Machining Processes: A Review." *International Journal of Machine Tools and Manufacture* 51 (5): 363-376

Quintana, Guillem, Joaquim Ciurana, Inés Ferrer, and Ciro A. Rodríguez. 2009. "Sound Mapping for Identification of Stability Lobe Diagrams in Milling Processes." *International Journal of Machine Tools and Manufacture* 49 (3): 203-211

Quintana, Guillem, Joaquim Ciurana, and Daniel Teixidor. 2008. "A New Experimental Methodology for Identification of Stability Lobes Diagram in Milling Operations." *International Journal of Machine Tools and Manufacture* 48 (15): 1637-1645

Rahman, M., and Y. Ito. 1986. "Detection of the Onset of Chatter Vibration." *Journal of Sound and Vibration* 109 (2): 193-205

Sallese, Lorenzo, Giacomo Innocenti, Niccolò Grossi, Antonio Scippa, Roberto Flores, Michele Basso, and Gianni Campatelli. 2017. "Mitigation of Chatter Instabilities in Milling Using an Active Fixture with a Novel Control Strategy." *The International Journal of Advanced Manufacturing Technology* 89 (9): 2771-2787

Sam, Turner. 2011. "Process Damping Parameters." *IOP Conference Series: Materials Science and Engineering* 26 (1): 012008

Schulz, Herbert, and Toshimichi Moriwaki. 1992. "High-Speed Machining." *CIRP Annals - Manufacturing Technology* 41 (2): 637-643

Seguy, Sébastien, Tamás Insperger, Lionel Arnaud, Gilles Dessein, and Grégoire Peigné. 2010. "On the Stability of High-Speed Milling with Spindle Speed Variation." *The International Journal of Advanced Manufacturing Technology* 48 (9): 883-895

Shashidhara, Y. M., and S. R. Jayaram. 2010. "Vegetable Oils as a Potential Cutting Fluid—an Evolution." *Tribology International* 43 (5–6): 1073-1081

Shokrani, Alborz, Vimal Dhokia, and Stephen T. Newman. 2017. "Hybrid Cooling and Lubricating Technology for Cnc Milling of Inconel 718 Nickel Alloy." *Procedia Manufacturing* 11: 625-632

Sims, N. D., B. Mann, and S. Huyanan. 2008. "Analytical Prediction of Chatter Stability for Variable Pitch and Variable Helix Milling Tools." *Journal of Sound and Vibration* 317 (3): 664-686

Slavicek, Jan. 1965. "The Effect of Irregular Tooth Pitch on Stability of Milling" *Proc. of the 6th Int. MTDR Conf.*,

Takemura, Tadashi, Takashi Kitamura, and Tetsutaro Hoshi. 1975. *Active Suppression of Chatter by Programed Variation of Spindle Speed*. Vol. 41.

Taylor, C. M., N. D. Sims, and S. Turner. 2011. "Process Damping and Cutting Tool Geometry in Machining." *IOP Conference Series: Materials Science and Engineering* 26 (1): 012009

Thakur, D. G., B. Ramamoorthy, and L. Vijayaraghavan. 2009. "Study on the Machinability Characteristics of Superalloy Inconel 718 During High Speed Turning." *Materials & Design* 30 (5): 1718-1725

Thakur, DineshG, B. Ramamoorthy, and L. Vijayaraghavan. 2010. "Investigation and Optimization of Lubrication Parameters in High Speed Turning of Superalloy Inconel 718." *The International Journal of Advanced Manufacturing Technology* 50 (5-8): 471-478

Tian, Xianhua, Jun Zhao, Jiabang Zhao, Zhaochao Gong, and Ying Dong. 2013. "Effect of Cutting Speed on Cutting Forces and Wear Mechanisms in High-Speed Face Milling of Inconel 718 with Sialon Ceramic Tools." *The International Journal of Advanced Manufacturing Technology* 69 (9-12): 2669-2678

Tlusty, J., and M. Polacek. 1963. "The Stability of the Machine Tool against Self-Excited Vibration in Machining." *ASME Int. res. in production* 1: 465-474

Tobias, SA, and W Fishwick. 1958. "Theory of Regenerative Machine Tool Chatter." *The engineer* 205 (7): 199-203

Tsai, N-C, D-C Chen, and R-M Lee. 2010. "Chatter Prevention and Improved Finish of Workpiece for a Milling Process." *Proceedings of the Institution of Mechanical Engineers, Part B: Journal of Engineering Manufacture* 224 (4): 579-588

Tunç, L. T., and E. Budak. 2012. "Effect of Cutting Conditions and Tool Geometry on Process Damping in Machining." *International Journal of Machine Tools and Manufacture* 57: 10-19

Turner, Sam, Doruk Merdol, Yusuf Altintas, and Keith Ridgway. 2007. "Modelling of the Stability of Variable Helix End Mills." *International Journal of Machine Tools and Manufacture* 47 (9): 1410-1416

Uhlmann, E., J. A. Oyanedel Fuentes, and M. Keunecke. 2009. "Machining of High Performance Workpiece Materials with Cbn Coated Cutting Tools." *Thin Solid Films* 518 (5): 1451-1454

Wang, Bing, and Zhanqiang Liu. 2016. "Cutting Performance of Solid Ceramic End Milling Tools in Machining Hardened Aisi H13 Steel." *International Journal of Refractory Metals and Hard Materials* 55: 24-32

Wang, Yong, Taiyong Wang, Zhiqiang Yu, Yue Zhang, Yulong Wang, and Hengli Liu. 2015. "Chatter Prediction for Variable Pitch and Variable Helix Milling." *Shock and Vibration* 2015: 9

Wiercigroch, Marian, and Erhan Budak. 2001. "Sources of Nonlinearities, Chatter Generation and Suppression in Metal Cutting." *Philosophical Transactions of the Royal Society of London A: Mathematical, Physical and Engineering Sciences* 359 (1781): 663-693

Wiercigroch, Marian, and Anton M Krivtsov. 2001. "Frictional Chatter in Orthogonal Metal Cutting." *Philosophical Transactions of the Royal Society of London A: Mathematical, Physical and Engineering Sciences* 359 (1781): 713-738

Xavior, M. Anthony, M. Manohar, P. Jeyapandiarajan, and Patil Mahesh Madhukar. 2017. "Tool Wear Assessment During Machining of Inconel 718." *Procedia Engineering* 174: 1000-1008

Yan, Sijie, Dahu Zhu, Kejia Zhuang, Xiaoming Zhang, and Han Ding. 2014. "Modeling and Analysis of Coated Tool Temperature Variation in Dry Milling of Inconel 718 Turbine Blade Considering Flank Wear Effect." *Journal of Materials Processing Technology* 214 (12): 2985-3001

Yao, Zhehe, Deqing Mei, and Zichen Chen. 2010. "On-Line Chatter Detection and Identification Based on Wavelet and Support Vector Machine." *Journal of Materials Processing Technology* 210 (5): 713-719

Yusoff, Ahmad R., and Neil D. Sims. 2011. "Optimisation of Variable Helix Tool Geometry for Regenerative Chatter Mitigation." *International Journal of Machine Tools and Manufacture* 51 (2): 133-141

Yusoff, Ahmad R., Sam Turner, Chris M. Taylor, and Neil D. Sims. 2010. "The Role of Tool Geometry in Process Damped Milling." *The International Journal of Advanced Manufacturing Technology* 50 (9): 883-895

Zetek, Miroslav, Ivana Česáková, and Vojtěch Švarc. 2014. "Increasing Cutting Tool Life When Machining Inconel 718." *Procedia Engineering* 69: 1115-1124

Zhang, S., J. F. Li, and Y. W. Wang. 2012. "Tool Life and Cutting Forces in End Milling Inconel 718 under Dry and Minimum Quantity Cooling Lubrication Cutting Conditions." *Journal of Cleaner Production* 32: 81-87

Zheng, Guangming, Jun Zhao, Xiang Cheng, Rufeng Xu, and Guoyong Zhao. 2016. "Experimental Investigation on Sialon Ceramic Inserts for Ultra-High-Speed Milling of Inconel 718." *Materials and Manufacturing Processes* 31 (5): 633-640

Zhong, Weiwu, Dongbiao Zhao, and Xi Wang. 2010. "A Comparative Study on Dry Milling and Little Quantity Lubricant Milling Based on Vibration Signals." *International Journal of Machine Tools and Manufacture* 50 (12): 1057-1064

Zhu, Dahu, Xiaoming Zhang, and Han Ding. 2013. "Tool Wear Characteristics in Machining of Nickel-Based Superalloys." *International Journal of Machine Tools and Manufacture* 64: 60-77

APPENDIX

Tool wear progression: Cutting tool A

Cutting speed: 50m/s, Feed rate: 0.04mm/z, DoC_a: 0.1mm

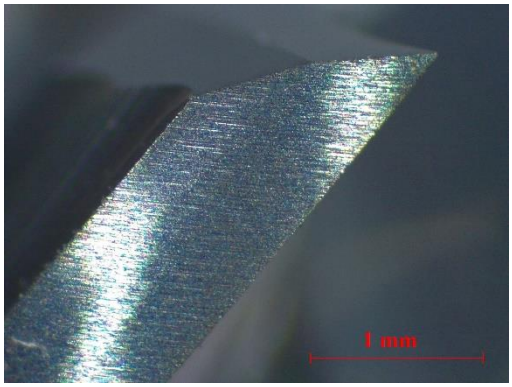

0 cutting pass

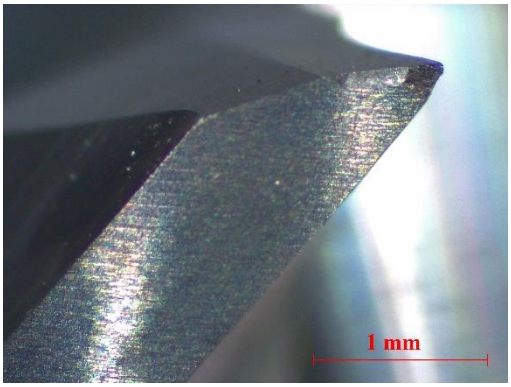

10 cutting pass

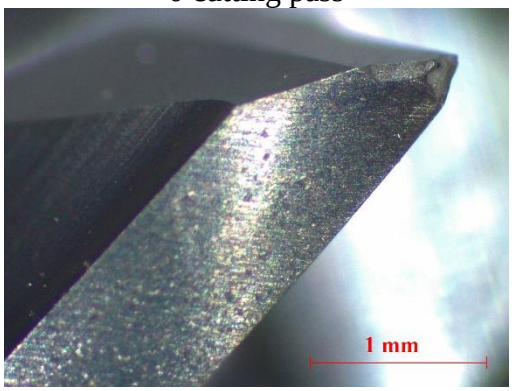

20 cutting pass

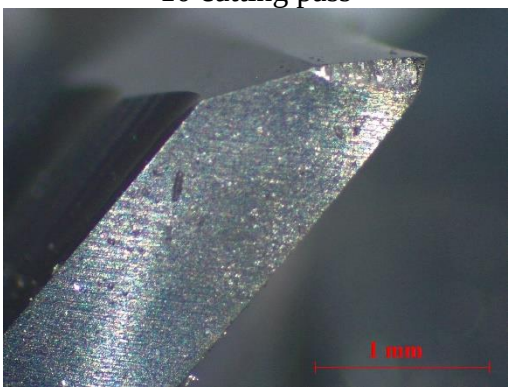

30 cutting pass

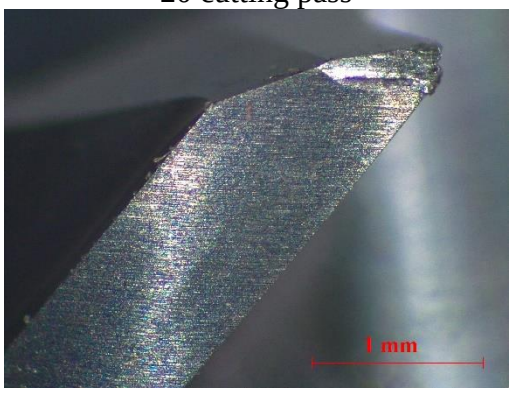

40 cutting pass

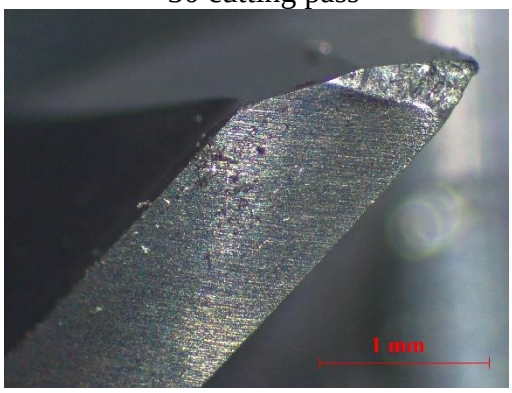

50 cutting pass

Tool wear progression: Cutting tool B

Cutting speed: 50m/s, Feed rate: 0.04mm/z, DoC_a: 0.1mm

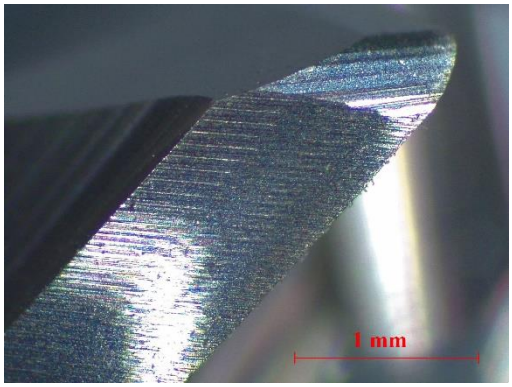

0 cutting pass

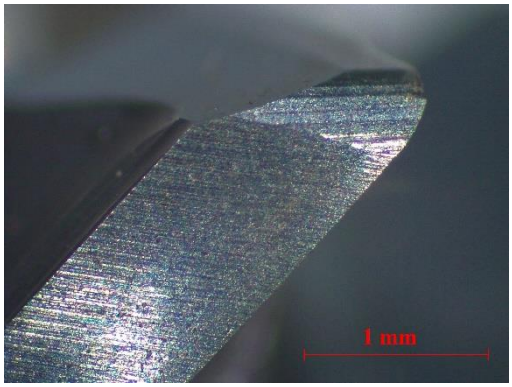

10 cutting pass

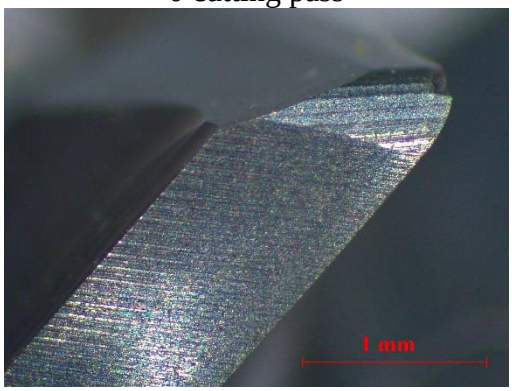

20 cutting pass

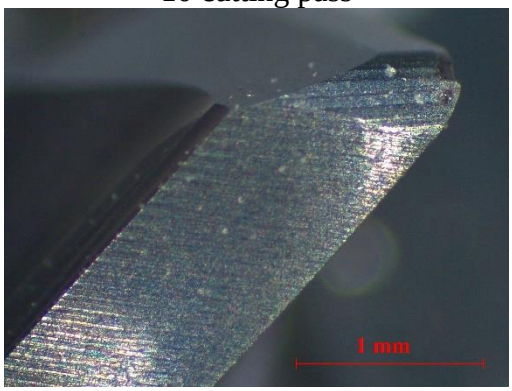

30 cutting pass

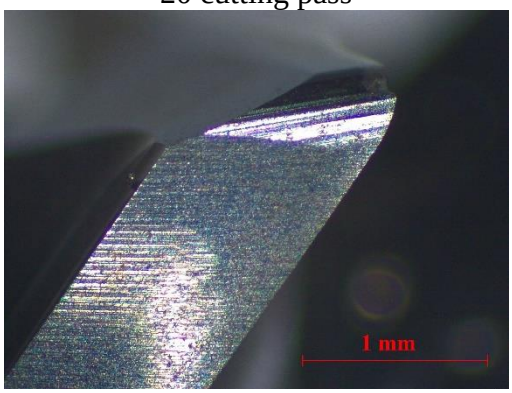

40 cutting pass

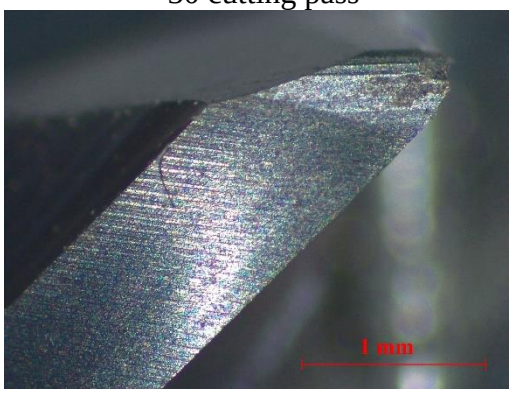

50 cutting pass

Tool wear progression: Cutting tool C

Cutting speed: 50m/s, Feed rate: 0.04mm/z, DoC_a: 0.1mm

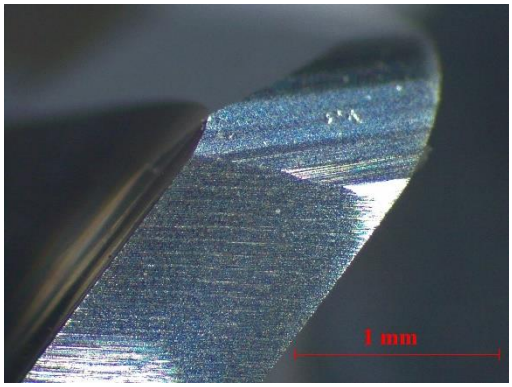

0 cutting pass

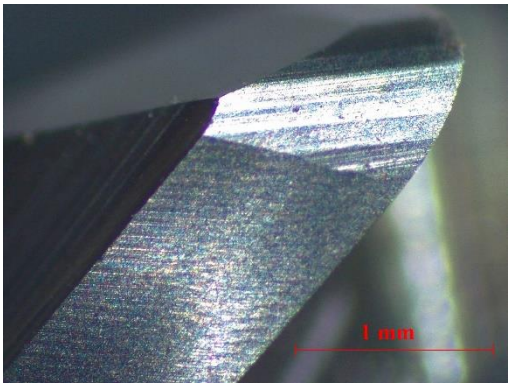

10 cutting pass

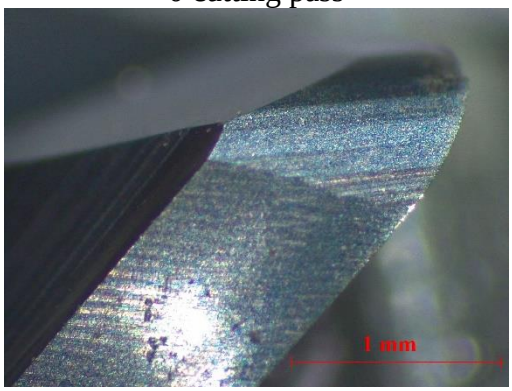

20 cutting pass

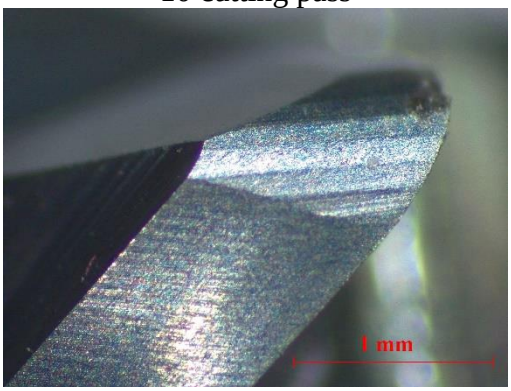

30 cutting pass

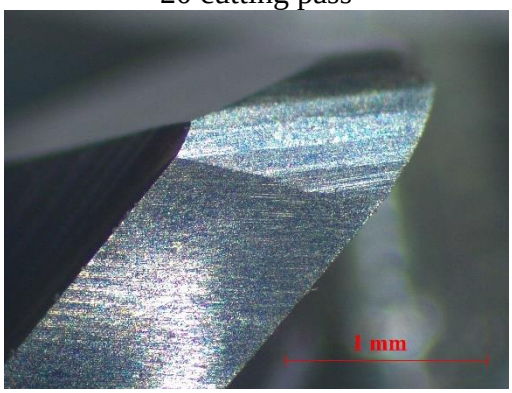

40 cutting pass

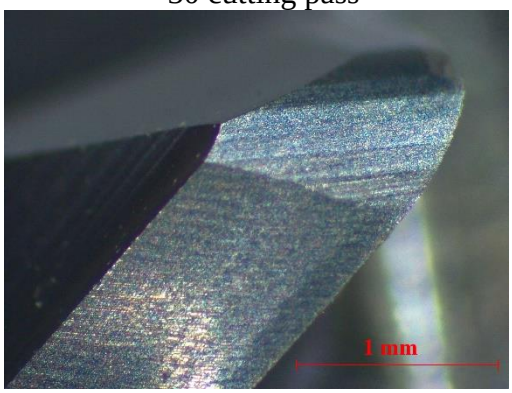

50 cutting pass

Tool wear progression: Cutting tool A

Cutting speed: 50m/s, Feed rate: 0.04mm/z, DoC_a: 0.3mm

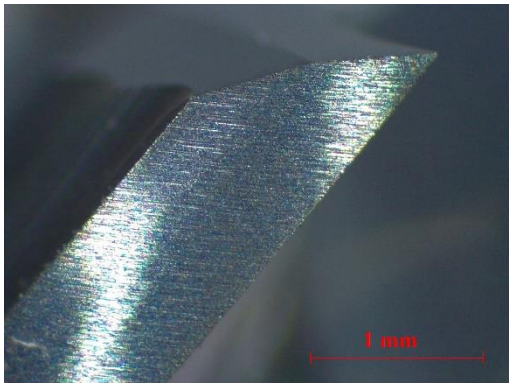

0 cutting pass

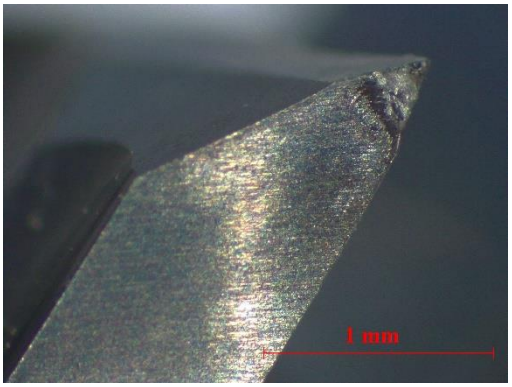

10 cutting pass

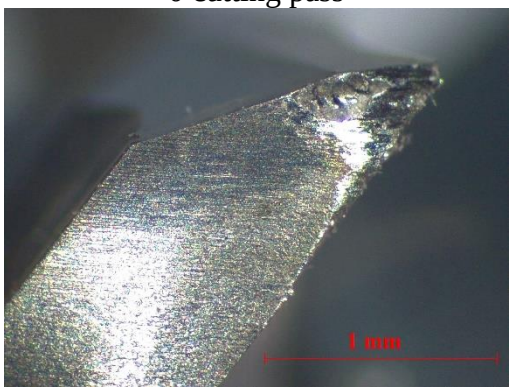

20 cutting pass

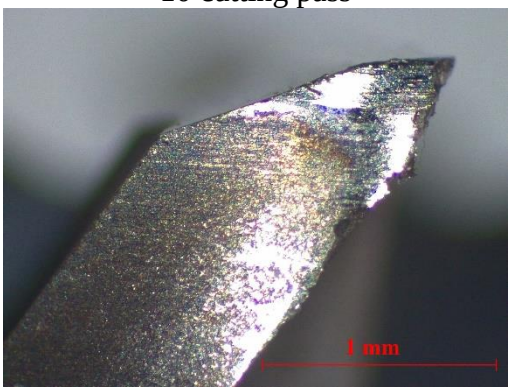

30 cutting pass

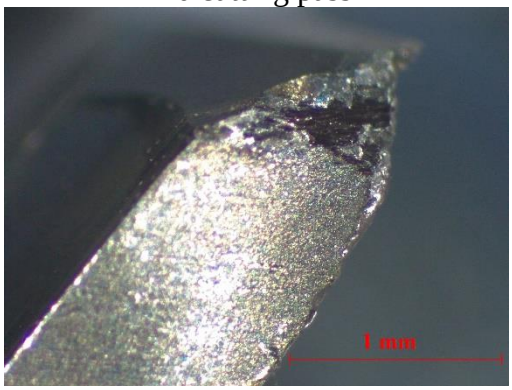

40 cutting pass

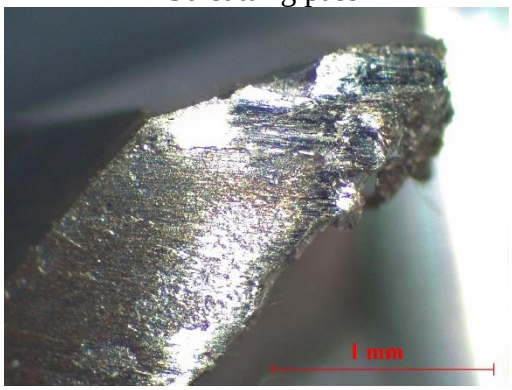

50 cutting pass

Tool wear progression: Cutting tool B

Cutting speed: 50m/s, Feed rate: 0.04mm/z, DoC_a: 0.3mm

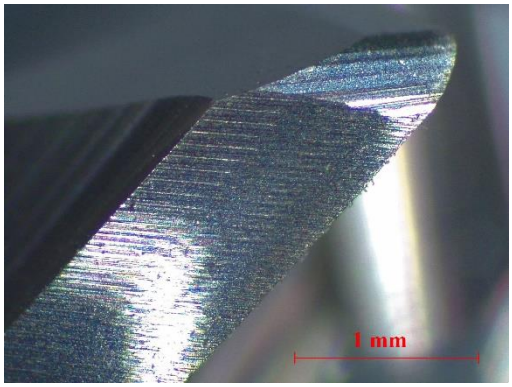

0 cutting pass

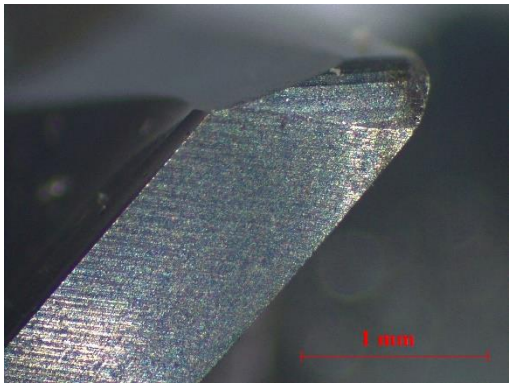

10 cutting pass

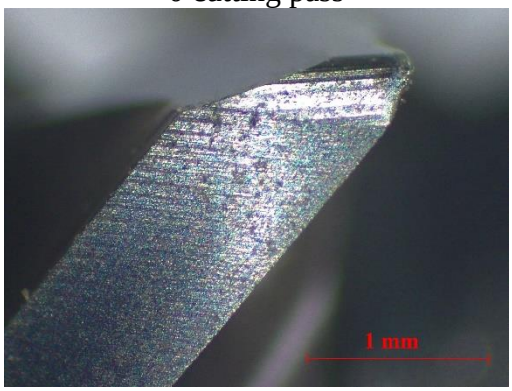

20 cutting pass

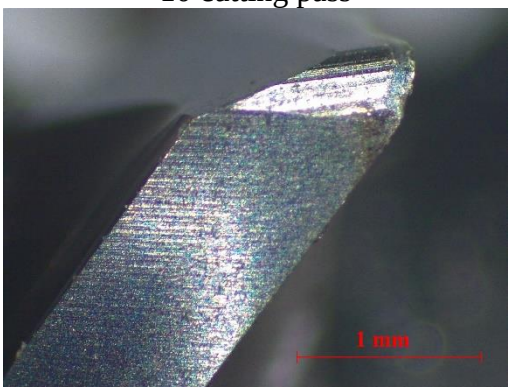

30 cutting pass

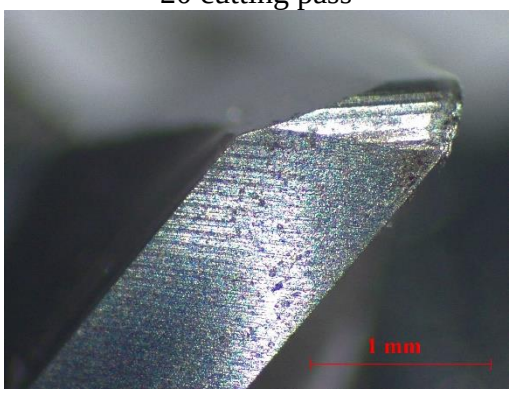

40 cutting pass

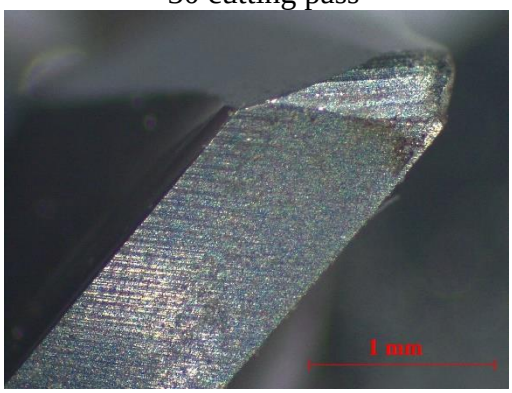

50 cutting pass

Tool wear progression: Cutting tool C

Cutting speed: 50m/s, Feed rate: 0.04mm/z, DoC_a: 0.3mm

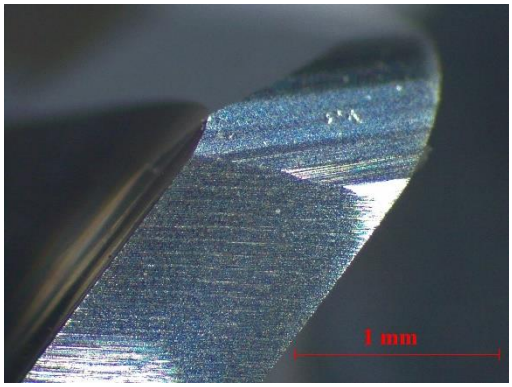

0 cutting pass

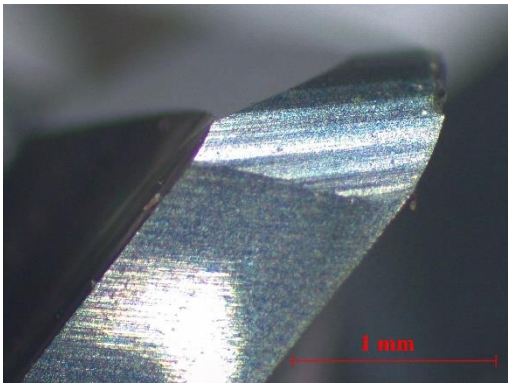

10 cutting pass

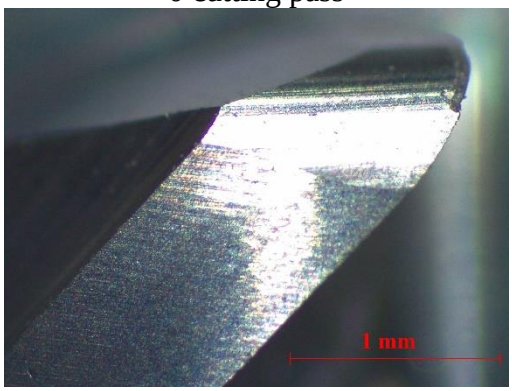

20 cutting pass

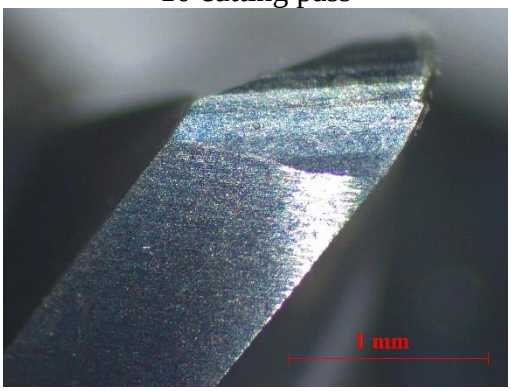

30 cutting pass

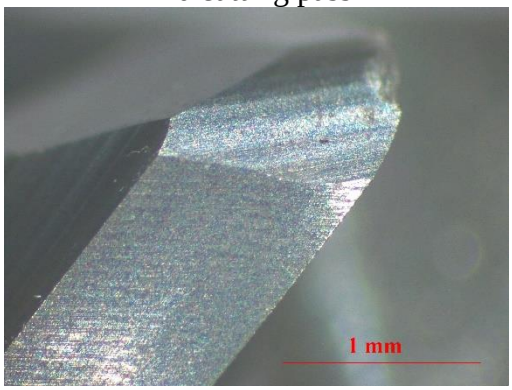

40 cutting pass

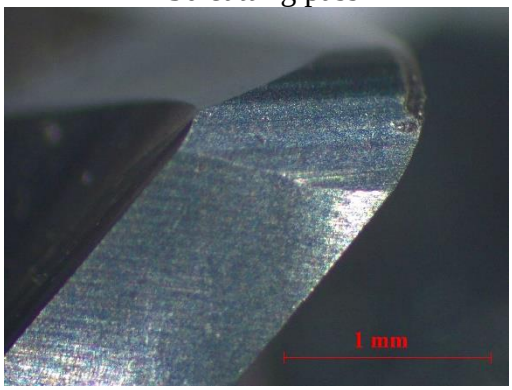

50 cutting pass